**CANADA**
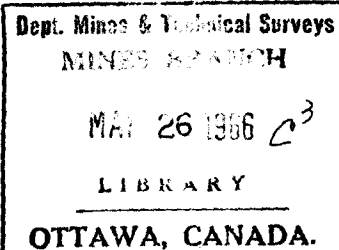
# PILLAR LOADING
## Part II: Model Studies

D. F. COATES

RTMENT OF MINES AND
ICAL SURVEYS, OTTAWA

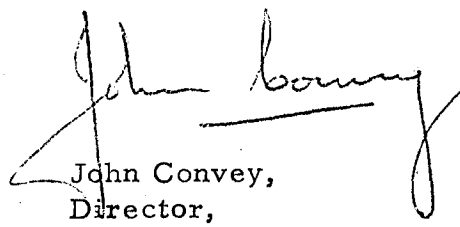FUELS AND MINING PRACTICE DIVISION

MINES BRANCH

RESEARCH REPORT

R 170

NOVEMBER 1965

# FOREWORD

It is Mines Branch policy to promote research, support universities and to disseminate information on subjects of importance to the mineral industry. With the traditional strength, among other subjects, of McGill University in applied mechanics, it has been natural for its Department of Mining Engineering and Applied Geophysics to display a leading interest in the development of the new subject of rock mechanics and in the training of postgraduate students in this subject. The co-operative effort of our two organizations has produced in a doctoral thesis, on which this report is based, what seems to be a significant contribution to the science of mining.

Dean D. L. Mordell and Professor R. G. K. Morrison, Chairman of the Department of Mining Engineering and Applied Geophysics, are to be commended for promoting this work. Mines Branch is glad to publish this work, in a series of three reports of which this is the second, so that it can receive wide distribution amongst those interested in a basic study of an important element of mine structures -- the pillar.

John Convey,
Director,
Mines Branch.

Mines Branch Research Report R 170

# PILLAR LOADING.  Part II:  Model Studies

by

D. F. Coates[*]

- - -

## ABSTRACT

The research work on pillar loading has been concerned with the combining of existing scientific theories into a rational hypothesis for predicting the loading of pillars.  With the establishment of this hypothesis empirical substantiation or modification became required.  The data from existing model work was analysed and supplementary experimental work conducted, so that the various parameters indicated by the hypothesis as being significant could be examined.

Measurements of pillar stresses in laboratory models of gelatin, Araldite-type materials, mortar and steel showed that it is possible to predict the variation of pillar loading with location within the mining zone, with variation of pillar height, with variation of pillar breadth, with the number of pillars across the mining zone, with the variation of the compressibility of the pillar ground with respect to that of the walls, with variation in the magnitude of the field stress component acting transversely to the mining zone or vein, and, above all, with the extraction ratio.

However, by analysing data with respect to the various parameters it was found necessary to modify the theoretical equations for the functions including the location of the pillar, the effect of the stress component acting transversely to the mining zone, and the effect of pillar breadth in a mining zone having pillars of unequal width.  These modifications have been made following the traditional engineering procedure

[*] Head, Mining Research Laboratories, Fuels and Mining Practice Division, Mines Branch, Department of Mines and Technical Surveys, Ottawa, Canada.

of taking into account both the empirical evidence and the mechanism (if it can be recognized but has not been included in the theory) that is causing the deviation of the data from theory.

The most significant parameters, aside from the extraction ratio, affecting the pillar loading have been shown to be the ratio of compressibility of the pillar rock to wall rock, the height of the pillar, and the breadth of the pillar in mines with pillars of unequal width.

# LA CHARGE DES PILIERS. PARTIE II: ÉTUDES DE MODELES

par

D. F. Coates*

- - - -

## RÉSUMÉ

Les travaux de recherches sur le régime de charge des piliers ont porté sur la combinaison de théories scientifiques connues en une hypothèse rationnelle afin de prédire le régime de charge des piliers. Avec l'élaboration de cette hypothèse, la vérification ou la modification empirique devint nécessaire. Les résultats provenant de travaux déjà réalisés sur des maquettes furent analysés, et l'on a effectué des travaux expérimentaux supplémentaires, pour que les divers paramètres, que l'hypothèse indiquait comme étant notables, puissent être examinés.

Les mesures de contraintes de piliers dans des modèles de laboratoire en gélatine, en matériaux de type Araldite, en mortier et en acier, ont montré qu'on peut prédire la variation du régime de charge des piliers avec leur emplacement à l'intérieur de la zone d'exploitation, avec la variation de hauteur des piliers, avec la variation de largeur des piliers, avec le nombre de piliers à travers la zone d'exploitation, avec la variation de la compressibilité de la roche du pilier par rapport à celle des parois, avec la variation d'intensité de la composante de la contrainte du terrain agissant transversalement à la veine ou à la zone d'exploitation, et par dessus tout avec le taux d'extraction.

Cependant, en analysant les résultats à l'égard des divers paramètres, on trouva nécessaire de modifier les équations théoriques pour les fonctions comprenant l'emplacement du pilier, l'effet de la composante de contrainte agissant transversalement à la zone d'exploitation, ainsi que l'effet de la largeur de pilier dans une zone d'exploitation ayant des piliers de largeurs inégales. On a fait ces modifications en suivant la méthode technique traditionnelle, tenant compte à la fois des observations empiriques et du mécanisme faisant dévier les résultats de la théorie (si ce mécanisme peut être reconnu mais n'a pas été inclus dans la théorie).

On a montré que, outre le taux d'extraction, les paramètres les plus importants, qui influent sur le régime de charge des piliers, sont le rapport de la compressibilité de la roche du pilier à celle de la roche des parois, la hauteur du pilier, et la largeur du pilier dans les mines où les piliers sont de largeurs inégales.

*Chef, Laboratoires de recherche en génie minier, Division des combustibles et du génie minier, Direction des mines, ministère des Mines et des Relevés techniques, Ottawa, Canada.

# CONTENTS

# FIGURES

## TABLES

# INTRODUCTION

## Hypothesis

A hypothesis has been presented that provides physical concepts for the mechanisms affecting pillar loadings (1). The equations relating the parameters that are judged to be most significant are:

$$\therefore \frac{\Delta \sigma_p}{S_o} = \frac{(2R - kh(1-w))(\sqrt{1-x^2} + h) - w_p\, khn}{hn + \pi(1-R)(1+1/N)(1+h/\sqrt{1-x^2})/2 + 2Rb(1-w)/\pi}, \qquad \text{Eq. 1}$$

$$\frac{\Delta \sigma_p}{S_o} = \frac{(2R - kh(1-w))(\sqrt{1-x^2} + 2h) + RK_b' - 2w_p\, khn}{2hn + (\pi/2(1+h/\sqrt{1-x^2}) + 2K_b'/3(1+h/(1-x^2)))(1-R)(1+1/N) + 4bR(1-w)/\pi},$$

$$\text{Eq. 2}$$

where $\Delta \sigma_p$ is the increase in pillar stress resulting from mining; $S_o$ is the field, or pre-mining, stress normal to the vein; R is the general extraction ratio; k is the ratio of transverse to normal field stress components, $S_t/S_o$; h is the normalized height parameter, $H/L$; H is the height of the pillar from wall to wall; L is the span of the mining zone from one abutment to the other; $w = \mu/(1-\mu)$; $\mu$ is Poisson's ratio; x is the normalized x-coordinate of the pillar, $x'/l$; $x'$ is the distance from the centre of the mining zone to the centre of the pillar in question; $l$ is the semi-span or distance from the centre of the mining zone to one abutment; $w_p$ applies to the pillar rock; $n = M/M_p$; $M = E/(1-\mu^2)$; E is the modulus of elasticity; b is the normalized breadth of the pillar, $B/L$; B is the breadth of the pillar; and $K_b'$ is a depth parameter defined as follows:

$$K_b' = \frac{1 - x^2}{2z'^3} + \frac{1.2(1+w)(1-x^2)}{z'}$$

$$+ \left[ 13 - 2w \left\{ \frac{12(1-x'^2)}{z'^2} + 1 - \frac{8}{z'^2} - 3w \right\} \right] \frac{z'}{32}$$

$$+ \frac{0.884\,F\,(1-x'^2)}{z'^2}$$

and

$$F = 1 - \frac{1}{2.26/z'+1}, \quad z' = z/l.$$

These equations require empirical substantiation or modification. The modifications made below follow the traditional engineering procedure of taking into account both the empirical evidence and the mechanism, if it can be recognized, and is not included in the theory that is causing the deviation of the data from theory.

## Model Requirements

The review of the subject showed that additional empirical data are required to establish the relationship between pillar stresses and the various geometrical aspects of mining zones (1). Model experiments can be designed to provide this information. To use models that will provide valid data equivalent to the actual mining geometries, certain specifications are required.

For underground openings, the resultant stresses can be considered to be caused by the combination of gravitational stresses, residual stresses from crustal disturbances, and stresses arising from mining operations.

To fulfil the requirements of dynamic as well as geometric similitude, it has been proven that if certain dimensionless ratios or parameters can be kept constant between the model and the prototype, then similitude will be achieved (2). A list of the variables involved in producing pillar stresses, together with the dimensions, follows:

$\gamma$ (density of the rock) $\qquad FL^{-3}$

z (depth below ground surface) $\qquad L$

$S_o$ (field stress normal to the vein) $\qquad FL^{-2}$

$S_t$ (field stress parallel to the vein
   and normal to the strike) $\qquad FL^{-2}$

i (dip angle of vein) $\qquad D$

x' (distance from centreline of
   mining zone) $\qquad L$

L (span of mining zone) $\qquad L$

H (height of pillar) $\qquad L$

B (breadth of pillar) $\qquad L$

E (modulus of deformation of
   wall rock) $\qquad FL^{-2}$

$E_p$ (modulus of deformation of
   pillar rock) $\qquad FL^{-2}$

$\mu$ (Poisson's ratio for all ground) $\qquad D$

  With twelve significant variables and two primary dimensions (force and length) in the system, there are then ten dimensionless ratios or parameters that are significant with respect to pillar stresses, namely:

1) $= \gamma z/E$     6) $= H/L = h$

2) $= S_t/S_o = k$    7) $= B/L = b$

3) $= i$       8) $= E/E_p = n$

4) $= x'/L = x/2$    9) $= \mu$

5) $= z/L$      10) $= \gamma z/S_o$

  It has been established that if the model and the prototype have equal ratios, the model will then be dynamically and geometrically similar to the prototype. If all of these ratios cannot be maintained constant, sufficient knowledge about the functional relations between these ratios and the pillar stresses might exist to confirm that it is not essential for all parameters to be constant to have an adequate model.

  $\gamma z/E$ usually would be important if the model were to predict deformations. However, the hypothesis of pillar loadings indicates that for pillar stresses this should not be a significant ratio, so long as E is constant with respect to stress level.

k is likely to be quite significant with respect to pillar stresses, and is a factor hitherto ignored in previous theories of pillar loading and in the presentation of the results of model tests.

i would seem to be an important parameter, that should be maintained constant between model and prototype. On the other hand, if the normal stresses perpendicular $(S_o)$ and tangential $(S_t)$ to the mining area are used, it may not be an essential parameter.

The ratio $x'/L$, or just x, is a ratio, as indicated by the pillar loading hypothesis, that is likely to be significant and again one that has been hitherto ignored, both in theory and in experimental work.

The ratio $z/L$ might, as indicated by the pillar loading hypothesis, be significant for relatively shallow workings. However, the hypothesis also indicates that, when the ratio is greater than about 1, the significance of $z/L$ should diminish very quickly.

The ratio $H/L$, or h, probably is of some significance when large, but diminishes into insignificance for values that are representative of pillars in thin seams or very wide stoping areas. The same comments apply to $B/L$ or b.

The ratio $E/E_p$, or n, is likely to be very significant and takes into account what will probably be found to be a frequently occurring geological condition, where the modulus of deformation of the pillar rock is less than that of the surrounding rocks.

Poisson's ratio, $\mu$, according to the pillar loading hypothesis, should have some significance.

$\gamma z/S_o$ might have some significance for shallow mining zones at dips other than $90^o$.

Another aspect of the requirements of a model is the amount of edge distance beyond any openings that is required to produce conditions equivalent to an infinite mass. This requirement can be examined by analysing the difference in stress distribution between that in an infinite plate and that in a finite plate.

For an elliptical opening, the compression of the abutments and the deflection of the boundaries in the vertical direction will be influenced by the total force in the finite width of plate A, as shown in Figure 1. If the force over this width is the same as for an infinite plate, then the vertical deflections should be substantially the same.
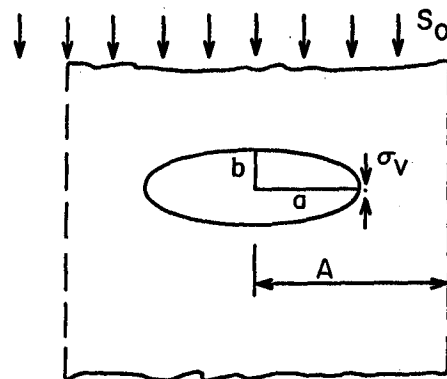
Figure 1. Elliptical hole in infinite and finite plates.

It has been established that for an infinite plate the average vertical stress over (A-a), as shown in Figure 1, is (3):

$$\bar{\sigma}_v = S_o \left[ 1 + \frac{a}{A} + \frac{1}{2}\left(\frac{a}{A}\right)^2 + \frac{1}{2}\left(\frac{a}{A}\right)^3 + \frac{(a-b)(3a^2 + 3ab + 3b^2)}{8a^3}\left\{\left(\frac{a}{A}\right)^4 + \left(\frac{a}{A}\right)^5\right\} \right],$$

with powers of a/A greater than 5 being ignored. It is of value to note here that only if $(a/A)^4$ is a significant number is the shape of the ellipse significant.

For a plate of finite width, half the force in the plate will be represented by $S_m A$. Then, if the two cases produce equal forces on the strip (A-a), it follows that:

$$S_m A = \bar{\sigma}_v (A-a)$$

$$\therefore S_m = S_o \left[ 1 - \frac{1}{2}\left(\frac{a}{A}\right)^2 - \frac{a^3(a+b)(a^2 + 2b^2 - ab)}{8A^3} - \frac{(a+b)(a^2 - b^2)(a^2 - ab + 4b^2)a}{16A} \right].$$

From this equation, if A = 2a,    $S_m = 0.875 S_o$;

= 3a,    = 0.944 $S_o$;

= 4a,    = 0.969 $S_o$.

These numbers indicate that the edge distance (A-a) in models should be about 3a, or A = 4a, if an error of 3 per cent is acceptable. If A = 3a, an error of a little more than 5 per cent would occur, which might not be too serious.

Other analyses have shown that, for a circular hole, the tangential, boundary stress parallel to the plate boundary would be increased by about 6 per cent if A = 4a, and by about 10 per cent if A = 3a (4).

In the case of a plate of finite dimensions, experimental work has indicated that the vertical, tangential boundary stress around a hole would be increased by about 10 per cent if the vertical distance from the centre of the hole to the plate boundary is four times the hole radius; the vertical radial stress on the centreline above the hole is increased by an amount varying from 0 to 10 per cent (5).

As a result of these analyses, it seems that the edge distances for any models should be three times, or more, the half-width of the opening.

The question arises, in models concerned with ground stress, as to whether a material that is sensitive to body forces must be used or whether a stiffer, conventional material can be used with boundary stresses. In general, if a mining opening is situated at sufficient depth from the ground surface that the weight of material removed is small in relation to that of the overlying rock, the difference between the stress distribution in a stress field created by a boundary pressure and that in a stress field created by gravitational body forces is insignificant. It has been shown that when the depth to an opening is 20 times the radius of the opening, or its equivalent, the error resulting from using a boundary force instead of a body force is negligible (6).

After examining the existing empirical data available for analysis, the areas where additional information is required can be determined. In many of the previous models that have been used, the edge distances were too small for the best results. The effects on the results may not be too significant; however, it would be useful to have some supplementary experiments performed with adequate dimensions so that the validity of previous experiments can be checked. For this reason, additional models providing data on the dependence of pillar loading on the factors probably of most significance, R, N and x, should be tested.

In addition, the factor k requires more study. Work has been done on models with N = 1 and k = 0, 1/3 and 1 (14), and on a variety of models with k = 0.5 (7). Consequently, it would be useful to have studies with a greater range in k on a series of models with different numbers of pillars.

In view of the existing data, the variables of height and breadth of pillar need less study than the above factors.

The depth of workings, z, or the ratio z/L, has been shown by the theoretical work above to be significant only within narrow limits. In round numbers, where z/L is less than 0.5, the tributary area theory for practical problems can probably be used to determine pillar loads. When z/L is greater than 1, the hypothesis for long, deep mining zones should be applicable. Hence, only for the range 0.5 to 1 is z/L likely to be important in predicting pillar loads through the use of the hypothesis of long, shallow, mining zones.

The effect of the pillar modulus of deformation being less than that of the surrounding rock has not been studied. Experiments designed to investigate the effect of this parameter should therefore be conducted.

In addition, if the effect of jointing, a widespread rock property, could be examined, the range of applicability of the hypothesis could be amplified.

Model Equation

Where models are created by cutting holes in unstressed material, and pressures are applied to the boundaries of the material, i.e., post-stressed, the reaction of the pillars will be different from the effect of cutting out openings in stressed, i.e., pre-stressed, materials. The difference in the reaction of the pillars arises from several mechanisms. Any empirical modifications that might result from such experimental work would then be made to the hypothesis through an analysis, rather than through a direct modification.

In the case of the post-stressed model, assuming a plane stress condition and $\mu_p = \mu$, it can be established that the deflection, $\delta$, caused by the field stresses will be as follows (1):

$$\delta = \frac{S_o l}{E} (2 + h - kh) ((1 - x^2)^{\frac{1}{2}} + h).$$

This deflection results from cutting out both the rooms and the pillars and applying the field stresses.

Then following the hypothesis and recognizing that the openings or rooms in the model are cut out before any stress is applied, it follows that the reverse deflection, $\delta'$, resulting from placing the pillars back in the model is:

$$\delta' = \frac{\pi \sigma_p l (1 - R)(1 + h/(1 - x^2)^{\frac{1}{2}})}{2E(1 - R/(1 + N))}.$$

The local penetration of the pillars in excess of the average reverse deflection can be determined as in the hypothesis, recognizing that this deflection is a function of the total pillar stress and not just the increase in pillar stress due to mining. The following equation is obtained:

$$\delta'_p = \frac{\sigma_p R B (1 - \mu)}{\pi E}.$$

Then, since the total pillar deflection, equal to $\sigma_p h'/E_p$, is the algebraic sum of the above components, it follows that:

$$\delta_p = \delta - \delta' - \delta'_p.$$

Solving for $\sigma_p$, the following equation is obtained:

$$\frac{\sigma_p}{S_o} = \frac{(2 + h - kh)((1 - x^2)^{\frac{1}{2}} + h)}{hh + \pi (1 - R)(1 + R/(1 + N - R))(1 + h/(1 - x^2)^{\frac{1}{2}})/2 + 2 Rb(1 - \mu)/\pi}. \quad \text{Eq. 3}$$

## EXPERIMENTAL DATA

### Gelatin Models

Construction. The use of gelatin for these models arises from the desirability of having a material with a low modulus of elasticity and a high optical sensitivity so that stresses are produced in the model by the weight of the material similar to gravitational stresses produced in ground. A gelatin mixture can be 200 to 1000 times more sensitive than other conventional photoelastic materials. However, some minimum size of model is still required to obtain significant stresses (6).

The physical and mechanical properties of the resultant gelatin vary with the ambient temperature, e.g., it has been found that the elastic modulus doubles as the temperatures change from 20°C to 16°C (8) and it has also been suggested that Poisson's ratio for gelatin may vary with temperature (9). The modulus of elasticity and optical stress coefficient are fairly stable with time (6), but some experiments have detected mechanical and optical creep (10).

Another difficulty is that several types of calibration methods have been tested without obtaining a completely satisfactory one (11). Only recently has a good method been established. However, under controlled

conditions, deformation is substantially linear with stress and the variation of the path of the light beam is also linear with deformation (6).

The pillar models were made from gelatin (10-45 per cent by weight of the total mixture), pure glycerin (30 per cent), water (25-60 per cent), and B-napthol (to prevent rotting) (0-0.01 per cent) (6). It is possible, by varying the percentages of gelatin and water, to produce a specific gravity ranging from 1.06 to 1.16, a range of modulus of elasticity of from 0.5 ksc to 3.9 ksc, and a range of optical stress coefficients of 15 x $10^{-4}$ cm$^2$/kg to 3.4 x $10^{-4}$ cm$^2$/kg (6). As the gelatin content is increased, it becomes gradually more difficult to achieve a uniform mixture; the best method then seems to be to add enough water to obtain a uniform mixture and evaporate the excess water.

The ingredients are added together in a basin and mixed for up to eight hours, after which the mixture must be left, depending on quantity, for from 8 to 24 hours. It is then melted over a water bath at 75-80°C, with heating continuing for as much as 2 hours, depending on the gelatin content. During the heating the mixture is gently stirred periodically, and froth is removed from the surface. The mixture should then be cooled slowly to the casting temperature of 40-60°C (6).

The models are made by pouring molten gelatin into collapsible molds. The sides of the molds are generally made of plate glass set into U-shaped frames with appropriate seals. Silicon-oil on the surfaces of the mold prevents sticking, and silicon-grease in the corners assists in preventing leakage (11). During the pouring operation the mold is kept vertical to assist in the removal of air bubbles.

While the model is being cast, calibration samples are taken for the determination of the physical and mechanical properties of the material.

For large models the mold may be suspended in a water tank to control the ambient temperature to provide support for the sides of the mold and to reduce the tendency for leaks to occur. After the gelatin has cooled and set, the mold is taken apart. The free surfaces of the model are then covered with additional lubricant, and the mold is reassembled and left in a vertical position for about 24 hours.

Various lubricants can be used, such as mineral oils, fish oils, and glycerin. None of these lubricants completely eliminates the friction between the model and the glass supports, and they tend to be effective for only a short period of time. A mixture of 15 per cent rosin in pure vaseline seems more effective than the conventional lubricants. Also, it is transparent and does not penetrate the gelatin. The vaseline is heated

to 80°C and the rosin powder is then added. The mixture is heated in a
boiling water bath until all the rosin is dissolved (6).

After the model has stabilized during the 24-hour period,
the openings are cut to simulate the mine rooms. During this operation
the model is kept nearly vertical to maintain the gravity stress field.

In order to produce in a model the condition of plane strain,
there must not be any transverse strain; for this reason the sides of the
mold should be retained and the surfaces lubricated. Furthermore, in
order to reduce any effect of such frictional forces as may remain, the
model should be made as thick as possible while still permitting the passage
of light and the production of the isochromatic patterns.

Owing to the low modulus of elasticity and the large resultant
deformations that would occur with a condition of plane stress, this simpler
case has the disadvantage that the application of the theory of elasticity
based on infinitesimal strains is then questionable.

Operation. The photoelastic method of stress analysis
makes it possible to obtain the difference between the principal stresses in
the model and the angle of inclination of these stresses. At the points along
the unloaded boundary the difference between the principal stresses com-
pletely defines the stress condition, since one of the principal stresses
equals zero.

For determining the values of the principal stresses at an
internal point in the model, the method used in this work is the so-called
"Shear Difference Method" (12).

The general forms of the equations of equilibrium for these
models are:

$$\frac{\partial \sigma_x}{\partial x} + \frac{\partial \tau_{xy}}{\partial y} = 0$$

$$\frac{\partial \tau_{xy}}{\partial x} + \frac{\partial \sigma_y}{\partial y} = -\gamma$$

From these equations it follows that:

$$(\sigma_x)_x = (\sigma_x)_0 - \int_0^x \frac{\partial \tau_{xy}}{\partial y} \, dx,$$

where subscript x outside the bracket denotes the coordinate axis parallel

to which the integration is performed; $(\sigma_x)_0$ is the known value of $\sigma_x$ at the initial point of the integration (usually the value for $(\sigma_x)_0$ is taken on the free boundary).

In order to determine the stresses along a straight line parallel to the x-axis, an auxiliary section must be added on each side of this axis of the graphs showing the isochromatic and isoclinic lines. The next step is to determine the values of the shear stresses, as well as their difference $\Delta\tau_{xy}$, along these auxiliary sections.

The shear stresses are determined by using the equation:

$$\tau_{xy} = \frac{p-q}{2} \sin 2\emptyset,$$

where p-q is the isochromatic fringe value and $\emptyset$ is the parameter of the isoclinic line.

Using a summation instead of integration, the equation is obtained:

$$(\sigma_x)_x = (\sigma_x)_0 - \sum_{i=n}^{i=n} \frac{\Delta\tau_{xy_i}}{\Delta_{y_i}} \Delta x_i,$$

where $\Delta_y$ is the distance between the auxiliary sections and $\Delta_x$ is the distance between the points of integration. Using this equation, $\sigma_x$ can be determined.

The value of $(\sigma_y)_x$ is determined by using the relation of stresses at a point:

$$(\sigma_y)_x = (\sigma_x)_x \pm \sqrt{(p-q)^2 - 4\tau_{xy}^2}.$$

The stresses $(\sigma_y)_y$ at points along the straight line parallel to the y-axis are found from an analogous equation:

$$(\sigma_y)_y = (\sigma_y)_0 - \sum_{i=n}^{i=n} \frac{\Delta\tau_{xy_i}}{\Delta x_i} \Delta y_i - \gamma y,$$

where $\gamma$ is the density of the material. $(\sigma_x)_y$ is found from the equation:

$$(\sigma_x)_y = (\sigma_y)_y \pm \sqrt{(p-q)^2 - 4\tau_{xy}^2}.$$

With the values of $\sigma_x$ and $\sigma_y$, the principal stresses p and q can now be found from the formulae

$$p = \frac{\sigma_x + \sigma_y}{2} + \tau_{max}; \quad q = \frac{\sigma_x + \sigma_y}{2} - \tau_{max}.$$

Experimental Results. Figure 2 shows typical model geometry used in the gelatin experiments (7, 13). These models were constructed as described above.

In Table 1 the experimental results from the gelatin models are tabulated. Models T-1 to T-15 were 700 mm wide by 600 mm high. This required the mixing and molding of about 110 lb of gelatin for each model. It can be seen that in spite of the size of the models the edge distances for numbers T-1 to T-10 were somewhat less than ideal.

Each model was tested in a condition of plane stress contained within rigid ends so that there was no expansion laterally in the plane of the model. As the gelatin has a Poisson's ratio of 0.5 the horizontal or tangential field stress, $S_t$, can be determined as follows:

$$\epsilon_h = 0 = (\sigma_h - u\sigma_v)/E$$

$$\therefore \sigma_h = 0.5\,\sigma_v$$

$$\therefore k = 0.5.$$

Detailed analyses of the principal stresses were conducted on several models. It was found that the horizontal stresses at the mid-section of the pillars were relatively insignificant. As a result of these analyses, the pillar loadings of models T-2, 3, 4, 7 and 9 were calculated assuming the major principal stress to be twice the maximum shear stress(7).

These detailed analyses also showed quite clearly the mechanism of wall deflections adjacent to a mining zone producing the loading on the pillar. In Figure 3 the greater stress concentration at the tops of the pillars on the sides towards the centreline of the mining zone is a manifestation of the deflection curve of the roof, or wall of the vein, which gives rise in the hypothesis to the factor $\sqrt{1 - x^2}$ in the basic formula.
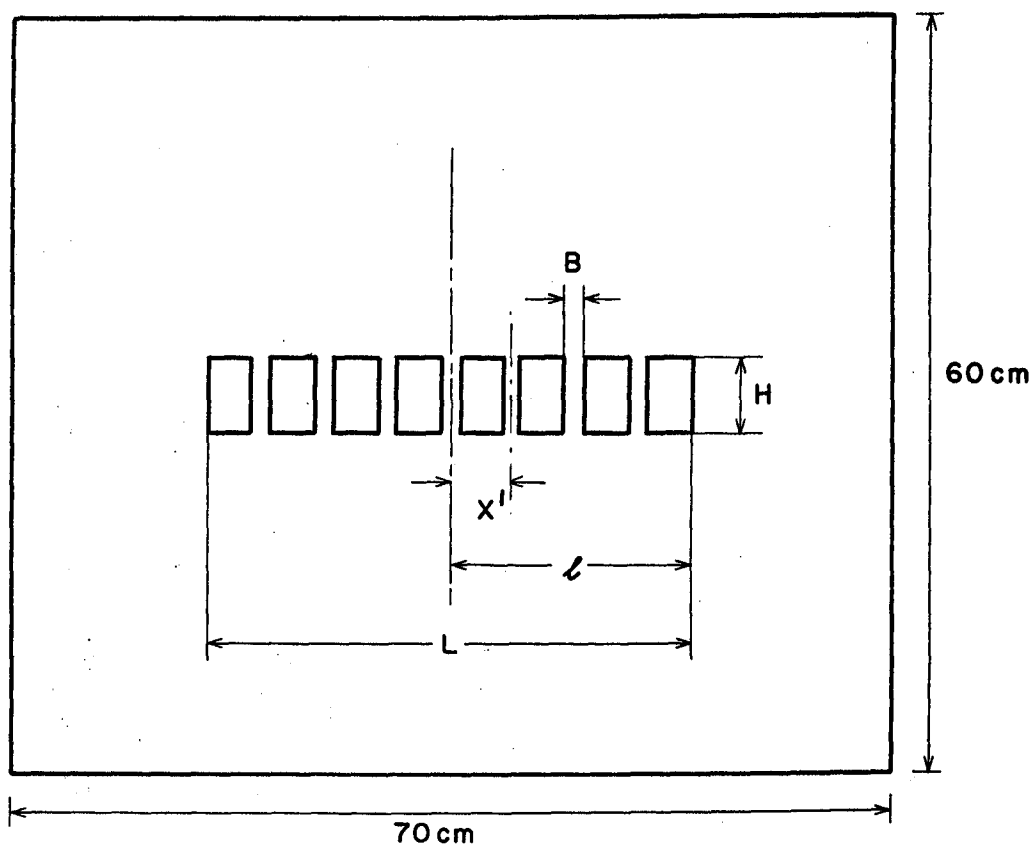
Figure 2. Typical gelatin model geometry with seven pillars (Ref. 7).

## TABLE 1

Experimental Results from Gelatin Models (7, 13)

B = 15 mm,  z = 300 mm,  k = 0.5,  $\mu$ = 0.5,  n = 1

| No. | N | R | L mm | H mm | x | $\Delta\sigma_p{}'$ |
|-----|---|---|------|------|---|---------------------|
| T-1 | 7 | 0.604 | 265 | 60 | 0 | 1.12 |
|     |   |       |     |    | 0.264 | 1.03 |
|     |   |       |     |    | 0.528 | 1.00 |
|     |   |       |     |    | 0.792 | 0.75 |
| T-2 | 7 | 0.656 | 305 | 60 | 0 | 1.35 |
|     |   |       |     |    | 0.262 | 1.22 |
|     |   |       |     |    | 0.525 | 1.22 |
|     |   |       |     |    | 0.787 | 1.11 |
| T-3 | 7 | 0.696 | 345 | 60 | 0 | 1.77 |
|     |   |       |     |    | 0.261 | 1.56 |
|     |   |       |     |    | 0.522 | 1.51 |
|     |   |       |     |    | 0.783 | 1.35 |
| T-4 | 7 | 0.728 | 385 | 60 | 0 | 2.06 |
|     |   |       |     |    | 0.260 | 2.06 |
|     |   |       |     |    | 0.520 | 1.56 |
|     |   |       |     |    | 0.780 | 1.36 |
| T-5 | 7 | 0.753 | 425 | 60 | 0 | 3.17 |
|     |   |       |     |    | 0.259 | 2.00 |
|     |   |       |     |    | 0.518 | 1.84 |
|     |   |       |     |    | 0.777 | 1.55 |
| T-6 | 7 | 0.696 | 345 | 30 | 0 | 1.61 |
|     |   |       |     |    | 0.261 | 1.55 |
|     |   |       |     |    | 0.522 | 1.46 |
|     |   |       |     |    | 0.783 | 1.38 |
| T-7 | 7 | 0.696 | 345 | 45 | 0 | 1.56 |
|     |   |       |     |    | 0.261 | 1.56 |
|     |   |       |     |    | 0.522 | 1.51 |
|     |   |       |     |    | 0.783 | 1.38 |
| T-9 | 7 | 0.696 | 345 | 80 | 0 | 1.78 |
|     |   |       |     |    | 0.261 | 1.56 |
|     |   |       |     |    | 0.522 | 1.51 |
|     |   |       |     |    | 0.783 | 1.38 |
| T-10 | 7 | 0.696 | 345 | 100 | 0 | 1.72 |
|     |   |       |     |    | 0.261 | 1.55 |
|     |   |       |     |    | 0.522 | 1.43 |
|     |   |       |     |    | 0.783 | 0.94 |
| T-11 | 1 | 0.727 | 55 | 60 | 0 | 0.83 |
| T-12 | 1 | 0.800 | 75 | 60 | 0 | 1.16 |
| T-13 | 1 | 0.833 | 95 | 60 | 0 | 1.50 |
| T-14 | 1 | 0.800 | 75 | 30 | 0 | 1.30 |
| T-15 | 1 | 0.800 | 75 | 100 | 0 | 1.05 |
| V-1 | 8 | 0.600 | - | - | 0 | 1.03 |
|     |   |       |     |    | 0.300 | 0.97 |
|     |   |       |     |    | 0.584 | 0.91 |
|     |   |       |     |    | 0.817 | 0.74 |
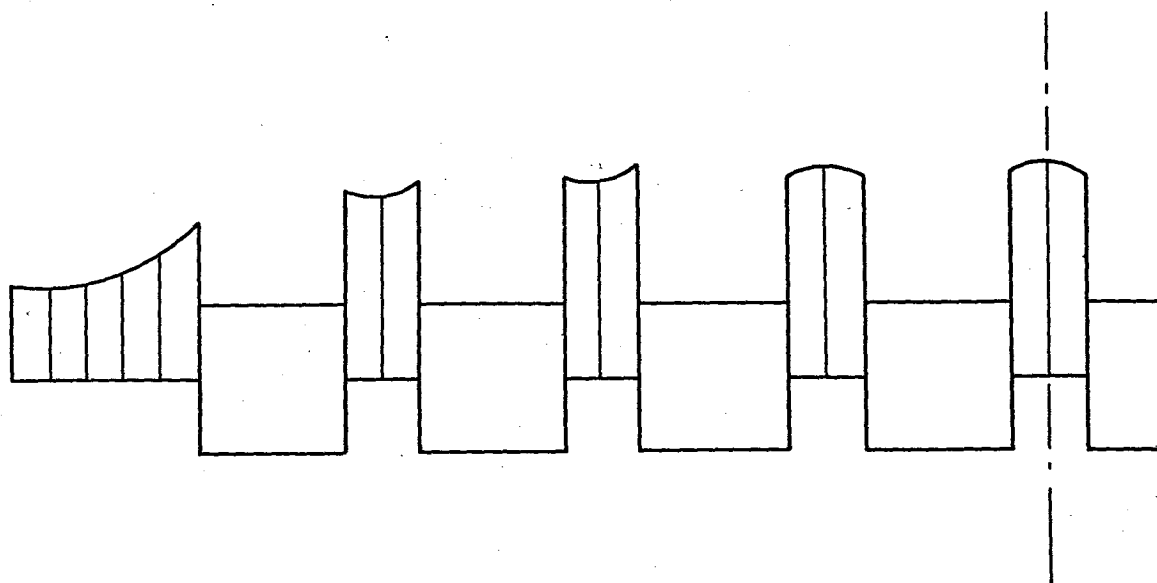
Figure 3. Stress in pillars of gelatin model T-6 (Ref. 7).

Araldite Models

Construction. Model series A, B, C, D, E and F were made out of Ciba Araldite Type B with sheet sizes of 30 cm x 15 cm x 1.5 cm for the multiple openings and 15 cm x 15 cm x 1.5 cm for the single pillar models (14). Series U models were made out of Homalite CR-39 with a sheet size of 4 in. x 4 in. x 1/4 in. (15).

The openings were made either square or rectangular with the corners filleted to a radius equal to 2/15 of the width of the opening, with the exceptions of Models F which had the shape of an inverted horseshoe with a flat bottom and Models U which were horizontal ovals.

Operation. For the various series of Models A, B, C and D (see Table 2 for details on dimensions), the boundary loading was applied through weights hung on the upper edge of the plate at equally spaced points along the top edge. The strains were determined photoelastically. Because the strains that were produced by this type of loading were not great enough to produce fringes of a high enough order to be useful, a modification of the normal technique was required. Under this loading the model was placed in an oven and heated at 120°C for 24 hours and then cooled to room temperature at the rate of 4°C/hr. In this way the sensitivity of the Araldite was increased about ten-fold, and the fringe patterns were "frozen" into the plastic (14).

For each of these models a separate test specimen was made from the same plate. These test specimens were loaded by hanging a weight on one end to produce a simple uniaxial tensile stress field. This sample then went through the same heating and cooling cycle as the model plate. In this way a calibration of the fringe orders was obtained (14).

For the U-series the plates were loaded through metal platens plus thin rubber gaskets; this was shown to produce, within the accuracy of the technique, substantially uniform loading (15).

Each model was tested in a condition of plane stress with free ends so that no horizontal field stresses existed and the parameter k = 0. For Models E, F and U the experiments included loading the plates both vertically and horizontally at different times and then combining the results by superposition.

Experimental Results. Figure 4 shows model geometry typical of the multi-pillar experiments.

In Table 2 the experimental results are tabulated. With model plates 300 mm long, it can be seen that series A, B, C and D all had less than desirable edge distances. For model series E and F the plates
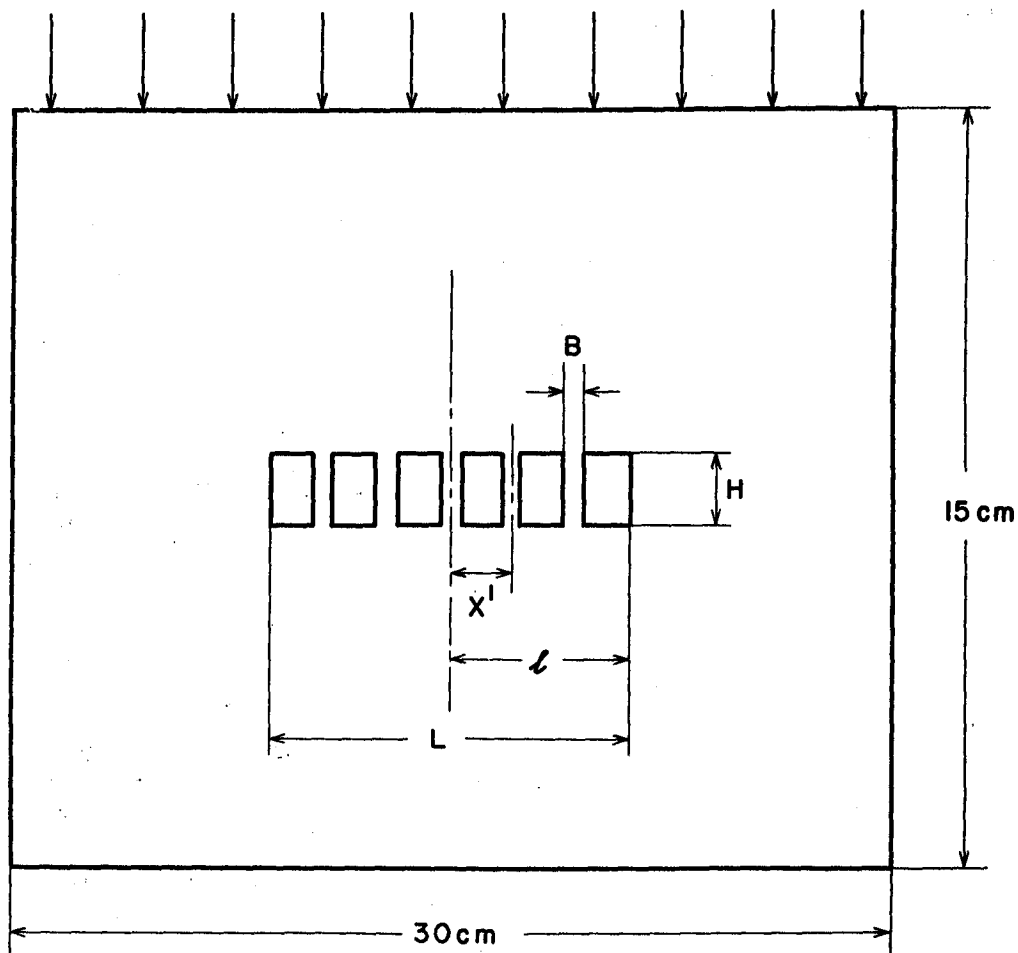
Figure 4. Typical Araldite model geometry with five pillars (Ref. 14).

TABLE 2

Experimental Results from Araldite Models (14, 15, 17)

$z = 75$ mm, $\mu = 0.435$, $n = 1$

| No. | N | L mm | H mm | B mm | x | k | $\sigma_p'$ |
|---|---|---|---|---|---|---|---|
| A-1 | 5 | 165 | 15 | 15 | 0 | 0 | 2.0 |
| | | | | | 0.364 | 0 | 2.0 |
| | | | | | 0.726 | 0 | 1.9 |
| A-2 | 5 | 169 | 19 | 11 | 0 | 0 | 2.6 |
| | | | | | 0.355 | 0 | 2.6 |
| | | | | | 0.711 | 0 | 2.5 |
| A-3 | 5 | 173 | 23 | 7 | 0 | 0 | 3.8 |
| | | | | | 0.348 | 0 | 3.7 |
| | | | | | 0.095 | 0 | 3.5 |
| A-4 | 5 | 177 | 27 | 3 | 0 | 0 | 7.7 |
| | | | | | 0.339 | 0 | 7.4 |
| | | | | | 0.678 | 0 | 6.7 |
| B-1 | 5 | 110 | 20 | 10 | 0 | 0 | 1.9 |
| | | | | | 0.364 | 0 | 1.9 |
| | | | | | 0.726 | 0 | 1.8 |
| B-2 | 5 | 116 | 32 | 4 | 0 | 0 | 3.6 |
| | | | | | 0.345 | 0 | 3.5 |
| | | | | | 0.090 | 0 | 3.3 |
| B-3 | 5 | 117 | 34 | 3 | 0 | 0 | 4.1 |
| | | | | | 0.342 | 0 | 4.0 |
| | | | | | 0.684 | 0 | 3.9 |
| C-1 | 5 | 90 | 10 | 10 | 0 | 0 | 2.1 |
| | | | | 5 | 0.389 | 0 | 2.8 |
| | | | | 5 | 0.722 | 0 | 2.6 |
| C-2 | 5 | 90 | 12 | 12 | 0 | 0 | 2.1 |
| | | | | 4 | 0.398 | 0 | 3.2 |
| | | | | 4 | 0.720 | 0 | 3.0 |
| C-3 | 5 | 108 | 13 | 10 | 0 | 0 | 2.3 |
| | | | | 4 | 0.334 | 0 | 3.4 |
| | | | | 4 | 0.712 | 0 | 3.1 |
| C-4 | 5 | 94 | 12 | 10 | 0 | 0 | 2.6 |
| | | | | 3 | 0.394 | 0 | 4.1 |
| | | | | 3 | 0.712 | 0 | 3.7 |
| C-5 | 5 | 100.9 | 13 | 10.1 | 0 | 0 | 2.7 |
| | | | | 3.2 | 0.391 | 0 | 4.2 |
| | | | | 3.2 | 0.712 | 0 | 3.8 |
| C-6 | 5 | 97 | 14.5 | 7 | 0 | 0 | 3.4 |
| | | | | 2.5 | 0.370 | 0 | 4.9 |
| | | | | 2.5 | 0.691 | 0 | 4.5 |
| C-7 | 5 | 96 | 13 | 10 | 0 | 0 | 2.8 |
| | | | | 2 | 0.796 | 0 | 4.5 |
| | | | | 2 | 0.709 | 0 | 4.2 |
| C-8 | 5 | 100 | 14 | 8 | 0 | 0 | 3.2 |
| | | | | 2 | 0.380 | 0 | 5.1 |
| | | | | 2 | 0.700 | 0 | 4.8 |

(Continued)

TABLE 2 (Concluded)

| No. | N | L mm | H mm | B mm | x | k | $\sigma_p'$ |
|---|---|---|---|---|---|---|---|
| D-1 | 5 | 179 | 19 | 11 | 0 | 0 | 2.5 |
|  |  |  |  | 16 | 0.363 | 0 | 2.1 |
|  |  |  |  | 11 | 0.726 | 0 | 2.4 |
| D-2 | 5 | 183 | 23 | 7 | 0 | 0 | 4.0 |
|  |  |  |  | 12 | 0.356 | 0 | 3.4 |
|  |  |  |  | 7 | 0.712 | 0 | 3.8 |
| D-3 | 5 | 183 | 25 | 3 | 0 | 0 | 6.2 |
|  |  |  |  | 12 | 0.355 | 0 | 4.3 |
|  |  |  |  | 3 | 0.710 | 0 | 5.9 |
| E-1 | 1 | 45 | 15 | 15 | 0 | 0 | 1.9 |
|  |  |  |  |  |  | 1/3 | 1.9 |
|  |  |  |  |  |  | 1 | 1.8 |
| E-2 | 1 | 50 | 20 | 10 | 0 | 0 | 2.6 |
|  |  |  |  |  |  | 1/3 | 2.5 |
|  |  |  |  |  |  | 1 | 2.3 |
| E-3 | 1 | 54 | 24 | 6 | 0 | 0 | 3.7 |
|  |  |  |  |  |  | 1/3 | 3.4 |
|  |  |  |  |  |  | 1 | 3.1 |
| F-1[x] | 1 | 2.91H | H | 1.24H | 0 | 0 | 1.8 |
|  |  |  |  |  |  | 1/3 | 1.7 |
|  |  |  |  |  |  | 1 | 1.6 |
| F-2 | 1 | 2.19H | H | 0.52H | 0 | 0 | 2.55 |
|  |  |  |  |  |  | 1/3 | 2.45 |
|  |  |  |  |  |  | 1 | 2.25 |
| F-3 | 1 | 1.70 | H | 0.177 | 0 | 0 | 3.85 |
|  |  |  |  |  |  | 1/3 | 3.7 |
|  |  |  |  |  |  | 1 | 3.4 |
| U-1[y] | 1 | 76 | 12 | 10 | 0 | 0 | 4.3 |
|  |  |  |  |  |  | 1/3 | 4.6 |
|  |  |  |  |  |  | 1 | 4.0 |
|  |  |  |  |  |  | 3 | 2.8 |

[x]Horseshoe section openings.

[y]Horizontal oval openings.

were 150 mm long, which produced just about the desirable edge distance.
For series U the length of the plate was 4 in., or 102 mm; edge distance
was much less than it should have been for the best results.

## Mortar Models

Construction. The mortar models were constructed with
various mixes of sand and a cement (7, 16). An attempt was made to
preserve similitude in the physical properties of the mortars with respect
to the mine conditions that were being modelled. For models I-1 to I-21,
the geometrical scale was 1:100 and the modulus of deformation of the
rock was 400,000 ksc. In the case of models T-16 to T-20 the scale was
also 1:100.

Models I-1 to I-11 were constructed with the pillars supported
on a rigid base as shown in Figure 5. This can be considered as a valid
construction for the case of a deep mining zone, with the rigid base
representing the horizontal centreline of the mining zone, which should
be the datum for symmetrical deflections in both the roof and floor. In
models I-10 to I-21 the rigid base was replaced with rubber, permitting
some penetration of the pillars into the base.

All models were constructed within rigid frames so that
away from the mining openings horizontal strain was zero and the hori-
zontal field stress was a function of Poisson's number (i.e., $S_z/(m - 1)$).
The I-series models were of the order of 5 m long, so that for most of
the experiments there was ample edge distance. The T-series models
were 70 cm long, which provided more than enough edge distance.

Operation. For models I-1 to I-21 the pillar loads resulting
from the overlying strata were measured with a compressible, electrical
wire pressure gauge about 1/8 in. thick, working on a three-point beam
loading principle.

For models T-16 to T-20, the pillar loads resulting from the
overlying ground plus boundary load were determined by knowing the
crushing strength of the mortar and loading to the point which produced
crushing.

Experimental Results. Table 3 contains the experimental
results obtained with these models. All of the symbols have their usual
meanings. The height of the model pillars, 8 cm, is given as H/2,
recognizing that by constructing the pillars on a base, only the upper half
of the pillars have been simulated. The coefficient of subgrade reaction,
$k_s$, is the deflection in centimetres to be expected from the bearing pressure
of the pillars on the rubber base in ksc, kilograms per square centimetre.
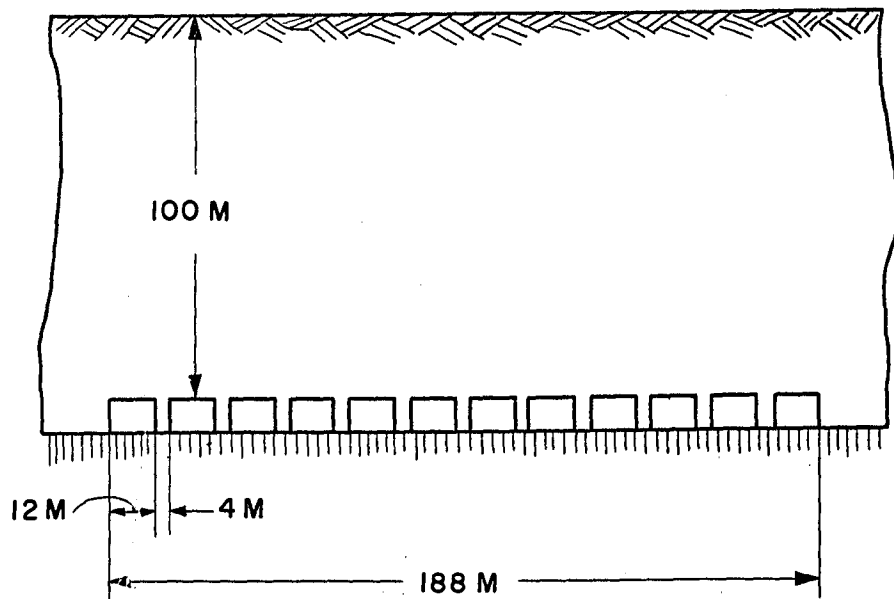
Figure 5. Typical mortar model geometry (Ref. 16).

## TABLE 3

Experimental Results from Mortar Models (7, 16)

H/2 = 8 cm,  B = 4 cm,  x = 0,  n = 1

| No. | N | R | L cm | z cm | E ksc | $k_s$ cm³/kg | $\sigma_p'$ |
|---|---|---|---|---|---|---|---|
| I-1 | 1 | 0.858 | 28 | 100 | 800 | 0 | 1.32 |
| I-2 | 7 | 0.774 | 124 | 100 | 800 | 0 | 1.40 |
| I-3 | 11 | 0.766 | 188 | 100 | 800 | 0 | 2.92 |
| I-4 | 1 | 0.858 | 28 | 285 | 600 | 0 | 1.12 |
| I-5 | 1 | 0.858 | 28 | 285 | 2000 | 0 | 1.12 |
| I-6 | 7 | 0.774 | 124 | 285 | 600 | 0 | 2.12 |
| I-7 | 7 | 0.774 | 124 | 285 | 2000 | 0 | 2.36 |
| I-8 | 11 | 0.776 | 188 | 285 | 600 | 0 | 2.72 |
| I-9 | 11 | 0.776 | 188 | 285 | 2000 | 0 | 2.96 |
| I-10 | 1 | 0.858 | 28 | 285 | 600 | 0.1 | 1.40 |
| I-11 | 1 | 0.858 | 28 | 285 | 2000 | 0.1 | 1.24 |
| I-12 | 3 | 0.800 | 60 | 285 | 600 | 0.1 | 1.48 |
| I-13 | 3 | 0.800 | 60 | 285 | 2000 | 0.1 | 1.44 |
| I-14 | 5 | 0.783 | 92 | 285 | 600 | 0.1 | 1.76 |
| I-15 | 5 | 0.783 | 92 | 285 | 2000 | 0.1 | 1.72 |
| I-16 | 7 | 0.774 | 124 | 285 | 600 | 0.1 | 2.04 |
| I-17 | 7 | 0.774 | 124 | 285 | 2000 | 0.1 | 2.00 |
| I-18 | 9 | 0.770 | 156 | 285 | 600 | 0.1 | 2.28 |
| I-19 | 9 | 0.770 | 156 | 285 | 2000 | 0.1 | 2.28 |
| I-20 | 11 | 0.766 | 188 | 285 | 600 | 0.1 | 2.58 |
| I-21 | 11 | 0.766 | 188 | 285 | 2000 | 0.1 | 2.53 |

B = 1.5 cm,  x = 0,  n = 1

| No. | N | R | H cm | L cm | z cm | $\sigma_p'$ |
|---|---|---|---|---|---|---|
| T-16 | 1 | 0.727 | 6.0 | 5.5 | 30 | 1.90 |
| T-17 | 1 | 0.800 | 6.0 | 7.5 | 30 | 2.36 |
| T-18 | 1 | 0.833 | 6.0 | 9.5 | 30 | 2.74 |
| T-19 | 1 | 0.800 | 3.0 | 7.5 | 30 | 2.51 |
| T-20 | 1 | 0.800 | 10.0 | 7.5 | 30 | 2.34 |

Besides the data contained in Table 3, an experiment was conducted in one of the models whereby the net pillar deflection, $\delta_p$, was artificially increased by cutting out 7.2 mm of the pillar ground. This resulted in reducing the pillar load by 12 per cent, and the increased roof sag occurred without fracture or spalling.

## Steel Models

Introduction. To supplement the empirical data required to verify the hypothesis, several model types were considered. Whereas gelatin models had been used to provide a material with a significant body force with respect to its deformation properties, it had some unsatisfactory aspects. The modulus of deformation was found to vary with temperature and time (11). In addition, the absolute fringe value was difficult to determine. Both of these factors would not necessarily be important for comparative studies; however, for the studying of pillar loading with respect to field stresses these parameters are critical. Other difficulties that are not critical but cannot be ignored are: the presence of some friction between the side plates and the gelatin for experiments in plane strain, the large strains accompanying experiments in plane stress, the great amount of work entailed in constructing the large models required by this material, and the difficulties encountered in varying the parameter k (i.e., the resistance on the bottom of the model to lateral compression would provide a very complex stress field ) which was required for this supplementary testing.

The use of soft rubber, combined with the Moire technique, for measuring deformations was considered as an alternative to using gelatin. However, it was found that the modulus of deformation of soft rubber also is not constant with respect to temperature and time. Similar minor problems as for the gelatin models would be encountered with the rubber models.

The alternate approach was to use a stiffer model material with boundary loadings but with the boundaries sufficiently far from the openings that the stress distributions would be the same as with body force loadings. Conventional photoelastic materials, such as araldite, were examined. Again, for comparative work, these materials are satisfactory; however, for absolute comparison of pillar stresses with field stresses the modulus of deformation of material is critical. It was found that the modulus of deformation of these materials would vary to some extent under loading with time. Although the variation was not great, it would be an unsatisfactory source of experimental error. This factor, combined with the lack of precision in converting isochromatic fringes to maximum shear stresses and thence to principal stresses, makes this technique less than ideal.

Mortar is not a good material for models used to study stress distributions. It is difficult to obtain homogeneity, and stress or load measurements cannot be made with any perfectly satisfactory technique. Mortar might be a good material where fracture patterns are to be studied.

Steel plate models have the advantage, over the above materials, of having constant elastic properties with respect to both time and temperature. Also, the use of strain gauges provides a direct and accurate method of determining principal stresses in a moderately homogeneous stress field. For any study involving steep stress gradients, this technique would not be satisfactory.

In pillars, areas both of steep stress gradients and of relative homogeneity exist. The distribution of vertical and horizontal stresses to be expected in a vertical pillar has been examined both theoretically and experimentally. In Figure 6(a) the theoretical variation of the vertical stress across the width of a cylindrical pillar is shown for both the section at the wall line and the section at the horizontal centreline (9). This solution was obtained by assuming that the ends of the pillar would remain plane, that no radial slipping at the ends would occur at any point and that the height to diameter ratio was equal to 1. An alternate theoretical solution produced almost identical results for the case where the ends remain plane, no expansion of the perimeter of the ends occurs and the height to diameter ratio is equal to $\pi/3$ (8). These theoretical solutions indicate that whereas the variation of vertical stress across the ends is large with a high stress concentration occurring towards the exterior of the pillar, the variation of vertical stress at the horizontal centreline is very small.

As a comparison, in Figure 6(b), the experimental results obtained on gelatin models are shown (7). These models were cases of plane stress, rather than having (as above) axial symmetry, with the breadth of the pillars being 50 mm and the dimension normal to the plane of the pillars being 15 mm. The great variation in the vertical principal stress at the wall line for both the cases where the height to breadth ratio was equal to 0.5 and 2 is almost identical with the theoretical solution shown in Figure 6(a). In addition, the variation of the vertical stress at the horizontal centreline, for the case of height-to-breadth equal to 2, is almost identical with the above theoretical solution; however, the variation obtained for the height-to-breadth ratio of 0.5 is somewhat greater, although still less than the variation occurring at the wall line. Others have also shown that the variation at the horizontal centreline decreases with an increase in the ratio of height-to-breadth and also with an increase in the ratio of height-to-breadth and also with an increase in extraction ratio (13, 14).

These experiments, in addition, produced information on the variation of the horizontal or minor principal stress in these model pillars (7).
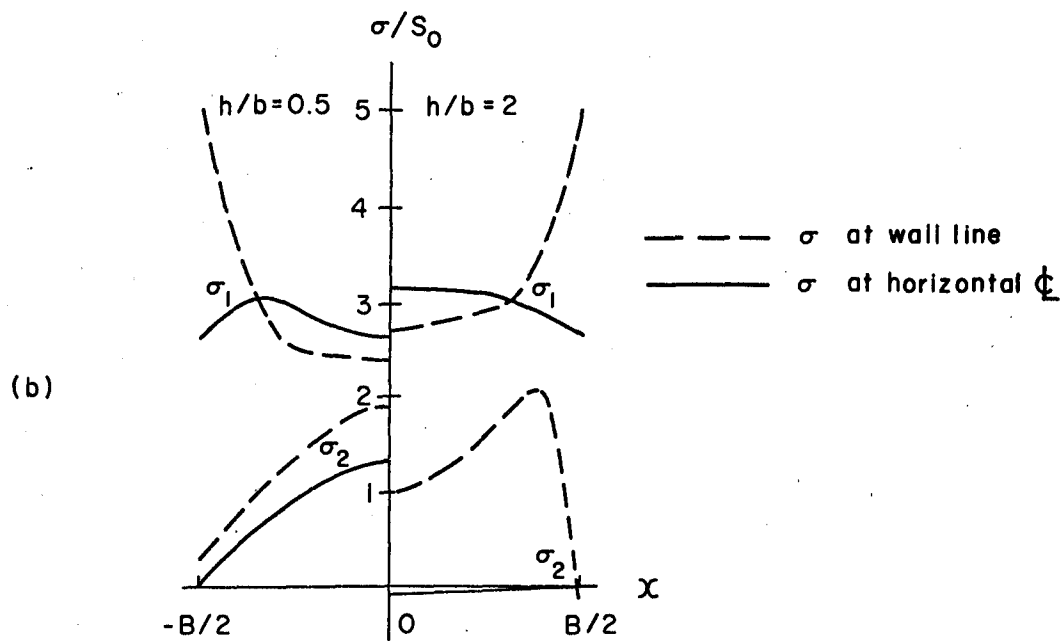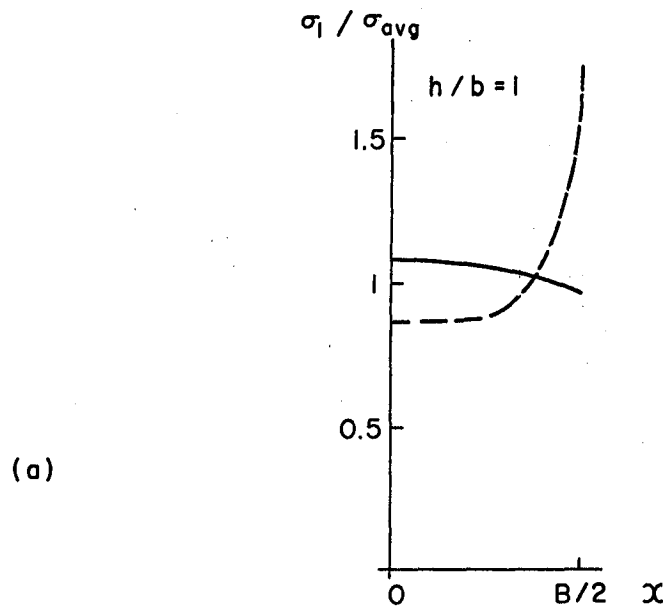
Figure 6.  Stress distributions in pillars, (a) theoretical and
(b) experimental (Ref. 7, 8, 9).

It can be seen in Figure 6(b) that again the variation at the wall line for the two cases is greater than at the horizontal centreline. At the horizontal centreline for the case of height-to-breadth ratio of 0.5, the horizontal stress is a significant amount in the central part of the pillar; however, for the case of height-to-breadth ratio of 2, the horizontal stress at the central section of the pillar is no more than about 3 per cent of the vertical stress.

In Figure 7, the results of experimental determinations in a steel plate 1 in. x 1 in. x 1/4 in. are shown (3). Again the variation of vertical stress at the contact with the walls is large and in close agreement with the theoretical solution. (The curve representing the variation of stress adjacent to the ends of the plate is not equivalent to the full load; it was established that this was the result of the loading conditions in the experiment (3).) Also, these experiments not only showed that the variation at the centreline was small and consistent with the theoretical solution, but, in addition, the results showed that for a distance of 30 per cent of the height of the plate above and below the horizontal centreline this zone of minor variation prevailed. The dotted curve represents the variation of vertical stress at a horizontal section 30 per cent above or below the horizontal centreline.

Recent work using the Moire technique, which shows displacements rather than shear strain, indicates quite clearly the conditions to be expected at the horizontal centreline of a pillar (20). Figure 8, from this work, shows the uniform displacements over the central cross-sections of the pillar.

As a result of the stress distribution that can be expected, based on both theoretical and experimental evidence, the measurement of strain in the central zone of a pillar in a two-dimensional model, and as was done in the steel models, will produce a figure which is closely representative of the average strain in that pillar.

The steel models also provided the advantage, compared to some of the other techniques, of being able to vary the parameter k by loading in different directions and combining the results by superposition. Also, the very important parameter n, the modulus of deformation of the pillars, can be easily varied. Finally, the fabrication of the models is much simpler than any of the other techniques considered.

Construction. Models were constructed for this work out of mild steel plates 12 in. x 12 in. x 0.25 in., as shown in Figure 9. The elastic properties of the steel, as determined by tests, were $E = 30.2 \times 10^6$ psi and $\mu = 0.290$ (see Figure 10).
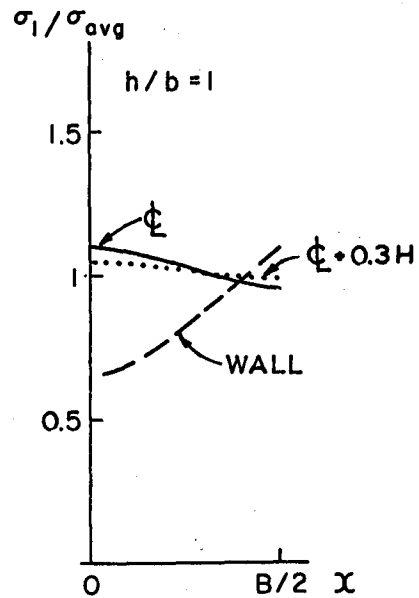
Figure 7. Experimental stress distributions in a plate (Ref. 3).
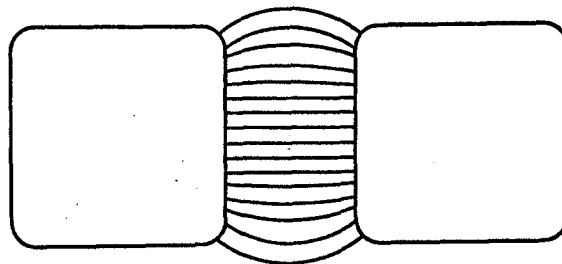


Figure 8. Moire diagram of deflection in a pillar (Ref. 21).
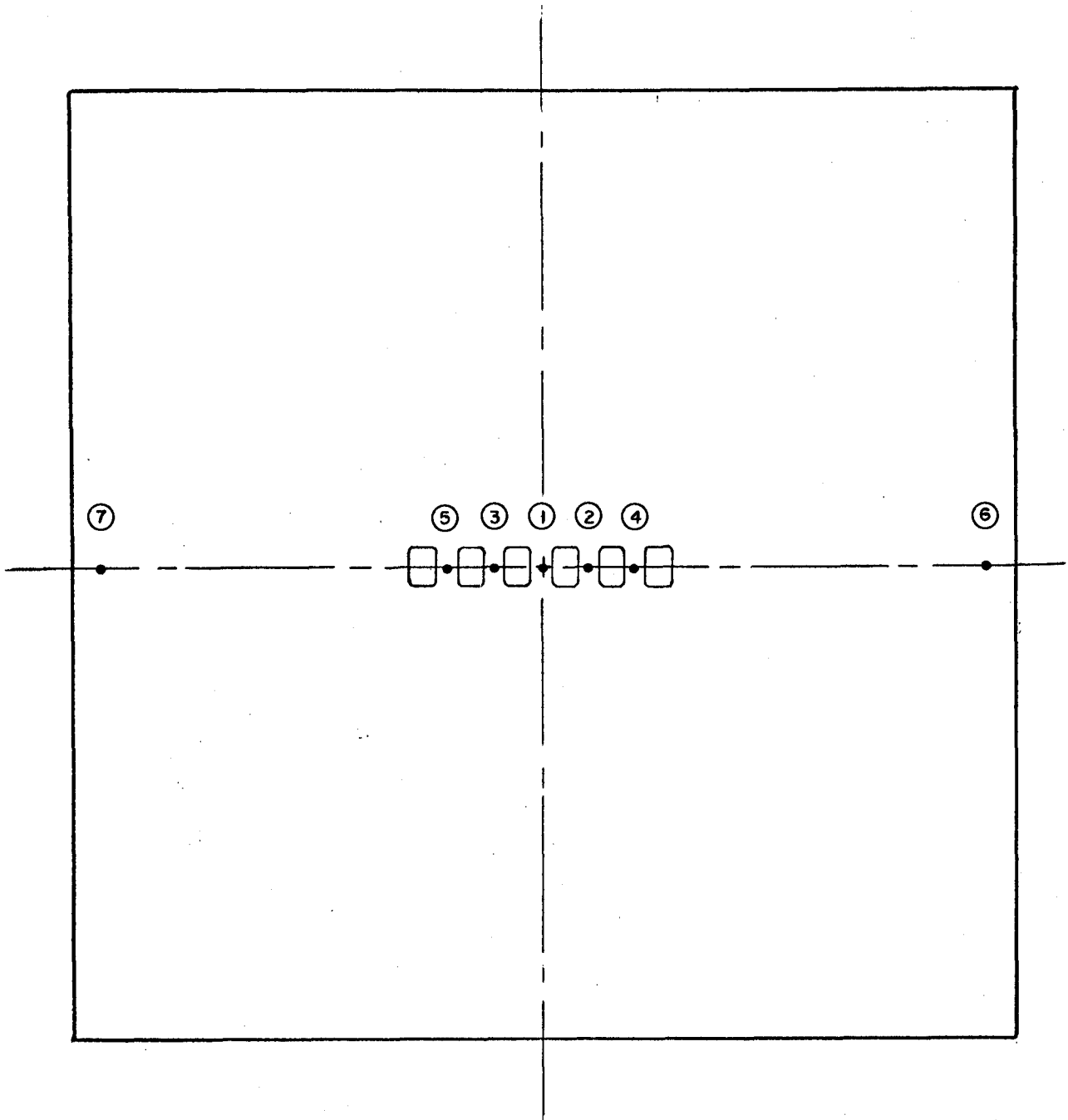
Figure 9.  Typical steel model geometry and gauge positions.
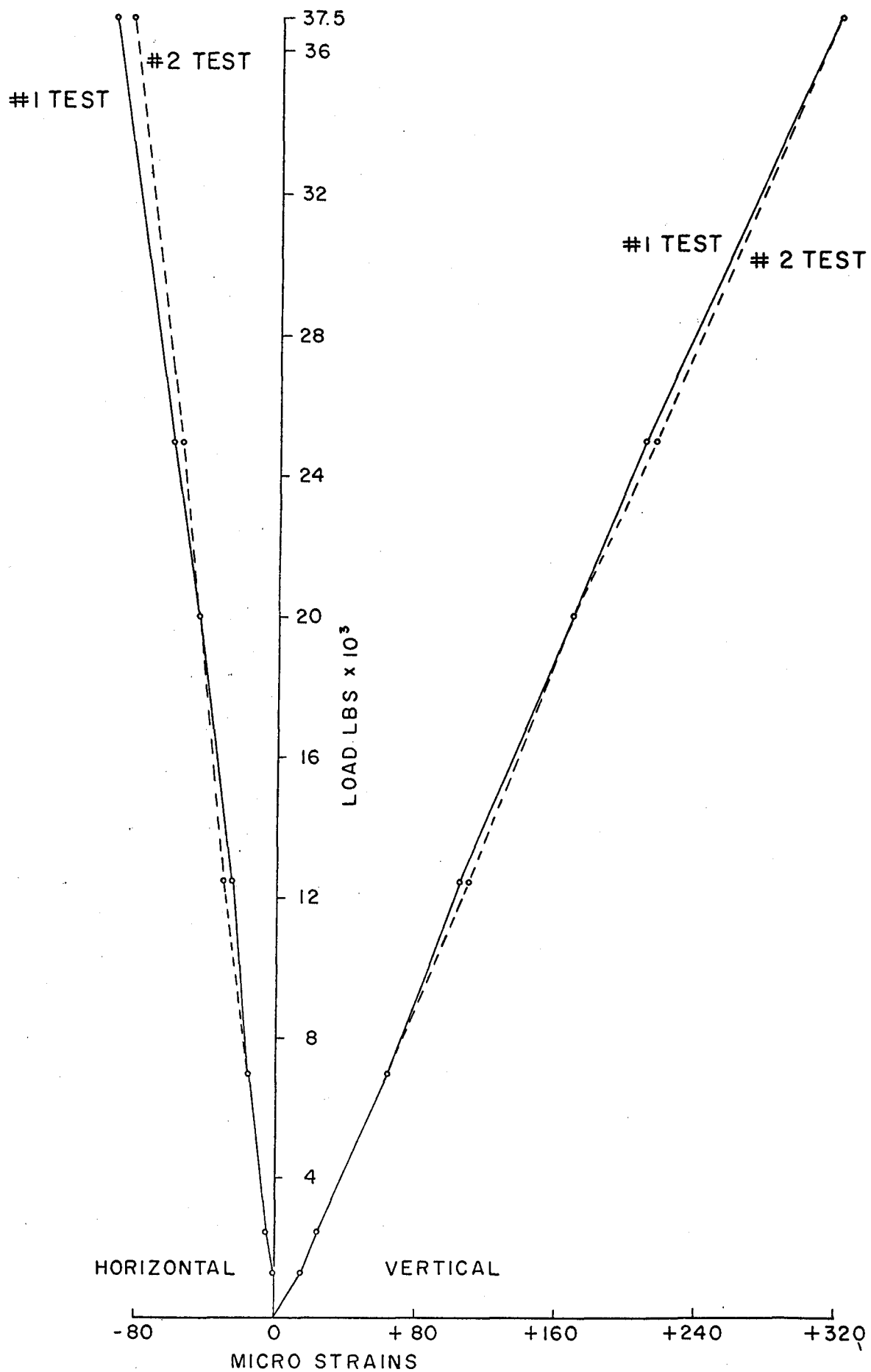
Although a tolerance, in machining the plates, of 0.002 in. was called for, the actual work was generally done to a tolerance of 0.001 in. The various configurations of pillars and openings were designed taking into account the desirability of having the edge distance three times half the span of the mining zone or, in other words, the plate width being four times the entire span of the mining zone, and the cover distance between openings and loaded boundaries being more than 20 times the equivalent radius of the openings.

To simulate the effects of having pillar compressibility greater than that of the wall rocks, plates were constructed with the pillars milled down approximately 0.025 in. on each side for one series of tests (making the pillars approximately 0.200 in. thick rather than equal to the plate's 0.250 in.), and in many cases an additional milling of approximately the same amount further increased the compressibility of the pillars.

To simulate the effects of joints in the roof and floor, or in the wall rocks, cuts were made at the centre of some of the openings in both walls to a depth of approximately 25 per cent of the span of the opening, the maximum depth to which tensile stresses could occur. A special saw was designed, using jeweller's saw blades, so that experiments could be run, both before and after the cuts were made, without removing the strain gauges.

Operation. Biaxial two-element, foil-type strain gauges were used on the majority of the pillars, to measure both longitudinal and transverse strains. On some of the pillars, only single-element, foil-type strain gauges were used to measure longitudinal strain. The experiments using the biaxial gauges indicated that in the majority of cases the effect of the transverse strain on the calculated longitudinal stress was less than 1 per cent.

In addition, single-element strain gauges were placed longitudinally on the horizontal centreline of the mining zone at the outer edge of the plate, to provide a comparison with theory of the distribution of the stresses throughout the plate (22) and on the magnitude of the loading on the plate. The location of these gauges, No. 6 and No. 7, are shown in Figure 9.

Gauges were applied to both sides of each pillar and then connected in series so that an average of the two gauges was obtained directly from the single reading. This compensated for any eccentric loading or slight warping of the plates which might have caused a higher stress on one side than on the other.

To load the plates in the testing machine, two aluminum blocks, 12 in. x 12 in. x 9 in., were used for supports. Attached to these blocks as "spacers" were steel strips 12 in. x 1/4 in. x 1/4 in. at both top and bottom edge of each block. Then a plate of cold-rolled steel 12 in. x 3/4 in. x 3/16 in. was placed on the bottom platen under the model plate and under the two bottom spacers attached to the aluminum blocks. When the two aluminum blocks were brought together, the model plate was held firmly in a vertical position so that a load could be applied or removed without the plate moving. On top of the model plate and under the top platen of the testing machine, a cold-rolled steel bar 12 in. x 2 in. x $1\frac{1}{2}$ in. was placed to transmit the load from the 10-in.-diameter upper platen.

To reduce the friction between the model plate and the loading plates, thereby permitting lateral expansion of the plate as a result of loading, it was found, after experimenting with various alternatives, that two layers of 2 mil teflon ribbon placed under and on top of the model plate permitted the development of a homogeneous uniaxial stress field in the plate.

After the load on the plate was cycled 2 to 3 times, a zero was set on the bridge for the strain gauges. The plate was then loaded up to 20,000 lb and unloaded, obtaining two sets of readings at 1,000, 2,000, 6,000, 10,000, 16,000 and 20,000 lb. The plate was then turned end for end and the same series of readings was taken. The readings were then combined into an average and plotted on the graph, with the slope being the strain produced by a unit load on the plate.

Experimental Results. Table 4 contains the experimental results obtained with these models. Pillar stresses were calculated from the measured longitudinal and transverse strains obtained in the majority of pillars. In some of the pillars, only longitudinal strain was measured, in which case the ratio of transverse strain to longitudinal strain was obtained from the measured results on geometrically similar models. It was found that by including the effect on the calculated longitudinal stress of the transverse strain, the difference was generally less than 1 per cent. In a few cases the differences were as high as 2 per cent.

## TABLE 4

### Experimental Results from Steel Models

z = 6 in., μ = 0.290

| No. | N | R | L in. | H in. | B in. | x | k | J in. | n | i | $\sigma'_p$ |
|---|---|---|---|---|---|---|---|---|---|---|---|
| S-1 | 1 | 0.800 | 2.505 | 0.503 | 0.502 | 0 | 0 | 0 | 1 | 0 | 2.48 |
| S-2 | 1 | 0.800 | 2.505 | 0.503 | 0.502 | 0 | 0 | 0.25 | 1 | 0 | 2.45 |
| S-3 | 1 | 0.800 | 2.505 | 0.503 | 0.502 | 0 | 0 | 0.25 | 1.300 | 0 | 2.28 |
| S-4 | 1 | 0.800 | 2.505 | 0.503 | 0.502 | 0 | 0 | 0.25 | 1.732 | 0 | 2.17 |
| S-5 | 1 | 0.800 | 2.505 | 0.503 | 0.502 | 0 | 1/3 | 0.25 | 1.732 | 0 | 2.14 |
|  |  |  |  |  |  |  | 1 |  |  |  | 2.09 |
|  |  |  |  |  |  |  | 3 |  |  |  | 1.93 |
| S-6 | 1 | 0.800 | 2.503 | 1.004 | 0.502 | 0 | 0 | 0 | 1 | 0 | 2.15 |
| S-7 | 1 | 0.800 | 2.503 | 1.004 | 0.502 | 0 | 1/3 | 0 | 1 | 0 | 2.09 |
|  |  |  |  |  |  |  | 1 |  |  |  | 1.98 |
|  |  |  |  |  |  |  | 3 |  |  |  | 1.65 |
| S-8 | 1 | 0.800 | 2.503 | 1.004 | 0.502 | 0 | 0 | 0 | 1.416 | 0 | 1.92 |
| S-9 | 1 | 0.800 | 2.503 | 1.004 | 0.502 | 0 | 1/3 | 0 | 1.416 | 0 | 1.87 |
|  |  |  |  |  |  |  | 1 |  |  |  | 1.78 |
|  |  |  |  |  |  |  | 3 |  |  |  | 1.51 |
| S-10 | 3 | 0.644 | 3.130 | 0.509 | 0.373 | 0 | 0 | 0 | 1 | 0 | 2.21 |
|  |  |  |  |  | 0.368 | 0.560 |  |  |  |  | 2.16 |
|  |  |  |  |  | 0.361 | 0.560 |  |  |  |  | 2.18 |
| S-11 | 3 | 0.644 | 3.130 | 0.509 | 0.373 | 0 | 0 | 0.25 | 1 | 0 | 2.21 |
|  |  |  |  |  | 0.368 | 0.560 |  |  |  |  | 2.16 |
|  |  |  |  |  | 0.361 | 0.560 |  |  |  |  | 2.17 |
| S-12 | 3 | 0.644 | 3.130 | 0.509 | 0.373 | 0 | 0 | 0.25 | 1.250 | 0 | 2.12 |
|  |  |  |  |  | 0.368 | 0.560 |  |  |  |  | 2.05 |
|  |  |  |  |  | 0.361 | 0.560 |  |  |  |  | 2.06 |
| S-13 | 3 | 0.644 | 3.130 | 0.509 | 0.373 | 0 | 0 | 0.25 | 1.695 | 0 | 1.94 |
|  |  |  |  |  | 0.368 | 0.560 |  |  |  |  | 1.82 |
|  |  |  |  |  | 0.361 | 0.560 |  |  |  |  | 1.85 |
| S-14 | 3 | 0.644 | 3.130 | 0.509 | 0.373 | 0 | 1/3 | 0.25 | 1.250 | 0 | 2.05 |
|  |  |  |  |  |  |  | 1 |  |  |  | 1.92 |
|  |  |  |  |  |  |  | 3 |  |  |  | 1.52 |
|  |  |  |  |  | 0.368 | 0.560 | 1/3 |  |  |  | 1.99 |
|  |  |  |  |  |  |  | 1 |  |  |  | 1.86 |
|  |  |  |  |  |  |  | 3 |  |  |  | 1.48 |
|  |  |  |  |  | 0.361 | 0.560 | 1/3 |  |  |  | 1.96 |
|  |  |  |  |  |  |  | 1 |  |  |  | 1.81 |
|  |  |  |  |  |  |  | 3 |  |  |  | 1.21 |
| S-15 | 3 | 0.644 | 3.130 | 0.509 | 0.373 | 0 | 1/3 | 0.25 | 1.695 | 0 | 1.90 |
|  |  |  |  |  |  |  | 1 |  |  |  | 1.80 |
|  |  |  |  |  |  |  | 3 |  |  |  | 1.51 |
|  |  |  |  |  | 0.368 | 0.560 | 1/3 |  |  |  | 1.76 |
|  |  |  |  |  |  |  | 1 |  |  |  | 1.63 |
|  |  |  |  |  |  |  | 3 |  |  |  | 1.24 |
|  |  |  |  |  | 0.361 | 0.560 | 1/3 |  |  |  | 1.79 |
|  |  |  |  |  |  |  | 1 |  |  |  | 1.68 |
|  |  |  |  |  |  |  | 3 |  |  |  | 1.33 |
| S-17 | 5 | 0.630 | 3.306 | 0.500 | 0.244 | 0 | 0 | 0 | 1 | 0 | 2.19 |
|  |  |  |  |  | 0.244 | 0.357 |  |  |  |  | 2.18 |
|  |  |  |  |  | 0.244 | 0.357 |  |  |  |  | 2.17 |
|  |  |  |  |  | 0.246 | 0.715 |  |  |  |  | 2.11 |
|  |  |  |  |  | 0.245 | 0.715 |  |  |  |  | 2.11 |

(Continued)

TABLE 4 (Continued)

| No. | N | R | L in. | H in. | B in. | x | k | J in. | n | i | $\sigma'_p$ |
|---|---|---|---|---|---|---|---|---|---|---|---|
| S-18 | 5 | 0.630 | 3.306 | 0.500 | 0.244 | 0 | 0 | 0 | 1.262 | 0 | 2.08 |
| | | | | | 0.244 | 0.357 | | | | | 2.01 |
| | | | | | 0.244 | 0.357 | | | | | 1.98 |
| | | | | | 0.246 | 0.715 | | | | | 1.87 |
| | | | | | 0.245 | 0.715 | | | | | 1.87 |
| S-19 | 5 | 0.630 | 3.306 | 0.500 | 0.244 | 0 | 0 | 0 | 1.665 | 0 | 2.06 |
| | | | | | 0.244 | 0.357 | | | | | 2.03 |
| | | | | | 0.244 | 0.357 | | | | | 2.01 |
| | | | | | 0.246 | 0.715 | | | | | 1.86 |
| | | | | | 0.245 | 0.715 | | | | | 1.88 |
| S-20 | 5 | 0.630 | 3.306 | 0.500 | 0.244 | 0 | 0 | 0.10 | 1.665 | 0 | 2.06 |
| | | | | | 0.244 | 0.357 | | | | | 2.03 |
| | | | | | 0.244 | 0.357 | | | | | 2.02 |
| | | | | | 0.246 | 0.715 | | | | | 1.86 |
| | | | | | 0.245 | 0.715 | | | | | 1.87 |
| S-21 | 5 | 0.630 | 3.306 | 0.500 | 0.244 | 0 | 1/3 | 0 | 1.262 | 0 | 2.07 |
| | | | | | | | 1 | | | | 2.06 |
| | | | | | | | 3 | | | | 2.02 |
| | | | | | 0.244 | 0.357 | 1/3 | | | | 2.01 |
| | | | | | | | 1 | | | | 2.01 |
| | | | | | | | 3 | | | | 2.01 |
| | | | | | 0.244 | 0.357 | 1/3 | | | | 1.98 |
| | | | | | | | 1 | | | | 1.98 |
| | | | | | | | 3 | | | | 1.98 |
| | | | | | 0.246 | 0.715 | 1/3 | | | | 1.87 |
| | | | | | | | 1 | | | | 1.86 |
| | | | | | | | 3 | | | | 1.84 |
| | | | | | 0.245 | 0.715 | 1/3 | | | | 1.85 |
| | | | | | | | 1 | | | | 1.82 |
| | | | | | | | 3 | | | | 1.72 |
| S-22 | 5 | 0.630 | 3.306 | 0.500 | 0.244 | 0 | 1/3 | 0 | 1.665 | 0 | 2.06 |
| | | | | | | | 1 | | | | 2.06 |
| | | | | | | | 3 | | | | 2.06 |
| | | | | | 0.244 | 0.357 | 1/3 | | | | 2.03 |
| | | | | | | | 1 | | | | 2.03 |
| | | | | | | | 3 | | | | 2.03 |
| | | | | | 0.244 | 0.357 | 1/3 | | | | 2.01 |
| | | | | | | | 1 | | | | 1.97 |
| | | | | | | | 3 | | | | 1.86 |
| | | | | | 0.246 | 0.715 | 1/3 | | | | 1.84 |
| | | | | | | | 1 | | | | 1.81 |
| | | | | | | | 3 | | | | 1.71 |
| | | | | | 0.245 | 0.715 | 1/3 | | | | 1.86 |
| | | | | | | | 1 | | | | 1.82 |
| | | | | | | | 3 | | | | 1.71 |
| S-23 | 5 | 0.630 | 3.306 | 0.500 | 0.244 | 0 | 1/3 | 0.10 | 1.665 | 0 | 2.05 |
| | | | | | | | 1 | | | | 2.02 |
| | | | | | | | 3 | | | | 1.94 |
| | | | | | 0.244 | 0.357 | 1/3 | | | | 2.02 |
| | | | | | | | 1 | | | | 2.00 |
| | | | | | | | 3 | | | | 1.94 |
| | | | | | 0.244 | 0.357 | 1/3 | | | | 2.00 |
| | | | | | | | 1 | | | | 1.97 |
| | | | | | | | 3 | | | | 1.87 |
| | | | | | 0.246 | 0.715 | 1/3 | | | | 1.84 |
| | | | | | | | 1 | | | | 1.81 |
| | | | | | | | 3 | | | | 1.71 |
| | | | | | 0.245 | 0.715 | 1/3 | | | | 1.84 |
| | | | | | | 0.715 | 1 | | | | 1.79 |
| | | | | | | 0.715 | 3 | | | | 1.63 |

TABLE 4 (Concluded)

| No. | N | R | L in. | H in. | B in. | x | k | J in. | n | i | $\sigma_p'$ |
|---|---|---|---|---|---|---|---|---|---|---|---|
| S-29 | 5 | 0.621 | 3.380 | 0.502 | 0.239 | 0 | 0 | 0 | 1 | 0 | 2.32 |
| | | | | | 0.220 | 0.342 | | | | | 2.33 |
| | | | | | 0.300 | 0.367 | | | | | 2.14 |
| | | | | | 0.302 | 0.705 | | | | | 2.04 |
| | | | | | 0.220 | 0.729 | | | | | 2.22 |
| S-30 | 5 | 0.621 | 3.380 | 0.502 | 0.239 | 0 | 1/3 | 0 | 1 | 0 | 2.30 |
| | | | | | | | 1 | | | | 2.27 |
| | | | | | | | 3 | | | | 2.17 |
| | | | | | 0.220 | 0.342 | 1/3 | | | | 2.31 |
| | | | | | | | 1 | | | | 2.28 |
| | | | | | | | 3 | | | | 2.18 |
| | | | | | 0.300 | 0.367 | 1/3 | | | | 2.11 |
| | | | | | | | 1 | | | | 2.05 |
| | | | | | | | 3 | | | | 1.86 |
| | | | | | 0.302 | 0.705 | 1/3 | | | | 2.01 |
| | | | | | | | 1 | | | | 1.95 |
| | | | | | | | 3 | | | | 1.78 |
| | | | | | 0.220 | 0.729 | 1/3 | | | | 2.18 |
| | | | | | | | 1 | | | | 2.10 |
| | | | | | | | 3 | | | | 1.87 |
| S-31 | 5 | 0.621 | 3.380 | 0.502 | 0.239 | 0 | 0 | 0 | 1.410 | 0 | 2.10 |
| | | | | | 0.220 | 0.342 | | | | | 2.06 |
| | | | | | 0.300 | 0.367 | | | | | 1.91 |
| | | | | | 0.302 | 0.705 | | | | | 1.76 |
| | | | | | 0.220 | 0.729 | | | | | 1.89 |

## COMPARISON WITH HYPOTHESIS

### Analysis of Data for $f(x)$

The experimental results are analysed to determine whether the tributary area theory or the new hypothesis provides satisfactory explanations of the absolute values and their change with the various parameters.

Figures 11 to 18 show clearly that pillar loading varies with x. As the tributary area theory (TA) does not contain the parameter x --in other words, it predicts equal loading regardless of position--it can be set aside on that basis. It remains, then, to compare the variation of x obtained experimentally with that predicted by the hypothesis (HYP).

Because the determination of pillar loadings is a multivariable problem, it is not easy to isolate each variable to examine its functional relations. From the hypothesis that has been established, this problem can be seen in the general form as follows:

$$\Delta \sigma_p = \frac{C_1 f(x) + C_2}{C_3 + C_4 (1 + C_5/f(x)) + C_6} ,$$

where each of the C's is an independent parameter.

One way of analysing the experimental data is to determine the pillar loading that was measured in an experiment and then to compare this with the calculated pillar loading for that case, using the hypothesis. Such calculations are included in Tables 5 to 7.

Figures 11 to 15 show the results of the comparison of the experimental variation of loading with x to that predicted by the hypothesis. It is judged in these cases that the experimental results do not include any obvious anomalies. Figures 16 to 18, on the other hand, show results that clearly contain experimental errors. Not knowing but seeking the correct f(x) makes it difficult to separate all of these cases--hence the use of the scatter diagram and curve fitting influenced by judgment.

A scatter diagram is plotted in Figure 19 of the ratio of the experimental values to the hypothesis values of pillar loading versus x, the distance from the centreline of the mining area. The results of model series A, B, T, V and S have been used in this figure. Model series C and D are too strongly dependent on the varying pillar breadths to be usefully included in this examination. Series E, F and U have only one pillar and hence do not include x as a variable.

$$\frac{\Delta \sigma_p(x)}{\Delta \sigma_p(0)}$$

TA

T — 5

HYP

x

$$\frac{\Delta \sigma_p(x)}{\Delta \sigma_p(0)}$$

TA

T — 6

HYP

x
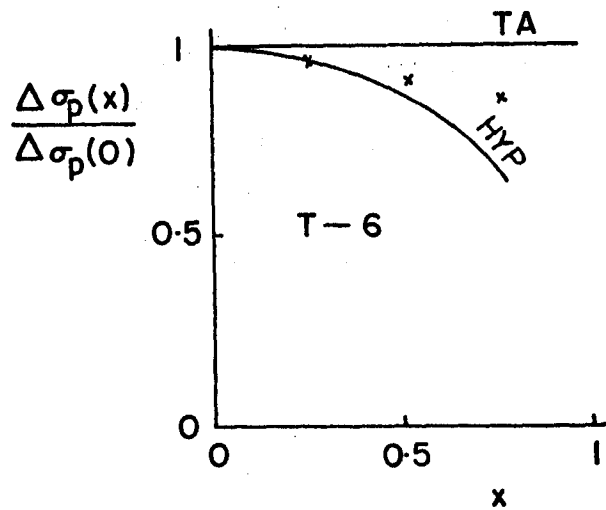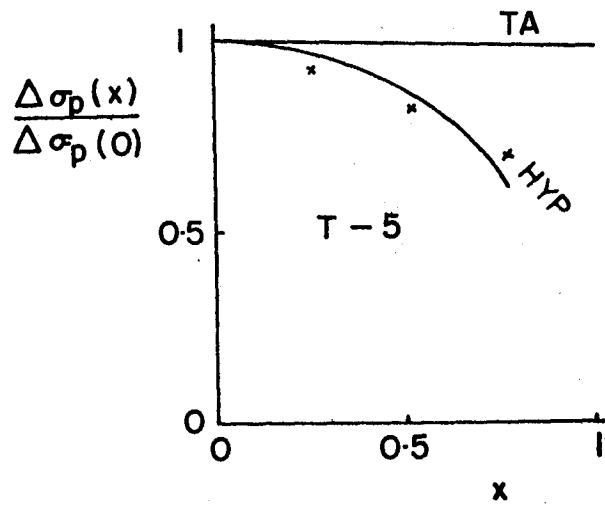
TA = tributary area theory prediction

HYP = new hypothesis prediction

Figure 11.  Variation of pillar loading with x.
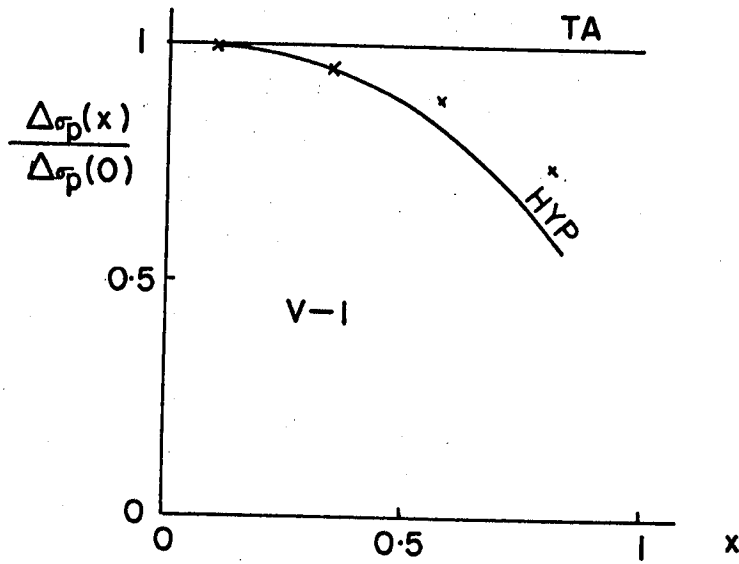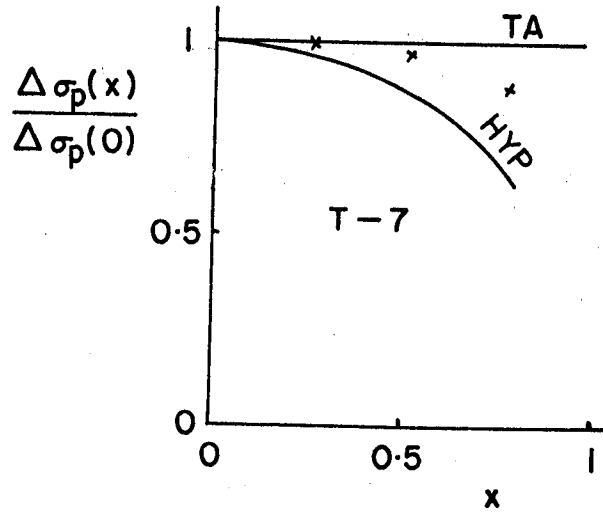
Figure 12. Variation of pillar loading with x.
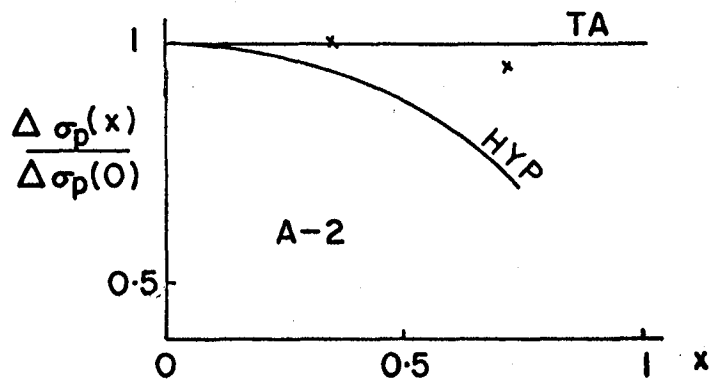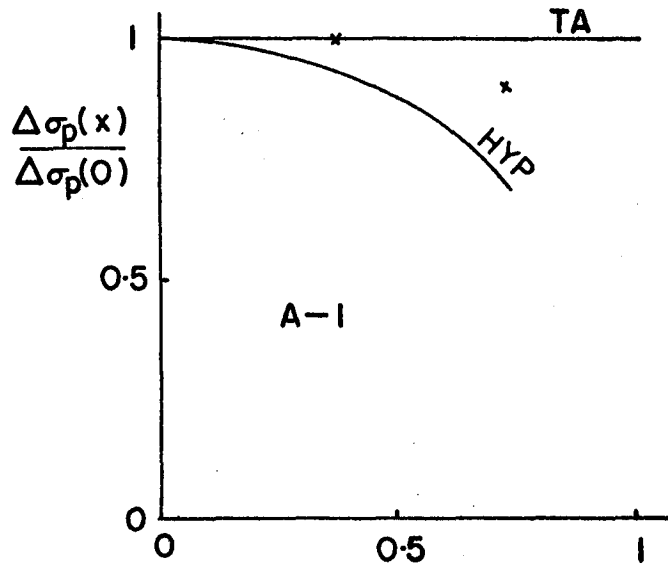
Figure 13. Variation of pillar loading with x.
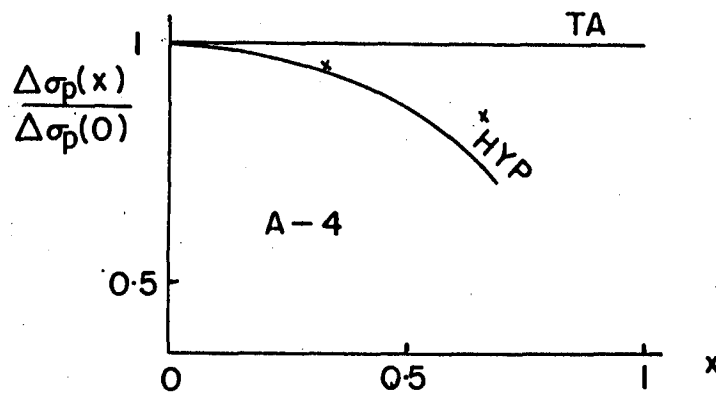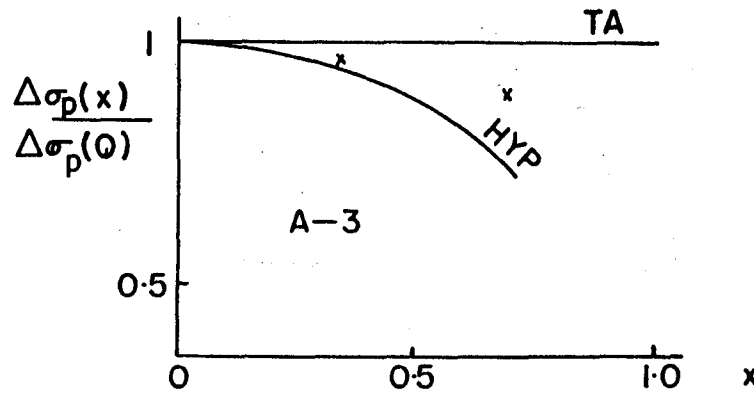
Figure 14. Variation of pillar loading with x.
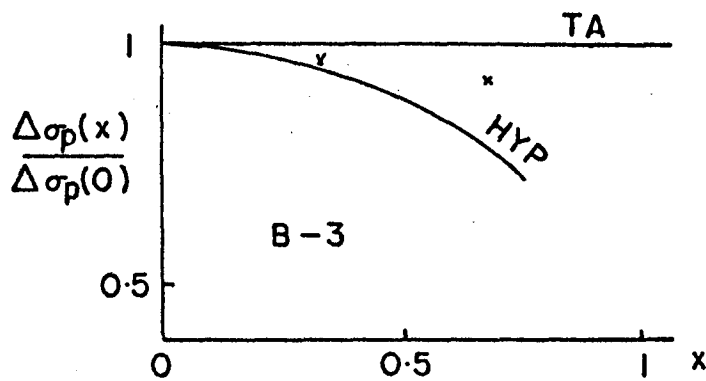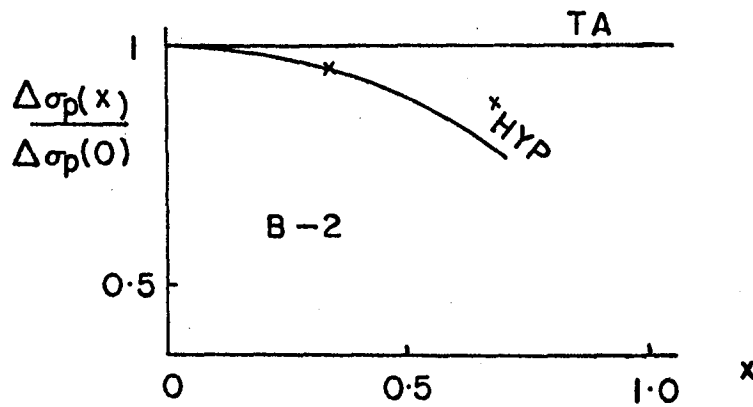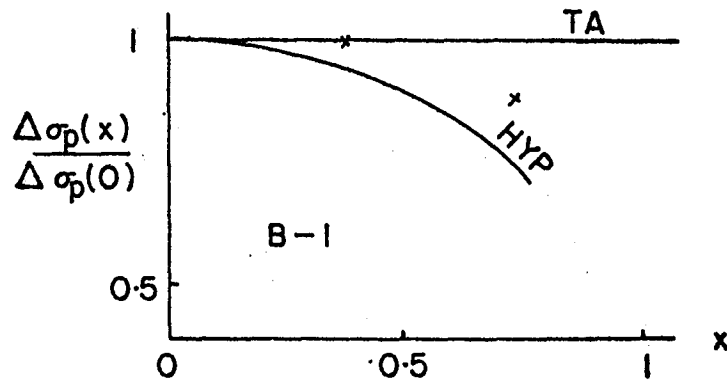
Figure 15. Variation of pillar loading with x.
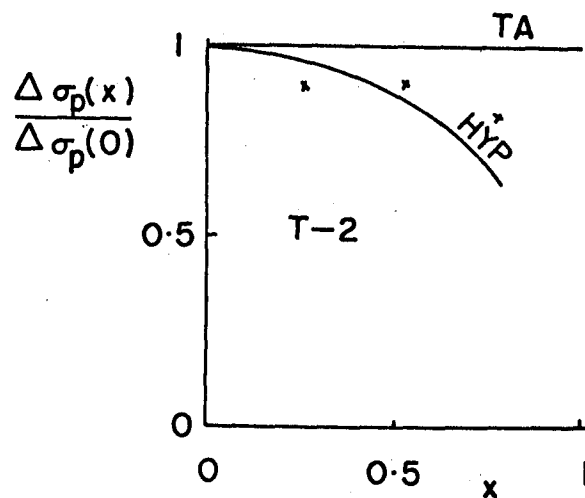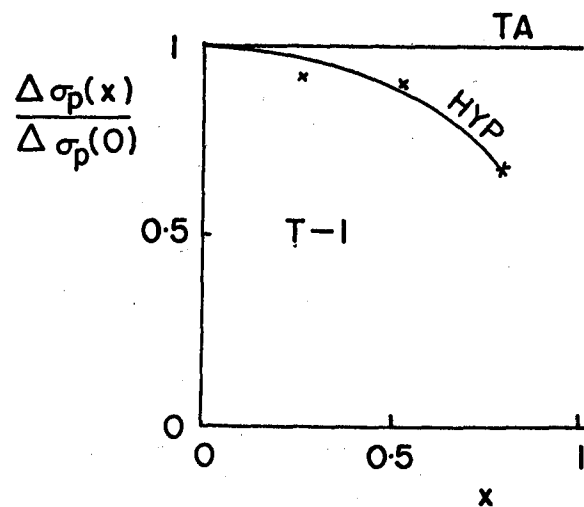
Figure 16.  Variation of pillar loading with x.
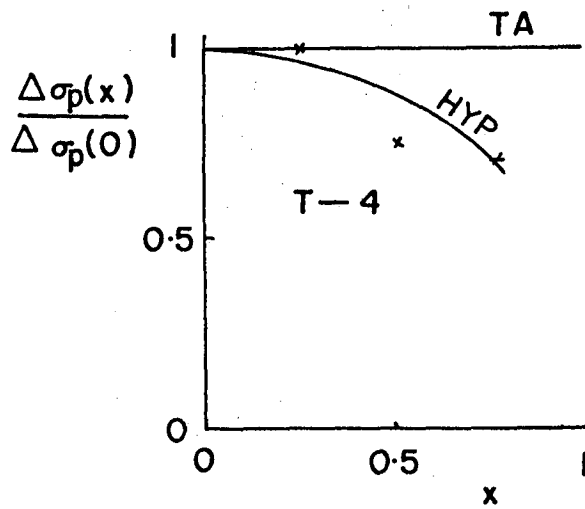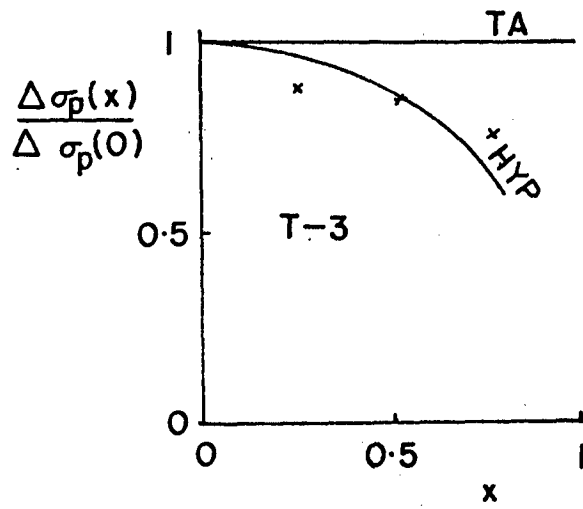
Figure 17.  Variation of pillar loading with x.
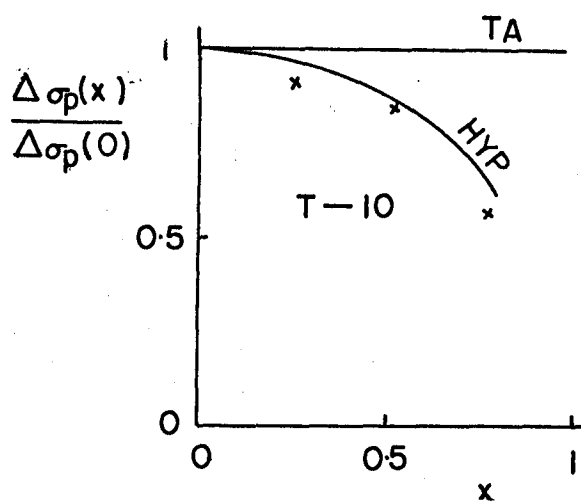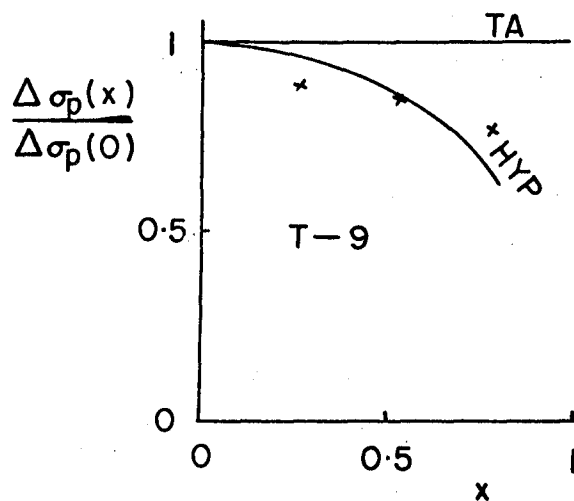
Figure 18. Variation of pillar loading with x.

## TABLE 5

### Analysis of Data from Gelatin Models for f(x)

$k = 0.5$, $\mu = 0.5$, $n = 1$

| No. | R | h | b | x | $\Delta\sigma_p{}'$ EXPT | $\Delta\sigma_p{}'$ TA | $\dfrac{\Delta\sigma_p(x)}{\Delta\sigma_p(0)}$ EXPT | $\dfrac{\Delta\sigma_p(x)}{\Delta\sigma_p(0)}$ HYP |
|---|---|---|---|---|---|---|---|---|
| T-1 | 0.604 | 0.226 | 0.057 | 0 | 1.12 | 1.33 | 1 | 1 |
| | | | | 0.264 | 1.03 | 1.33 | 0.92 | 0.96 |
| | | | | 0.528 | 1.00 | 1.33 | 0.89 | 0.87 |
| | | | | 0.792 | 0.75 | 1.33 | 0.67 | 0.67 |
| T-2 | 0.656 | 0.197 | 0.049 | 0 | 1.35 | 1.67 | 1 | 1 |
| | | | | 0.262 | 1.22 | 1.67 | 0.90 | 0.96 |
| | | | | 0.525 | 1.22 | 1.67 | 0.90 | 0.85 |
| | | | | 0.787 | 1.11 | 1.67 | 0.82 | 0.65 |
| T-3 | 0.696 | 0.174 | 0.043 | 0 | 1.77 | 2.00 | 1 | 1 |
| | | | | 0.261 | 1.56 | 2.00 | 0.88 | 0.97 |
| | | | | 0.522 | 1.51 | 2.00 | 0.85 | 0.85 |
| | | | | 0.783 | 1.35 | 2.00 | 0.76 | 0.62 |
| T-4 | 0.728 | 0.156 | 0.039 | 0 | 2.06 | 2.34 | 1 | 1 |
| | | | | 0.260 | 2.06 | 2.34 | 1 | 0.97 |
| | | | | 0.520 | 1.56 | 2.34 | 0.76 | 0.86 |
| | | | | 0.780 | 1.36 | 2.34 | 0.66 | 0.63 |
| T-5 | 0.753 | 0.141 | 0.035 | 0 | 2.17 | 2.87 | 1 | 1 |
| | | | | 0.259 | 2.00 | 2.87 | 0.92 | 0.97 |
| | | | | 0.518 | 1.78 | 2.87 | 0.82 | 0.86 |
| | | | | 0.777 | 1.52 | 2.87 | 0.70 | 0.63 |
| T-6 | 0.696 | 0.087 | 0.043 | 0 | 1.61 | 2.00 | 1 | 1 |
| | | | | 0.261 | 1.55 | 2.00 | 0.96 | 0.96 |
| | | | | 0.522 | 1.46 | 2.00 | 0.91 | 0.86 |
| | | | | 0.783 | 1.38 | 2.00 | 0.86 | 0.64 |
| T-7 | 0.696 | 0.130 | 0.043 | 0 | 1.56 | 2.00 | 1 | 1 |
| | | | | 0.261 | 1.56 | 2.00 | 1 | 0.96 |
| | | | | 0.522 | 1.51 | 2.00 | 0.97 | 0.86 |
| | | | | 0.783 | 1.38 | 2.00 | 0.88 | 0.64 |
| T-9 | 0.696 | 0.232 | 0.043 | 0 | 1.78 | 2.00 | 1 | 1 |
| | | | | 0.261 | 1.56 | 2.00 | 0.88 | 0.96 |
| | | | | 0.522 | 1.51 | 2.00 | 0.85 | 0.86 |
| | | | | 0.783 | 1.38 | 2.00 | 0.77 | 0.64 |
| T-10 | 0.696 | 0.290 | 0.043 | 0 | 1.72 | 2.00 | 1 | 1 |
| | | | | 0.261 | 1.55 | 2.00 | 0.90 | 0.97 |
| | | | | 0.522 | 1.43 | 2.00 | 0.83 | 0.86 |
| | | | | 0.783 | 0.94 | 2.00 | 0.55 | 0.63 |
| V-1 | 0.600 | 0.200 | 0.050 | 0.117 | 1.03 | 1.33 | 0.99 | 0.99 |
| | | | | 0.350 | 0.97 | 1.33 | 0.94 | 0.94 |
| | | | | 0.584 | 0.91 | 1.33 | 0.88 | 0.82 |
| | | | | 0.817 | 0.74 | 1.33 | 0.72 | 0.59 |

## TABLE 6

### Analysis of Data from Araldite Models for f(x)

$k = 0, \ \mu = 0.435, \ n = 1$

| No. | R | h | b | x | $\sigma_p'$ EXPT | $\sigma_p'$ TA | $\dfrac{\sigma_p(x)}{\sigma_p(0)}$ EXPT | $\dfrac{\sigma_p(x)}{\sigma_p(0)}$ HYP |
|---|---|---|---|---|---|---|---|---|
| A-1 | 0.545 | 0.091 | 0.091 | .0 | 2.0 | 2.0 | 1 | 1 |
|  |  |  |  | 0.364 | 2.0 | 2.0 | 1 | 0.93 |
|  |  |  |  | 0.726 | 1.9 | 2.0 | 0.95 | 0.69 |
| A-2 | 0.675 | 0.112 | 0.065 | 0 | 2.6 | 2.73 | 1 | 1 |
|  |  |  |  | 0.355 | 2.6 | 2.73 | 1 | 0.94 |
|  |  |  |  | 0.711 | 2.5 | 2.73 | 0.96 | 0.72 |
| A-3 | 0.798 | 0.133 | 0.040 | 0 | 3.8 | 4.19 | 1 | 1 |
|  |  |  |  | 0.348 | 3.7 | 4.19 | 0.97 | 0.96 |
|  |  |  |  | 0.695 | 3.5 | 4.19 | 0.92 | 0.74 |
| A-4 | 0.915 | 0.152 | 0.017 | 0 | 7.7 | 9.96 | 1 | 1 |
|  |  |  |  | 0.339 | 7.4 | 9.96 | 0.96 | 0.95 |
|  |  |  |  | 0.678 | 6.7 | 9.96 | 0.87 | 0.77 |
| B-1 | 0.545 | 0.182 | 0.091 | 0 | 1.9 | 2.0 | 1 | 1 |
|  |  |  |  | 0.364 | 1.9 | 2.0 | 1 | 0.93 |
|  |  |  |  | 0.726 | 1.8 | 2.0 | 0.95 | 0.70 |
| B-2 | 0.828 | 0.276 | 0.034 | 0 | 3.6 | 5.0 | 1 | 1 |
|  |  |  |  | 0.345 | 3.5 | 5.0 | 0.97 | 0.95 |
|  |  |  |  | 0.690 | 3.3 | 5.0 | 0.92 | 0.75 |
| B-3 | 0.873 | 0.291 | 0.026 | 0 | 4.1 | 6.72 | 1 | 1 |
|  |  |  |  | 0.342 | 4.0 | 6.72 | 0.98 | 0.95 |
|  |  |  |  | 0.684 | 3.9 | 6.72 | 0.95 | 0.76 |

## TABLE 7

### Analysis of Data from Steel Models for f(x)

$$k = 0, \quad \mu = 0.290$$

| No. | R | h | b | x | n | $\sigma_p'$ EXPT | $\sigma_p'$ TA | $\dfrac{\sigma_p(x)}{\sigma_p(0)}$ EXPT | $\dfrac{\sigma_p(x)}{\sigma_p(0)}$ HYP |
|---|---|---|---|---|---|---|---|---|---|
| S-10 | 0.644 | 0.162 | 0.119 | 0 | 1 | 2.21 | 2.36 | 1 | 1 |
| | | | 0.118 | 0.560 | 1 | 2.15 | 2.36 | 0.97 | 0.83 |
| | | | 0.115 | 0.560 | 1 | 2.18 | 2.36 | 0.99 | 0.83 |
| S-11 | 0.644 | 0.162 | 0.119 | 0 | 1 | 2.24 | 2.36 | 1 | 1 |
| | | | 0.118 | 0.560 | 1 | 2.19 | 2.36 | 0.98 | 0.83 |
| | | | 0.115 | 0 | 1 | 2.22 | 2.36 | 0.99 | 0.83 |
| S-12 | 0.644 | 0.162 | 0.119 | 0 | 1.250 | 2.06 | 2.36 | 1 | 1 |
| | | | 0.118 | 0.560 | 1.250 | 1.99 | 2.36 | 0.97 | 0.83 |
| | | | 0.115 | 0.560 | 1.250 | 2.03 | 2.36 | 0.99 | 0.83 |
| S-13 | 0.644 | 0.162 | 0.119 | 0 | 1.695 | 1.97 | 2.36 | 1 | 1 |
| | | | 0.118 | 0.560 | 1.695 | 1.88 | 2.36 | 0.95 | 0.83 |
| | | | 0.115 | 0.560 | 1.695 | 1.86 | 2.36 | 0.94 | 0.83 |
| S-17 | 0.630 | 0.151 | 0.074 | 0 | 1 | 2.19 | 3.33 | 1 | 1 |
| | | | | 0.357 | 1 | 2.18 | 3.33 | 0.995 | 0.94 |
| | | | | 0.357 | 1 | 2.17 | 3.33 | 0.99 | 0.94 |
| | | | | 0.715 | 1 | 2.11 | 3.33 | 0.96 | 0.705 |
| | | | | 0.715 | 1 | 2.11 | 3.33 | 0.96 | 0.705 |
| S-18 | 0.630 | 0.151 | 0.074 | 0 | 1.262 | 2.08 | 3.33 | 1 | 1 |
| | | | | 0.357 | 1.262 | 2.03 | 3.33 | 0.98 | 0.94 |
| | | | | 0.357 | 1.262 | 1.98 | 3.33 | 0.95 | 0.94 |
| | | | | 0.715 | 1.262 | 1.89 | 3.33 | 0.91 | 0.71 |
| | | | | 0.715 | 1.262 | 1.86 | 3.33 | 0.895 | 0.71 |
| S-19 | 0.630 | 0.151 | 0.074 | 0 | 1.665 | 2.07 | 3.33 | 1 | 1 |
| | | | | 0.357 | 1.665 | 2.04 | 3.33 | 0.99 | 0.93 |
| | | | | 0.357 | 1.665 | 2.02 | 3.33 | 0.98 | 0.93 |
| | | | | 0.715 | 1.665 | 1.86 | 3.33 | 0.90 | 0.71 |
| | | | | 0.715 | 1.665 | 1.89 | 3.33 | 0.91 | 0.71 |
| S-20 | 0.630 | 0.151 | 0.074 | 0 | 1.665 | 2.06 | 3.33 | 1 | 1 |
| | | | | 0.357 | 1.665 | 2.03 | 3.33 | 0.99 | 0.93 |
| | | | | 0.357 | 1.665 | 2.02 | 3.33 | 0.98 | 0.93 |
| | | | | 0.715 | 1.665 | 1.86 | 3.33 | 0.90 | 0.71 |
| | | | | 0.715 | 1.665 | 1.87 | 3.33 | 0.90 | 0.71 |
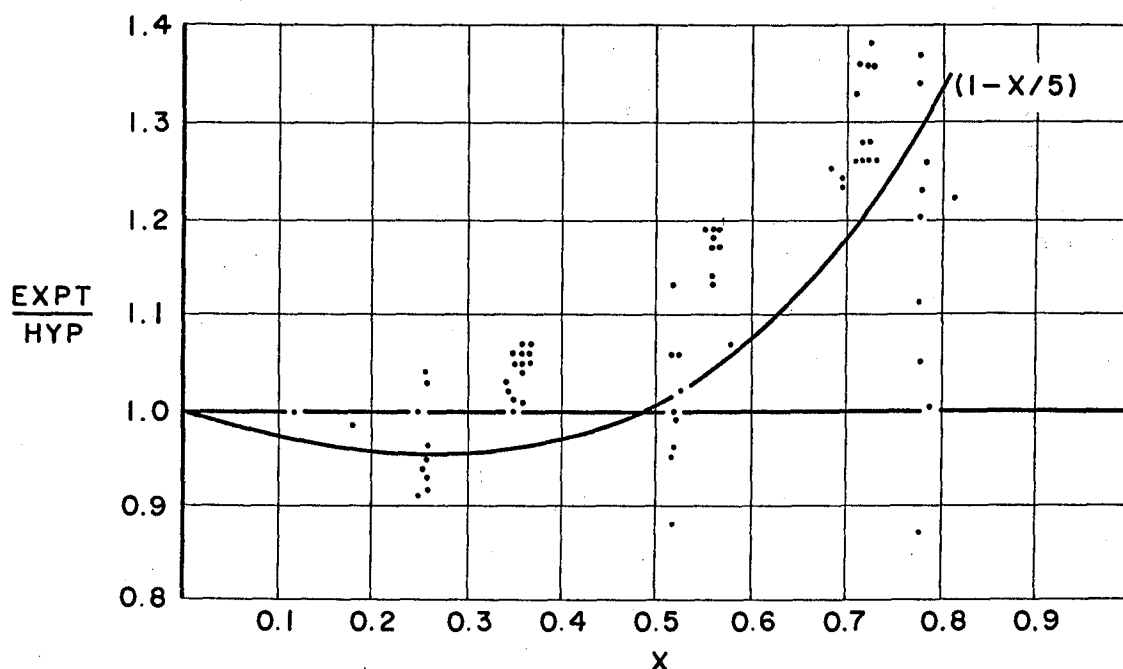
Figure 19. Scatter diagram of variation of pillar loading with x.

The function of x included in the hypothesis, as can be seen from the scatter diagram, is too strong when compared with the experimental data. Also, from an examination of Figures 16 to 18, the points representing experiments T-1, T-2, T-3, T-9 and T-10 at x approximately equal to 0.26, the points for T-4 at x = 0.520, and the points for T-10 at x = 0.783, are obviously all in error. These observations have influenced the judgment exercised in fitting a curve to the experimental data.

It seems probable that the function included in the hypothesis is correct for deflection but does not include all the significant factors connected with room-and-pillar geometry. For example, some of the experimental data show that the stress concentration on the sides of the pillars closest to the centreline of the mining area is greater than on the sides away from the centreline (see Figure 3). This is consistent with the concept of the pillar loading mechanism being the deflection of the roof or walls of the mining zone. However, the hypothesis does not take into account this eccentric loading condition. It is conceivable that the moment resistance of the pillars to this eccentric loading condition modifies the deflection curve of the walls of the mining zone, which in turn means that f(x) will be modified. Consequently, of all the various types of curves that might be fitted to the experimental data, the use of the same type of curve as included in f(x) is likely to provide the best fit.

To generalize the nature of $f(x)$, the function used in the hypothesis can be expanded in a binomial series as follows:

$$(1 - x^2)^{\frac{1}{2}} = 1 - x^2/2 - x^4/2^3 - x^6/2^4 - \ldots$$

For simplicity, a generalized form is used:

$$f(x) = 1 - x^s/t,$$

where s and t are constants.

Taking into account the utility that would result from having a function where the constants s and t are integers, several curves were tried on the scatter diagram. In addition, the selection of the best $f(x)$ has been influenced by some deflection measurements, shown in Table 8, which indicate a linear variation of deflection with x (23). Of the various curves that were tried it can be seen in Figure 19 that a good fit is obtained with the function $(1 - x/5)$.

Because there are recognizable mechanisms that have not been included in the hypothesis which could modify the variation of pillar loading with x, the function $f(x) = (1 - x/5)$, based on the empirical data, is used in the hypothesis. This will change Equation 1 (see page 1) to:

$$\frac{\Delta \sigma_p}{S_o} = \frac{(2R - kh(1-w))(1-x/5+h) - w_p khn}{hn + 1.8(1-R)(1+1/N)(1+h/(1-x/5)) + 2Rb(1-w)/\pi} . \qquad \text{Eq. 4}$$

Equation 2 (see page 1) will change to:

$$\frac{\Delta \sigma_p}{S_o} = \frac{(2R - kh(1-w))(1-x/5+2h) + RK_b' - 2w_p khn}{2hn + (1.8(1+h/(1-x/5)) + (2K_b'/3)(1+h/(1-x^2)))(1-R)(1+1/N) + 4Rb(1-w)/\pi}$$

$$\text{Eq. 5}$$

The model Equation 3 (see page 8) will change to:

$$\frac{\sigma_p}{S_o} = \frac{(2 + h - kh)(1-x/5+h)}{hn + 1.8(1-R)(1+R/(1+N-R))(1+h/(1-x/5)) + 2Rb(1-\mu)/\pi}$$

$$\text{Eq. 6}$$

TABLE 8

## Deflection Measurements from a Lead Mine (23)

H = 10-12 ft, L = 75 ft, z = 200-500 ft, E < 5 x 10$^6$ psi

| x | $\delta$ in. | $\delta_x/\delta_{\mathfrak{C}}$ |
|---|---|---|
| 0 | 0.15 | 1 |
| 0.25 | 0.12 | 0.83 |
| 0.5 | 0.07 | 0.54 |
| 0.75 | 0.03 | 0.30 |

## Analysis of Data for f(z)

It was shown above, in analysing the case of shallow mining zones, that when $z/l$ is less than 2, or $z/L$ is less than 1, Equation 2 theoretically should give a more accurate prediction of pillar loading than Equation 1. Needless to say, the tributary area theory makes no distinction for cases with different ratios of $z/L$. In Tables 9 and 10 the cases are analysed where $z/l$ varies between 0.85 and 1.97. These results are from model series A, B, and T. Model series C and D could not be usefully included in this analysis, in view of the variations due to different pillar breadths. Series E, F and S have sufficient cover to be clearly cases of deep mining zones. Model series I has not been used, inasmuch as the techniques produced data that have value only in studying the comparative effects of barrier pillars.

In Figure 20 a scatter diagram has been plotted of the parameter $z/l$ against the ratio of experimental to calculated values, using the modified hypothesis for deep mining zones as represented by Equations 4 and 6. The experimental loading as a ratio of the normal field stress should increase with a decrease in $z/l$. The scatter diagram should therefore indicate where the mechanics of a shallow mining zone govern the pillar loadings, by showing an increase in the ratio of experimental to hypothesis values for deep mining zones as $z/l$ decreases.

From the scatter diagram, it can be seen that the hypothesis for deep mining zones predicts the experimental values quite well down to at least $z/l = 0.86$. For lower values, one experiment indicates that the experimental loadings are starting to become greater than predicted by the analysis for deep mining zones. The wide dispersion of points above $z/l = 1.36$ is due, as can be seen from Tables 9 and 10, entirely to the gelatin models, which indicates that this technique is more difficult to control than that using the Araldite method.

TABLE 9

Analysis of Data from Gelatin Models for $f(z)$

$k = 0.5, \mu = 0.5, n = 1$

| No. | N | R | h | b | z/l | x | $\sigma_p'$ EXPT | $\sigma_p'$ SHAL | $\sigma_p'$ HYP$^x$ |
|-----|---|-----|-----|-----|------|-------|------|------|------|
| T-2 | 7 | 0.656 | 0.197 | 0.049 | 1.97 | 0' | 1.35 | 1.67 | 1.39 |
| | | | | | | 0.262 | 1.22 | 1.52 | 1.36 |
| | | | | | | 0.525 | 1.22 | 1.46 | 1.26 |
| | | | | | | 0.787 | 1.11 | 1.33 | 1.20 |
| T-3 | 7 | 0.696 | 0.174 | 0.043 | 1.74 | 0 | 1.77 | 1.89 | 1.71 |
| | | | | | | 1.261 | 1.56 | 1.82 | 1.61 |
| | | | | | | 0.522 | 1.51 | 1.75 | 1.50 |
| | | | | | | 0.783 | 1.35 | 1.61 | 1.45 |
| T-4 | 7 | 0.728 | 0.156 | 0.039 | 1.56 | 0 | 2.06 | 2.24 | 1.97 |
| | | | | | | 0.260 | 2.06 | 2.17 | 1.87 |
| | | | | | | 0.520 | 1.56 | 2.09 | 1.76 |
| | | | | | | 0.780 | 1.36 | 1.93 | 1.66 |
| T-5 | 7 | 0.753 | 0.141 | 0.035 | 1.41 | 0 | 2.17 | 2.58 | 2.24 |
| | | | | | | 0.259 | 2.00 | 2.51 | 2.13 |
| | | | | | | 0.518 | 1.84 | 2.26 | 2.03 |
| | | | | | | 0.777 | 1.55 | 2.10 | 1.94 |
| T-6 | 7 | 0.696 | 0.087 | 0.043 | 1.74 | 0 | 1.61 | 2.12 | 1.89 |
| | | | | | | 0.261 | 1.55 | 2.06 | 1.79 |
| | | | | | | 0.522 | 1.46 | 1.98 | 1.68 |
| | | | | | | 0.783 | 1.38 | 1.86 | 1.59 |
| T-7 | 7 | 0.696 | 0.130 | 0.043 | 1.74 | 0 | 1.56 | 2.00 | 1.77 |
| | | | | | | 0.261 | 1.56 | 1.94 | 1.69 |
| | | | | | | 0.522 | 1.51 | 1.88 | 1.59 |
| | | | | | | 0.783 | 1.38 | 1.73 | 1.49 |
| T-9 | 7 | 0.096 | 0.232 | 0.043 | 1.74 | 0 | 1.78 | 1.76 | 1.56 |
| | | | | | | 0.261 | 1.56 | 1.71 | 1.48 |
| | | | | | | 0.522 | 1.51 | 1.63 | 1.40 |
| | | | | | | 0.783 | 1.38 | 1.49 | 1.32 |
| T-10 | 7 | 0.696 | 0.290 | 0.043 | 1.74 | 0 | 1.72 | 1.65 | 1.48 |
| | | | | | | 0.261 | 1.55 | 1.60 | 1.40 |
| | | | | | | 0.522 | 1.43 | 1.52 | 1.33 |
| | | | | | | 0.783 | 0.94 | 1.38 | 1.25 |

SHAL = modified hypothesis as included in Equation 5.

HYP$^x$ = modified hypothesis as included in Equation 6.

## TABLE 10

### Analysis of Data from Araldite Models for $f(z)$

$k = 0, \mu = 0.435, n = 1$

| No. | N | R | h | b | $z/l$ | x | $\sigma_p'$ EXPT | $\sigma_p'$ SHAL | $\sigma_p'$ HYP$^x$ |
|-----|---|---|---|---|-------|---|------|------|------|
| A-1 | 5 | 0.545 | 0.091 | 0.091 | 0.91 | 0 | 2.0 | 2.42 | 2.09 |
|     |   |       |       |       |      | 0.364 | 2.0 | 2.33 | 1.94 |
|     |   |       |       |       |      | 0.726 | 1.9 | 2.19 | 1.79 |
| A-2 | 5 | 0.675 | 0.065 | 0.065 | 0.89 | 0 | 2.6 | 3.13 | 2.72 |
|     |   |       |       |       |      | 0.355 | 2.6 | 3.02 | 2.53 |
|     |   |       |       |       |      | 0.711 | 2.5 | 2.82 | 2.35 |
| A-3 | 5 | 0.798 | 0.040 | 0.040 | 0.87 | 0 | 3.8 | 4.62 | 4.02 |
|     |   |       |       |       |      | 0.348 | 3.7 | 4.45 | 3.72 |
|     |   |       |       |       |      | 0.695 | 3.5 | 4.15 | 3.46 |
| A-4 | 5 | 0.915 | 0.017 | 0.017 | 0.85 | 0 | 7.7 | 7.90 | 6.77 |
|     |   |       |       |       |      | 0.339 | 7.4 | 7.67 | 6.34 |
|     |   |       |       |       |      | 0.678 | 6.7 | 7.23 | 5.90 |
| B-1 | 5 | 0.545 | 0.182 | 0.091 | 1.36 | 0 | 1.9 | 2.22 | 2.03 |
|     |   |       |       |       |      | 0.364 | 1.9 | 2.13 | 1.89 |
|     |   |       |       |       |      | 0.726 | 1.8 | 1.95 | 1.75 |
| B-2 | 5 | 0.828 | 0.276 | 0.034 | 1.29 | 0 | 3.6 | 4.13 | 3.89 |
|     |   |       |       |       |      | 0.345 | 3.5 | 3.97 | 3.65 |
|     |   |       |       |       |      | 0.090 | 3.3 | 3.60 | 3.41 |
| B-3 | 5 | 0.873 | 0.291 | 0.026 | 1.28 | 0 | 4.1 | 4.81 | 4.56 |
|     |   |       |       |       |      | 0.342 | 4.0 | 4.62 | 4.27 |
|     |   |       |       |       |      | 0.684 | 3.9 | 4.10 | 3.99 |

SHAL = modified hypothesis as included in Equation 5.

HYP$^x$ = modified hypothesis as included in Equation 6.
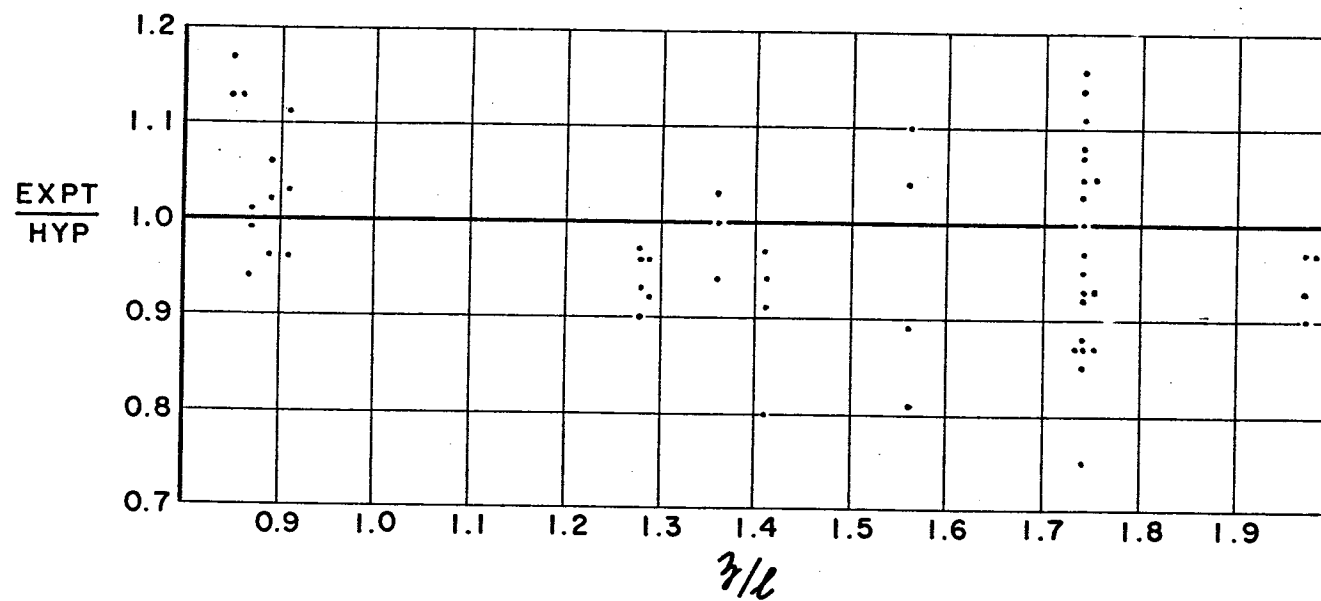
Figure 20. Scatter diagram of variation of pillar loading with z/ℓ.

In Table 12, where Equation 5 is used for model A-4, the analysis for a shallow mining zone predicts more closely the experimental values than does the equation for the deep mining zone. For values of $z/l$ lower than this case, presumably the comparison with the shallow case would be increasingly valid. However, if this is the range of values of $z/l$ for which the analysis of the shallow mining zone is applicable, it is even narrower than was indicated by the original theory. Consequently, the usefulness of the hypothesis for shallow mining zones seems to be rather limited.

## Analysis of Data for f(b)

In Table 11 the data obtained from the gelatin models, model series T and V, are analysed with respect to the tributary area theory and with respect to the modified hypothesis as expressed by Equation 5. It can be seen immediately that the tributary area theory predicts in all cases pillar loadings greater than are actually obtained. The modified hypothesis is in much closer agreement with the experimental data. It might be noted that the edge distances to the sides are much less than the desirable three times the half span for models T-1 to T-10.

Table 12 contains the results of analyses of the data from the Araldite-type models, series A, B, C, D, E, F and U, using the tributary area theory and the modified hypothesis as expressed by Equations 5 and 6. As for the gelatin experiments, all of the computed values of pillar loading by the tributary area theory exceed the experimental values, whereas those using the modified hypothesis produce very good agreement for the cases of equal pillar breadths. The majority of these models (series A, B, C, and D) had edge distances less than three times the half-span.

In Table 13 the results of the analysis of the data from the mortar models, series I and T, are presented. The experimental results are much less than the values obtained with the tributary area theory. In addition, the experimental results for the I-series of experiments are much less than those predicted by the modified hypothesis. This probably arises from the method of measuring the pillar loading which permitted some extra and non-representative deflection of the pillar. Models I-4 to I-9 were conducted on three identical cases with the exception of the modulus of deformation of the mortar. From the results it seems that the deformability of the ground did not affect the magnitudes of the pillar loads. This is consistent with the observation that E cancels out in the derivation of the hypothesis when the deformability of the pillars is the same as that of the wall rocks.

## TABLE 11

### Analysis of Data from Gelatin Models for f(b, h, N, R)

$k = 0.5, \; \mu = 0.5, \; n = 1$

| No. | N | R | h | b | x | $\Delta\sigma_p{'}$ EXPT | $\Delta\sigma_p{'}$ TA | $\Delta\sigma_p{'}$ HYP[x] |
|-----|---|---|---|---|---|------|----|------|
| T-1 | 7 | 0.604 | 0.226 | 0.057 | 0 | 1.12 | 1.33 | 1.10 |
| | | | | | 0.264 | 1.03 | 1.33 | 1.05 |
| | | | | | 0.528 | 1.00 | 1.33 | 0.99 |
| | | | | | 0.792 | 0.75 | 1.33 | 0.93 |
| T-2 | 7 | 0.656 | 0.197 | 0.049 | 0 | 1.35 | 1.67 | 1.39 |
| | | | | | 0.262 | 1.22 | 1.67 | 1.36 |
| | | | | | 0.525 | 1.22 | 1.67 | 1.26 |
| | | | | | 0.787 | 1.11 | 1.67 | 1.20 |
| T-3 | 7 | 0.696 | 0.174 | 0.043 | 0 | 1.77 | 2.00 | 1.71 |
| | | | | | 0.261 | 1.56 | 2.00 | 1.61 |
| | | | | | 0.522 | 1.51 | 2.00 | 1.50 |
| | | | | | 0.783 | 1.35 | 2.00 | 1.45 |
| T-4 | 7 | 0.728 | 0.156 | 0.039 | 0 | 2.06 | 2.34 | 1.97 |
| | | | | | 0.260 | 2.06 | 2.34 | 1.87 |
| | | | | | 0.520 | 1.56 | 2.34 | 1.76 |
| | | | | | 0.780 | 1.36 | 2.34 | 1.66 |
| T-5 | 7 | 0.753 | 0.141 | 0.035 | 0 | 2.17 | 2.87 | 2.24 |
| | | | | | 0.259 | 2.00 | 2.87 | 2.13 |
| | | | | | 0.518 | 1.84 | 2.87 | 2.03 |
| | | | | | 0.777 | 1.55 | 2.87 | 1.94 |
| T-6 | 7 | 0.696 | 0.087 | 0.043 | 0 | 1.61 | 2.00 | 1.89 |
| | | | | | 0.261 | 1.55 | 2.00 | 1.79 |
| | | | | | 0.522 | 1.46 | 2.00 | 1.68 |
| | | | | | 0.783 | 1.38 | 2.00 | 1.59 |
| T-7 | 7 | 0.696 | 0.130 | 0.043 | 0 | 1.56 | 2.00 | 1.77 |
| | | | | | 0.261 | 1.56 | 2.00 | 1.69 |
| | | | | | 0.522 | 1.51 | 2.00 | 1.59 |
| | | | | | 0.783 | 1.38 | 2.00 | 1.49 |
| T-9 | 7 | 0.696 | 0.232 | 0.043 | 0 | 1.78 | 2.00 | 1.56 |
| | | | | | 0.261 | 1.56 | 2.00 | 1.48 |
| | | | | | 0.522 | 1.51 | 2.00 | 1.40 |
| | | | | | 0.783 | 1.38 | 2.00 | 1.32 |
| T-10 | 7 | 0.696 | 0.290 | 0.043 | 0 | 1.72 | 2.00 | 1.48 |
| | | | | | 0.261 | 1.55 | 2.00 | 1.40 |
| | | | | | 0.522 | 1.43 | 2.00 | 1.33 |
| | | | | | 0.783 | 0.94 | 2.00 | 1.25 |
| T-11 | 1 | 0.727 | 1.090 | 0.273 | 0 | 0.83 | 1.33 | 0.69 |
| T-12 | 1 | 0.800 | 0.800 | 0.200 | 0 | 1.16 | 2.00 | 1.08 |
| T-13 | 1 | 0.833 | 0.632 | 0.158 | 0 | 1.50 | 2.50 | 1.40 |
| T-14 | 1 | 0.800 | 0.400 | 0.200 | 0 | 1.30 | 2.00 | 1.37 |
| T-15 | 1 | 0.800 | 1.333 | 0.200 | 0 | 1.05 | 2.00 | 0.86 |
| V-1 | 8 | 0.600 | 0.200 | 0.050 | 0.117 | 1.03 | 1.33 | 1.10 |
| | | | | | 0.350 | 0.97 | 1.33 | 1.05 |
| | | | | | 0.584 | 0.91 | 1.33 | 1.00 |
| | | | | | 0.817 | 0.74 | 1.33 | 0.94 |

HYP[x] = hypothesis modified as included in Equation 4.

## TABLE 12

Analysis of Data from Araldite Models for $f(b, N, h, R)$

$k = 0, \ \mu = 0.435, \ n = 1$

| No. | N | R | h | b | x | $\sigma_p'$ EXPT | $\sigma_p'$ TA | $\sigma_p'$ HYP[x] |
|-----|---|---|---|---|---|------|------|------|
| A-1 | 5 | 0.545 | 0.091 | 0.091 | 0 | 2.0 | 2.0 | 2.09 |
| | | | | | 0.364 | 2.0 | 2.0 | 1.94 |
| | | | | | 0.726 | 1.9 | 2.0 | 1.79 |
| A-2 | 5 | 0.675 | 0.117 | 0.065 | 0 | 2.6 | 2.73 | 2.72 |
| | | | | | 0.355 | 2.6 | 2.73 | 2.53 |
| | | | | | 0.711 | 2.5 | 2.73 | 2.34 |
| A-3 | 5 | 0.798 | 0.133 | 0.040 | 0 | 3.8 | 4.19 | 4.02 |
| | | | | | 0.348 | 3.7 | 4.19 | 3.72 |
| | | | | | 0.695 | 3.5 | 4.19 | 3.46 |
| A-4 | 5 | 0.915 | 0.152 | 0.017 | 0 | 7.7 | 9.96 | 7.90 |
| | | | | | 0.339 | 7.4 | 9.96 | 7.67 |
| | | | | | 0.678 | 6.7 | 9.96 | 7.23 |
| B-1 | 5 | 0.545 | 0.182 | 0.091 | 0 | 1.9 | 2.0 | 2.03 |
| | | | | | 0.364 | 1.9 | 2.0 | 1.89 |
| | | | | | 0.726 | 1.8 | 2.0 | 1.75 |
| B-2 | 5 | 0.828 | 0.276 | 0.034 | 0 | 3.6 | 5.0 | 3.89 |
| | | | | | 0.345 | 3.5 | 5.0 | 3.65 |
| | | | | | 0.090 | 3.3 | 5.0 | 3.41 |
| B-3 | 5 | 0.873 | 0.291 | 0.026 | 0 | 4.1 | 6.72 | 4.56 |
| | | | | | 0.342 | 4.0 | 6.72 | 4.27 |
| | | | | | 0.684 | 3.9 | 6.72 | 3.99 |
| C-1 | 5 | 0.667 | 0.111 | 0.111 | 0 | 2.1 | 3.0 | 2.64 |
| | | | | 0.055 | 0.389 | 2.8 | 3.0 | 2.48 |
| | | | | 0.055 | 0.722 | 2.6 | 3.0 | 2.31 |
| C-2 | 5 | 0.720 | 0.120 | 0.120 | 0 | 2.1 | 3.57 | 2.99 |
| | | | | 0.040 | 0.398 | 3.2 | 3.57 | 2.84 |
| | | | | 0.040 | 0.720 | 3.0 | 3.57 | 2.65 |
| C-3 | 5 | 0.750 | 0.125 | 0.096 | 0 | 2.3 | 4.0 | 3.29 |
| | | | | 0.038 | 0.384 | 3.4 | 4.0 | 3.11 |
| | | | | 0.038 | 0.712 | 3.1 | 4.0 | 2.89 |
| C-4 | 5 | 0.766 | 0.128 | 0.106 | 0 | 2.6 | 4.24 | 3.42 |
| | | | | 0.032 | 0.394 | 4.1 | 4.24 | 3.25 |
| | | | | 0.032 | 0.712 | 3.7 | 4.24 | 3.04 |
| C-5 | 5 | 0.780 | 0.130 | 0.101 | 0 | 2.7 | 4.55 | 3.58 |
| | | | | 0.030 | 0.391 | 4.2 | 4.55 | 3.40 |
| | | | | 0.030 | 0.712 | 3.8 | 4.55 | 3.21 |
| C-6 | 5 | 0.837 | 0.139 | 0.067 | 0 | 3.4 | 6.14 | 4.45 |
| | | | | 0.024 | 0.370 | 4.9 | 6.14 | 4.24 |
| | | | | 0.024 | 0.691 | 4.5 | 6.14 | 3.95 |

(Continued)

TABLE 12 (Concluded)

| No. | N | R | h | b | x | $\sigma_p'$ EXPT | $\sigma_p'$ TA | $\sigma_p'$ HYP$^x$ |
|-----|---|---|---|---|---|------|----|------|
| C-7 | 5 | 0.812 | 0.135 | 0.104 | 0 | 2.8 | 5.32 | 3.97 |
|  |  |  |  | 0.021 | 0.396 | 4.5 | 5.32 | 3.82 |
|  |  |  |  | 0.021 | 0.709 | 4.2 | 5.32 | 3.57 |
| C-8 | 5 | 0.850 | 0.140 | 0.080 | 0 | 3.2 | 6.25 | 4.48 |
|  |  |  |  | 0.020 | 0.380 | 5.1 | 6.25 | 4.29 |
|  |  |  |  | 0.020 | 0.700 | 4.8 | 6.25 | 4.01 |
| D-1 | 5 | 0.638 | 0.106 | 0.061 | 0 | 2.5 | 2.76 | 2.89 |
|  |  |  |  | 0.089 | 0.363 | 2.1 | 2.76 | 2.78 |
|  |  |  |  | 0.061 | 0.726 | 2.4 | 2.76 | 2.62 |
| D-2 | 5 | 0.755 | 0.126 | 0.038 | 0 | 4.0 | 4.08 | 3.92 |
|  |  |  |  | 0.066 | 0.356 | 3.4 | 4.08 | 3.75 |
|  |  |  |  | 0.038 | 0.712 | 3.8 | 4.08 | 3.51 |
| D-3 | 5 | 0.820 | 0.136 | 0.016 | 0 | 6.2 | 5.55 | 4.94 |
|  |  |  |  | 0.066 | 0.355 | 4.3 | 5.55 | 4.66 |
|  |  |  |  | 0.016 | 0.710 | 5.9 | 5.55 | 4.43 |
| E-1 | 1 | 0.667 | 0.333 | 0.333 | 0 | 1.9 | 1.5 | 1.92 |
| E-2 | 1 | 0.800 | 0.400 | 0.200 | 0 | 2.6 | 2.5 | 2.58 |
| E-3 | 1 | 0.889 | 0.444 | 0.111 | 0 | 3.7 | 4.52 | 3.54 |
| F-1 | 1 | 0.572 | 0.345 | 0.429 | 0 | 1.8 | 1.67 | 1.67 |
| F-2 | 1 | 0.762 | 0.457 | 0.238 | 0 | 2.55 | 2.60 | 2.35 |
| F-3 | 1 | 0.904 | 0.543 | 0.096 | 0 | 3.85 | 5.71 | 3.61 |

HYP$^x$ = modified hypothesis as included in Equations 5 and 6.

## TABLE 13

### Analysis of Data from Mortar Models for f(b, N, h, R)

x = 0,  k = 0.1,  μ = 0.1,  n = 1

| No. | N | R | h | b | z/l | $\sigma_p'$ EXPT | $\sigma_p'$ TA | $\sigma_p'$ HYP$^x$ | $\sigma_p'$ MOD |
|-----|---|---|---|---|-----|------|------|-------|-----|
| I-1 | 1 | 0.858 | 0.572 | 0.143 | 7.14 | 1.32 | 4.0 | 2.94 | - |
| I-2 | 7 | 774 | 0.129 | 0.032 | 1.61 | 1.40 | 4.0 | 3.67 | - |
| I-3 | 11 | 766 | 0.085 | 0.021 | 1.06 | 2.92 | 4.0 | 3.87 | - |
| I-4 | 1 | 858 | 0.572 | 0.143 | 20.4 | 1.12 | 4.0 | 2.94 | - |
| I-5 | 1 | 858 | 0.572 | 0.143 | 20.4 | 1.12 | 4.0 | 2.94 | - |
| I-6 | 7 | 774 | 0.129 | 0.032 | 4.60 | 2.12 | 4.0 | 3.67 | - |
| I-7 | 7 | 774 | 0.129 | 0.032 | 4.60 | 2.36 | 4.0 | 3.67 | - |
| I-8 | 11 | 766 | 0.085 | 0.021 | 3.04 | 2.72 | 4.0 | 3.87 | - |
| I-9 | 11 | 766 | 0.085 | 0.021 | 3.04 | 2.96 | 4.0 | 3.87 | - |
| I-10 | 1 | 858 | 0.572 | 0.143 | 20.4 | 1.40 | 4.0 | 2.94 | 1.46 |
| I-11 | 1 | 858 | 0.572 | 0.143 | 20.4 | 1.24 | 4.0 | 2.94 | 1.18 |
| I-12 | 3 | 800 | 0.276 | 0.067 | 9.50 | 1.48 | 4.0 | 3.30 | 1.69 |
| I-13 | 3 | 800 | 0.276 | 0.067 | 9.50 | 1.44 | 4.0 | 3.30 | 1.27 |
| I-14 | 5 | 783 | 0.174 | 0.043 | 6.20 | 1.76 | 4.0 | 3.51 | 1.90 |
| I-15 | 5 | 783 | 0.174 | 0.043 | 6.20 | 1.72 | 4.0 | 3.51 | 1.36 |
| I-16 | 7 | 774 | 0.129 | 0.032 | 4.60 | 2.04 | 4.0 | 3.67 | 2.07 |
| I-17 | 7 | 774 | 0.129 | 0.032 | 4.60 | 2.00 | 4.0 | 3.67 | 1.45 |
| I-18 | 9 | 770 | 0.102 | 0.026 | 3.65 | 2.28 | 4.0 | 3.79 | 2.24 |
| I-19 | 9 | 770 | 0.102 | 0.026 | 3.65 | 2.28 | 4.0 | 3.79 | 1.54 |
| I-20 | 11 | 766 | 0.085 | 0.021 | 3.03 | 2.58 | 4.0 | 3.87 | 2.37 |
| I-21 | 11 | 766 | 0.085 | 0.021 | 3.03 | 2.53 | 4.0 | 3.87 | 1.62 |
| T-16 | 1 | 0.727 | 1.09 | 0.273 | 5.45 | 1.90 | 2.33 | 2.20 | - |
| T-17 | 1 | 0.800 | 0.800 | 0.200 | 4.00 | 2.36 | 3.00 | 2.48 | - |
| T-18 | 1 | 0.833 | 0.632 | 0.158 | 3.16 | 2.74 | 3.50 | 2.71 | - |
| T-19 | 1 | 0.800 | 0.400 | 0.200 | 4.00 | 2.51 | 3.00 | 2.48 | - |
| T-20 | 1 | 0.800 | 1.333 | 0.200 | 4.00 | 2.34 | 3.00 | 2.64 | - |

HYP$^x$ = modified hypothesis as included in Equation 6.

MOD = modification to hypothesis to include penetration into the elastic base.

For experiments I-10 to I-21, where a rubber base was used, the hypothesis was modified to include this extra local penetration. The resulting equation is as follows:

$$\frac{\sigma_p}{S_o} = \frac{(2+h-kh)(1-x/5+h)+0.1E/\ell}{hn+1.8(1-R)(1+R/(1+N-R))(1+h/(1-x/5))+2Rb(1-\mu)\pi+0.1E/\ell} .$$

This modification in some cases produces values that are in good correspondence with the experimental values and always produces changes in the same direction as the experiments. This helps to confirm the validity of the concepts used in the hypothesis.

For experiments T-16 to T-20, the agreement between experimental results and those predicted by the hypothesis is quite good.

The results of the analysis of the data from the steel models, series S, are shown in Table 14. The experimental values of pillar loadings are all less than those calculated using the tributary area theory. The calculated values using the modified hypothesis as expressed by Equation 6 are in closer agreement with the measured values. In these models, edge distances were usually more than three times the half span, and the cover was generally about twenty-three times the equivalent radii of the openings, thus being in excess of the minimum desirable value of 20.

In Figure 21 the scatter diagram is shown of the parameter b, representing pillar breadth, plotted against the ratio of experimental values to those calculated by the modified hypothesis. The information for this scatter diagram comes from the model series A, B, C, D, E, F, T, V, and S. Series U was not considered appropriate for this examination, since the absolute values may not have been accurate owing to the small edge distance in the models. The scatter diagram indicates that the average pillar loading is fairly well predicted by the modified hypothesis. However, the dispersion of values is high.

On further examination it is found that the major contribution to the dispersion comes from the models with unequal pillar breadths. This is not a surprising result in view of the hypothesis using an average back pressure from all the pillars for the calculation of the reverse deflection, $\delta'$. To take into account the variation from pillar to pillar of this average back pressure, the concept of the reverse deflection varying as the local average back pressure, i.e., the pillar load divided by the area tributary to the pillar, leads to the function $(1+b_o/b)^{-1}$ (i.e., $B_o/B = b_o/b$ and $(B+B_o)/B = \sigma_p/S_p$) being used to replace the factors in the denominator of Equation 4 of $(1-R)(1+1/N)$ and of the similar two factors in Equation 6.

## TABLE 14

### Analysis of Data from Steel Models for f(b, N, h, n, R)

$$\mu = 0.290$$

| No. | N | R | h | b | x | k | n | $\sigma_p'$ EXPT | $\sigma_p'$ TA | $\sigma_p'$ HYP[x] |
|---|---|---|---|---|---|---|---|---|---|---|
| S-1 | 1 | 0.800 | 0.201 | 0.200 | 0 | 0 | 1 | 2.48 | 3.0 | 2.66 |
| S-2 | 1 | 0.800 | 0.201 | 0.200 | 0 | 0 | 1 | 2.45 | 3.0 | 2.66 |
| S-3 | 1 | 0.800 | 0.201 | 0.200 | 0 | 0 | 1.300 | 2.28 | 3.0 | 2.51 |
| S-4 | 1 | 0.800 | 0.201 | 0.200 | 0 | 0 | 1.732 | 2.17 | 3.0 | 2.32 |
| S-5 | 1 | 0.800 | 0.201 | 0.200 | 0 | 1/3 | 1.732 | 2.14 | 3.0 | 2.25 |
|  |  |  |  |  |  | 1 |  | 2.09 | 3.0 | 2.11 |
|  |  |  |  |  |  | 3 |  | 1.93 | 3.0 | 1.68 |
| S-6 | 1 | 0.800 | 0.401 | 0.200 | 0 | 0 | 1 | 2.15 | 3.0 | 2.56 |
| S-7 | 1 | 0.800 | 0.401 | 0.200 | 0 | 1/3 | 1 | 2.09 | 3.0 | 2.42 |
|  |  |  |  |  |  | 1 | 1 | 1.98 | 3.0 | 2.13 |
|  |  |  |  |  |  | 3 | 1 | 1.65 | 3.0 | 1.28 |
| S-8 | 1 | 0.800 | 0.401 | 0.200 | 0 | 0 | 1.416 | 1.92 | 3.0 | 2.27 |
| S-9 | 1 | 0.800 | 0.401 | 0.200 | 0 | 1/3 | 1.416 | 1.87 | 3.0 | 2.14 |
|  |  |  |  |  |  | 1 | 1.416 | 1.78 | 3.0 | 1.89 |
|  |  |  |  |  |  | 3 | 1.416 | 1.51 | 3.0 | 1.13 |
| S-10 | 3 | 0.644 | 0.162 | 0.119 | 0 | 0 | 1 | 2.21 | 2.36 | 2.32 |
|  |  |  |  | 0.118 | 0.560 |  | 1 | 2.16 | 2.36 | 2.06 |
|  |  |  |  | 0.115 | 0.560 |  | 1 | 2.18 | 2.36 | 2.06 |
| S-11 | 3 | 0.644 | 0.162 | 0.119 | 0 | 0 | 1 | 2.21 | 2.36 | 2.32 |
|  |  |  |  | 0.118 | 0.560 |  | 1 | 2.16 | 2.36 | 2.06 |
|  |  |  |  | 0.115 | 0.560 |  | 1 | 2.17 | 2.36 | 2.06 |
| S-12 | 3 | 0.644 | 0.162 | 0.119 | 0 | 0 | 1.250 | 2.12 | 2.36 | 2.24 |
|  |  |  |  | 0.118 | 0.560 |  |  | 2.05 | 2.36 | 1.99 |
|  |  |  |  | 0.115 | 0.560 |  |  | 2.06 | 2.36 | 1.99 |
| S-13 | 3 | 0.644 | 0.162 | 0.119 | 0 | 0 | 1.695 | 1.97 | 2.36 | 2.09 |
|  |  |  |  | 0.118 | 0.560 |  |  | 1.88 | 2.36 | 1.86 |
|  |  |  |  | 0.115 | 0.560 |  |  | 1.86 | 2.36 | 1.86 |
| S-14 | 3 | 0.644 | 0.162 | 0.119 | 0 | 1/3 | 1.250 | 2.05 | 2.36 | 2.18 |
|  |  |  |  |  |  | 1. |  | 1.92 | 2.36 | 2.07 |
|  |  |  |  |  |  | 3 |  | 1.52 | 2.36 | 1.74 |
|  |  |  |  | 0.118 | 0.560 | 1/3 |  | 1.99 | 2.36 | 1.94 |
|  |  |  |  |  |  | 1 |  | 1.86 | 2.36 | 1.84 |
|  |  |  |  |  |  | 3 |  | 1.48 | 2.36 | 1.54 |
|  |  |  |  | 0.115 | 0.560 | 1/3 |  | 1.96 | 2.36 | 1.94 |
|  |  |  |  |  |  | 1 |  | 1.81 | 2.36 | 1.84 |
|  |  |  |  |  |  | 3 |  | 1.21 | 2.36 | 1.54 |
| S-15 | 3 | 0.644 | 0.162 | 0.119 | 0 | 1/3 | 1.695 | 1.90 | 2.36 | 2.04 |
|  |  |  |  |  |  | 1 |  | 1.80 | 2.36 | 1.93 |
|  |  |  |  |  |  | 3 |  | 1.51 | 2.36 | 1.62 |
|  |  |  |  | 0.118 | 0.560 | 1/3 |  | 1.76 | 2.36 | 1.81 |
|  |  |  |  |  |  | 1 |  | 1.63 | 2.36 | 1.72 |
|  |  |  |  |  |  | 3 |  | 1.24 | 2.36 | 1.44 |
|  |  |  |  | 0.115 | 0.560 | 1/3 |  | 1.79 | 2.36 | 1.81 |
|  |  |  |  |  |  | 1 |  | 1.68 | 2.36 | 1.72 |
|  |  |  |  |  |  | 3 |  | 1.33 | 2.36 | 1.44 |
| S-17 | 5 | 0.630 | 0.151 | 0.074 | 0 | 0 | 1 | 2.19 | 3.33 | 2.40 |
|  |  |  |  |  | 0.357 |  |  | 2.18 | 3.33 | 2.24 |
|  |  |  |  |  | 0.357 |  |  | 2.17 | 3.33 | 2.24 |
|  |  |  |  |  | 0.715 |  |  | 2.11 | 3.33 | 2.07 |
|  |  |  |  |  | 0.715 |  |  | 2.11 | 3.33 | 2.07 |

(Continued)

TABLE 14 (Continued)

| No. | N | R | h | b | x | k | n | $\sigma_p'$ EXPT | $\sigma_p'$ TA | $\sigma_p'$ HYP$^x$ |
|---|---|---|---|---|---|---|---|---|---|---|
| S-18 | 5 | 0.630 | 0.151 | 0.074 | 0 | 0 | 1.262 | 2.08 | 3.33 | 2.31 |
|  |  |  |  |  | 0.357 |  |  | 2.01 | 3.33 | 2.16 |
|  |  |  |  |  | 0.357 |  |  | 1.98 | 3.33 | 2.16 |
|  |  |  |  |  | 0.715 |  |  | 1.87 | 3.33 | 1.99 |
|  |  |  |  |  | 0.715 |  |  | 1.87 | 3.33 | 1.99 |
| S-19 | 5 | 0.630 | 0.151 | 0.074 | 0 | 0 | 1.665 | 2.06 | 3.33 | 2.19 |
|  |  |  |  |  | 0.357 |  |  | 2.03 | 3.33 | 2.05 |
|  |  |  |  |  | 0.357 |  |  | 2.01 | 3.33 | 2.05 |
|  |  |  |  |  | 0.715 |  |  | 1.86 | 3.33 | 1.88 |
|  |  |  |  |  | 0.715 |  |  | 1.88 | 3.33 | 1.88 |
| S-20 | 5 | 0.630 | 0.151 | 0.074 | 0 | 0 | 1.665 | 2.06 | 3.33 | 2.19 |
|  |  |  |  |  | 0.357 |  |  | 2.03 | 3.33 | 2.05 |
|  |  |  |  |  | 0.357 |  |  | 2.02 | 3.33 | 2.05 |
|  |  |  |  |  | 0.715 |  |  | 1.86 | 3.33 | 1.88 |
|  |  |  |  |  | 0.715 |  |  | 1.87 | 3.33 | 1.88 |
| S-21 | 5 | 0.630 | 0.151 | 0.074 | 0 | 1/3 | 1.262 | 2.07 | 3.33 | 2.26 |
|  |  |  |  |  |  | 1 |  | 2.06 | 3.33 | 2.15 |
|  |  |  |  |  |  | 3 |  | 2.02 | 3.33 | 1.82 |
|  |  |  |  |  | 0.357 | 1/3 |  | 2.01 | 3.33 | 2.11 |
|  |  |  |  |  |  | 1 |  | 2.01 | 3.33 | 2.01 |
|  |  |  |  |  |  | 3 |  | 2.01 | 3.33 | 1.70 |
|  |  |  |  |  | 0.357 | 1/3 |  | 1.98 | 3.33 | 2.11 |
|  |  |  |  |  |  | 1 |  | 1.98 | 3.33 | 2.01 |
|  |  |  |  |  |  | 3 |  | 1.98 | 3.33 | 1.70 |
|  |  |  |  |  | 0.715 | 1/3 |  | 1.87 | 3.33 | 1.94 |
|  |  |  |  |  |  | 1 |  | 1.86 | 3.33 | 1.85 |
|  |  |  |  |  |  | 3 |  | 1.84 | 3.33 | 1.57 |
|  |  |  |  |  | 0.715 | 1/3 |  | 1.85 | 3.33 | 1.94 |
|  |  |  |  |  |  | 1 |  | 1.82 | 3.33 | 1.85 |
|  |  |  |  |  |  | 3 |  | 1.72 | 3.33 | 1.57 |
| S-22 | 5 | 0.630 | 0.151 | 0.074 | 0 | 1/3 | 1.665 | 2.05 | 3.33 | 2.14 |
|  |  |  |  |  |  | 1 |  | 2.04 | 3.33 | 2.04 |
|  |  |  |  |  |  | 3 |  | 1.99 | 3.33 | 1.73 |
|  |  |  |  |  | 0.357 | 1/3 |  | 2.02 | 3.33 | 2.00 |
|  |  |  |  |  |  | 1 |  | 2.00 | 3.33 | 1.91 |
|  |  |  |  |  |  | 3 |  | 1.93 | 3.33 | 1.62 |
|  |  |  |  |  | 0.357 | 1/3 |  | 2.00 | 3.33 | 2.00 |
|  |  |  |  |  |  | 1 |  | 1.97 | 3.33 | 1.91 |
|  |  |  |  |  |  | 3 |  | 1.88 | 3.33 | 1.62 |
|  |  |  |  |  | 0.715 | 1/3 |  | 1.84 | 3.33 | 1.84 |
|  |  |  |  |  |  | 1 |  | 1.80 | 3.33 | 1.75 |
|  |  |  |  |  |  | 3 |  | 1.67 | 3.33 | 1.48 |
|  |  |  |  |  | 0.715 | 1/3 |  | 1.85 | 3.33 | 1.84 |
|  |  |  |  |  |  | 1 |  | 1.80 | 3.33 | 1.75 |
|  |  |  |  |  |  | 3 |  | 1.66 | 3.33 | 1.48 |

TABLE 14 (Concluded)

| No. | N | R | h | b | x | k | n | $\sigma'_p$ EXPT | $\sigma'_p$ TA | $\sigma'_p$ HYP$^X$ |
|---|---|---|---|---|---|---|---|---|---|---|
| S-23 | 5 | 0.630 | 0.151 | 0.074 | 0 | 1/3 | 1.665 | 2.03 | 3.33 | 2.14 |
| | | | | | | 1 | | 1.98 | 3.33 | 2.04 |
| | | | | | | 3 | | 1.82 | 3.33 | 1.73 |
| | | | | | 0.357 | 1/3 | | 2.01 | 3.33 | 2.00 |
| | | | | | | 1 | | 1.96 | 3.33 | 1.91 |
| | | | | | | 3 | | 1.81 | 3.33 | 1.62 |
| | | | | | 0.357 | 1/3 | | 2.00 | 3.33 | 2.00 |
| | | | | | | 1 | | 1.95 | 3.33 | 1.91 |
| | | | | | | 3 | | 1.80 | 3.33 | 1.62 |
| | | | | | 0.715 | 1/3 | | 1.83 | 3.33 | 1.84 |
| | | | | | | 1 | | 1.77 | 3.33 | 1.75 |
| | | | | | | 3 | | 1.58 | 3.33 | 1.48 |
| | | | | | 0.715 | 1/3 | | 1.83 | 3.33 | 1.85 |
| | | | | | | 1 | | 1.75 | 3.33 | 1.75 |
| | | | | | | 3 | | 1.52 | 3.33 | 1.48 |
| S-29 | 5 | 0.621 | 0.148 | 0.0708 | 0 | 0 | 1 | 2.32 | 2.64 | 2.37 |
| | | | | 0.0651 | 0.342 | | | 2.33 | 2.64 | 2.23 |
| | | | | 0.0887 | 0.367 | | | 2.14 | 2.64 | 2.21 |
| | | | | 0.0893 | 0.705 | | | 2.04 | 2.64 | 2.04 |
| | | | | 0.0651 | 0.729 | | | 2.22 | 2.64 | 2.03 |
| S-30 | 5 | 0.621 | 0.148 | 0.0708 | 0 | 1/3 | 1 | 2.30 | 2.64 | 2.31 |
| | | | | | | 1 | | 2.27 | 2.64 | 2.20 |
| | | | | | | 3 | | 2.17 | 2.64 | 1.87 |
| | | | | 0.0651 | 0.342 | 1/3 | | 2.31 | 2.64 | 2.18 |
| | | | | | | 1 | | 2.28 | 2.64 | 2.08 |
| | | | | | | 3 | | 2.18 | 2.64 | 1.77 |
| | | | | 0.0887 | 0.367 | 1/3 | | 2.11 | 2.64 | 2.18 |
| | | | | | | 1 | | 2.05 | 2.64 | 2.11 |
| | | | | | | 3 | | 1.86 | 2.64 | 1.90 |
| | | | | 0.0893 | 0.705 | 1/3 | | 2.01 | 2.64 | 2.01 |
| | | | | | | 1 | | 1.95 | 2.64 | 1.95 |
| | | | | | | 3 | | 1.78 | 2.64 | 1.76 |
| | | | | 0.0651 | 0.729 | 1/3 | | 2.18 | 2.64 | 2.00 |
| | | | | | | 1 | | 2.10 | 2.64 | 1.94 |
| | | | | | | 3 | | 1.87 | 2.64 | 1.75 |
| S-31 | 5 | 0.621 | 0.148 | 0.0708 | 0 | 0 | 1.410 | 2.10 | 2.64 | 2.24 |
| | | | | 0.0651 | 0.342 | | | 2.06 | 2.64 | 2.08 |
| | | | | 0.0887 | 0.367 | | | 1.91 | 2.64 | 2.07 |
| | | | | 0.0893 | 0.705 | | | 1.76 | 2.64 | 1.96 |
| | | | | 0.0651 | 0.729 | | | 1.89 | 2.64 | 1.96 |

HYP$^X$ = modified hypothesis as included in Equation 6.
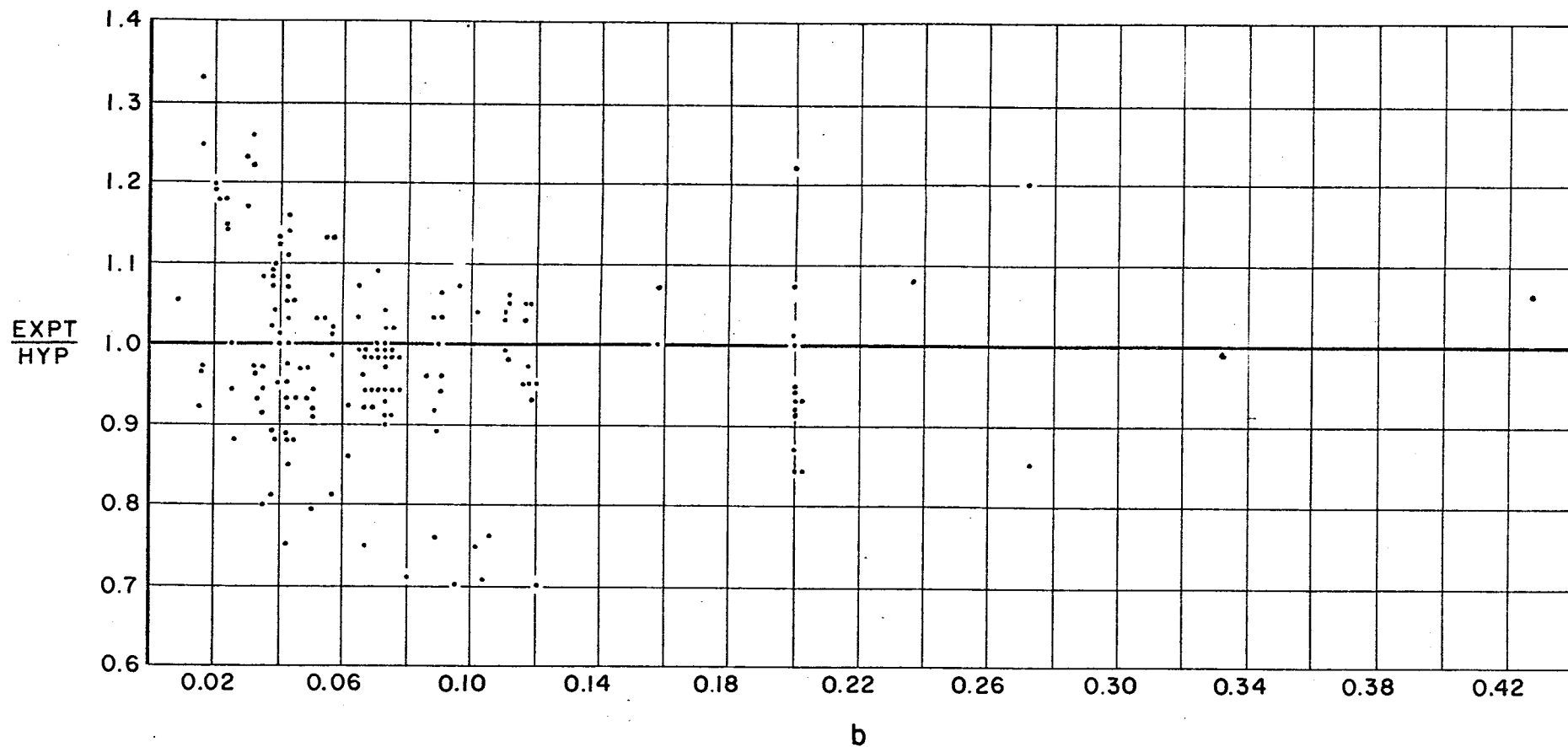
Figure 21. Scatter diagram of variation of pillar loading with b.

In Tables 15 and 16, this alternate form of the hypothesis is used to compute pillar loadings for the models with pillars of unequal breadth. It might be noted that where the pillar breadths are equal the two forms of the hypothesis give equal answers.

In Figure 22, a new scatter diagram is drawn using this alternate form of the hypothesis. This scatter diagram shows a reduction in dispersion of the ratio of experimental to calculated values. This reduction is illustrated principally by a change in the coefficient of variation for series C plus D of from 19.1 per cent to 13.3 per cent.

From this it is judged that the alternate form of the hypothesis is preferable, particularly with the further generalization of letting $(1 + b_0/b)^{-1} = (1 - r)$, where r is the local extraction ratio determined from the area of one pillar and the tributary area surrounding it. Equations 4 and 6 will thus be altered as follows:

$$\frac{\Delta\sigma_p}{S_o} = \frac{(2R - kh(1-w))(1 - x/5 + h) - w_p\, khn}{hn + 1.8(1-r)(1 + h/(1 - x/5)) + 2Rb(1-w)/\pi} \qquad \text{Eq. 7}$$

$$\frac{\sigma_p}{S_o} = \frac{(2 + h - kh)(1 - x/5 + h)}{hn + 1.8(1-r)(1 + h/(1 - x/5)) + 2Rb(1-\mu)/\pi} \qquad \text{Eq. 8}$$

## Analysis of Data for f(N)

To determine whether the function of N, the number of pillars, is correct in Equations 4 and 6, which would still be used where either the pillars are of equal breadth or only the general extraction ratio, R, is given, a scatter diagram is plotted of the ratio of experimental to calculated values against N. The results of the experiments from the model series A, B, E, F, T, V and S are used in this figure. Model series I was not used because, as explained above, these experiments did not produce good absolute values, and series U has been excluded owing to the small amount of edge distance that was provided, which probably influenced the absolute values of pillar loadings in these models.

Figure 23 shows this scatter diagram. From this figure it seems that the deviations of experimental values from calculated values does not arise from an incorrect function of N. In other words, there is no strong trend away from the x-axis as N increases.

TABLE 15

Analysis of Data from Araldite Models for Alternate f(b)

$k = 0, \mu = 0.435, n = 1$

| No. | N | R | h | b | $b_o/b$ | x | $\sigma_p'$ EXPT | $\sigma_p'$ HYP$^{xb}$ |
|-----|---|---|---|---|---------|---|-----------------|------------------------|
| C-1 | 5 | 0.667 | 0.111 | 0.111 | 1.00 | 0 | 2.0 | 2.11 |
|     |   |       |       | 0.055 | 2.00 | 0.389 | 2.8 | 2.70 |
|     |   |       |       | 0.055 | 2.00 | 0.722 | 2.6 | 2.49 |
| C-2 | 5 | 0.720 | 0.120 | 0.120 | 1.00 | 0 | 2.1 | 2.04 |
|     |   |       |       | 0.040 | 3.00 | 0.398 | 3.2 | 3.45 |
|     |   |       |       | 0.040 | 3.00 | 0.720 | 3.0 | 3.35 |
| C-3 | 5 | 0.750 | 0.125 | 0.096 | 1.30 | 0 | 2.3 | 2.32 |
|     |   |       |       | 0.038 | 3.25 | 0.384 | 3.4 | 3.64 |
|     |   |       |       | 0.038 | 3.25 | 0.712 | 3.1 | 3.36 |
| C-4 | 5 | 0.766 | 0.128 | 0.106 | 1.20 | 0 | 2.6 | 2.23 |
|     |   |       |       | 0.032 | 4.00 | 0.394 | 4.1 | 4.08 |
|     |   |       |       | 0.032 | 4.00 | 0.712 | 3.7 | 3.81 |
| C-5 | 5 | 0.780 | 0.130 | 0.101 | 1.29 | 0 | 2.7 | 2.29 |
|     |   |       |       | 0.030 | 4.30 | 0.391 | 4.2 | 4.12 |
|     |   |       |       | 0.030 | 4.30 | 0.712 | 3.8 | 3.84 |
| C-6 | 5 | 0.837 | 0.139 | 0.067 | 2.07 | 0 | 3.4 | 2.95 |
|     |   |       |       | 0.024 | 5.80 | 0.370 | 4.9 | 5.07 |
|     |   |       |       | 0.024 | 5.80 | 0.691 | 4.5 | 4.73 |
| C-7 | 5 | 0.812 | 0.135 | 0.104 | 1.30 | 0 | 2.8 | 2.31 |
|     |   |       |       | 0.021 | 6.50 | 0.396 | 4.5 | 5.38 |
|     |   |       |       | 0.021 | 6.50 | 0.709 | 4.2 | 5.02 |
| C-8 | 5 | 0.840 | 0.140 | 0.080 | 1.75 | 0 | 3.2 | 2.68 |
|     |   |       |       | 0.020 | 7.00 | 0.380 | 5.1 | 5.61 |
|     |   |       |       | 0.020 | 7.00 | 0.700 | 4.8 | 5.25 |
| D-1 | 5 | 0.638 | 0.106 | 0.061 | 1.73 | 0 | 2.5 | 2.75 |
|     |   |       |       | 0.089 | 1.19 | 0.363 | 2.1 | 2.09 |
|     |   |       |       | 0.061 | 1.73 | 0.726 | 2.4 | 2.36 |
| D-2 | 5 | 0.755 | 0.126 | 0.038 | 3.29 | 0 | 4.0 | 3.96 |
|     |   |       |       | 0.066 | 1.92 | 0.356 | 3.4 | 2.65 |
|     |   |       |       | 0.038 | 3.29 | 0.712 | 3.8 | 3.40 |
| D-3 | 5 | 0.820 | 0.136 | 0.016 | 8.33 | 0 | 6.2 | 6.73 |
|     |   |       |       | 0.066 | 2.08 | 0.355 | 4.3 | 2.73 |
|     |   |       |       | 0.016 | 8.33 | 0.710 | 5.9 | 5.86 |

$HYP^{xb}$ = modified hypothesis as included in Equation 8.

## TABLE 16

Analysis of Data from Steel Models for Alternate f(b)

$k = 0$, $\mu = 0.290$, $i = 0$

| No. | N | R | h | b | $b_o/b$ | x | n | $\sigma_p'$ EXPT | $\sigma_p'$ HYP$^{xb}$ |
|-----|---|---|---|---|---------|---|---|------|------|
| S-29 | 5 | 0.621 | 0.148 | 0.0708 | 1.462 | 0 | 1 | 2.32 | 2.45 |
|      |   |       |       | 0.0651 | 1.590 | 0.342 |   | 2.33 | 2.39 |
|      |   |       |       | 0.0887 | 1.167 | 0.367 |   | 2.14 | 2.03 |
|      |   |       |       | 0.0893 | 1.159 | 0.705 |   | 2.04 | 1.89 |
|      |   |       |       | 0.0651 | 1.590 | 0.729 |   | 2.22 | 2.19 |
| S-31 | 5 | 0.621 | 0.148 | 0.0708 | 1.462 | 0 | 1.410 | 2.10 | 2.31 |
|      |   |       |       | 0.0651 | 1.590 | 0.342 |   | 2.06 | 2.26 |
|      |   |       |       | 0.0887 | 1.167 | 0.367 |   | 1.91 | 1.93 |
|      |   |       |       | 0.0893 | 1.159 | 0.705 |   | 1.76 | 1.79 |
|      |   |       |       | 0.0651 | 1.590 | 0.729 |   | 1.89 | 2.06 |

HYP$^{xb}$ = modified hypothesis as included in Equation 8.
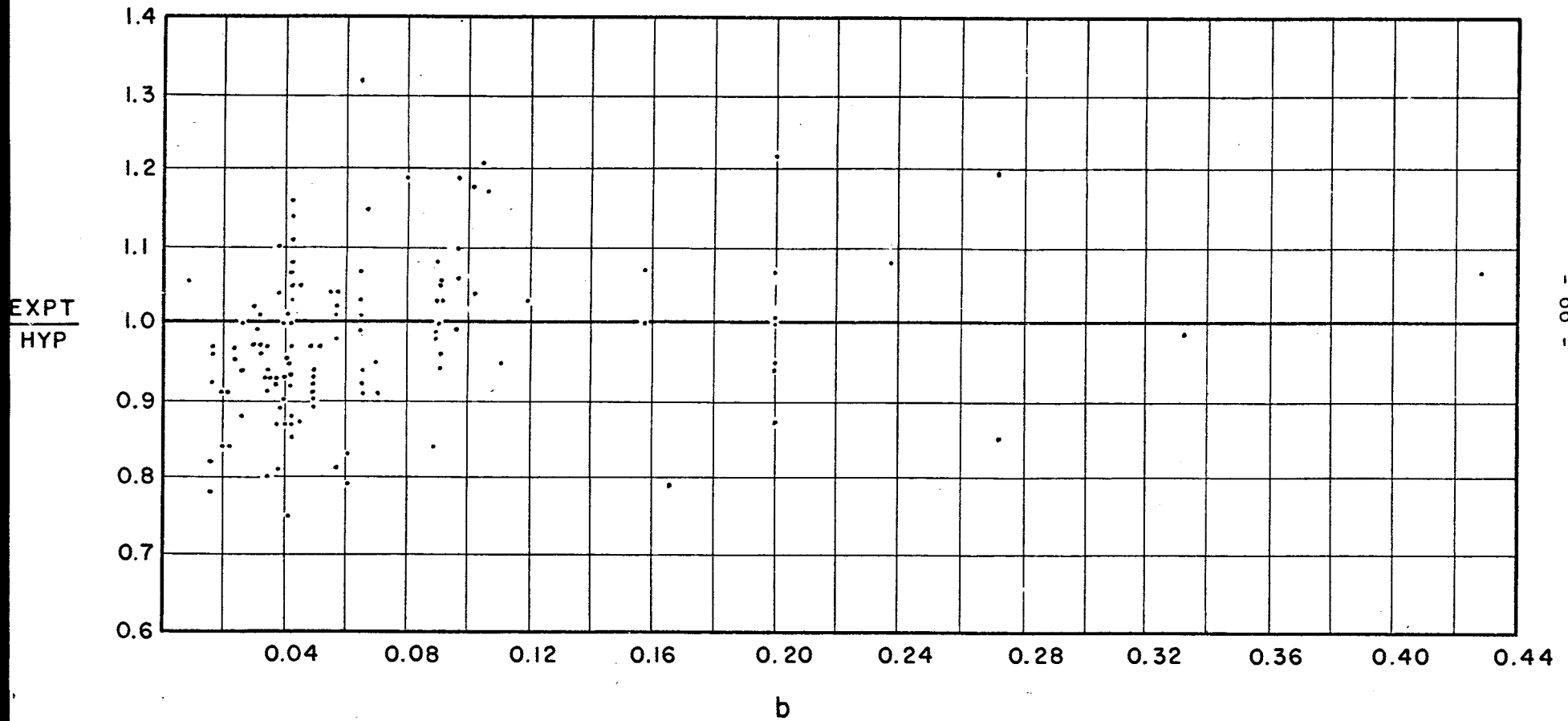
Figure 22. Scatter diagram of variation of pillar loading with b with the hypothesis modified.
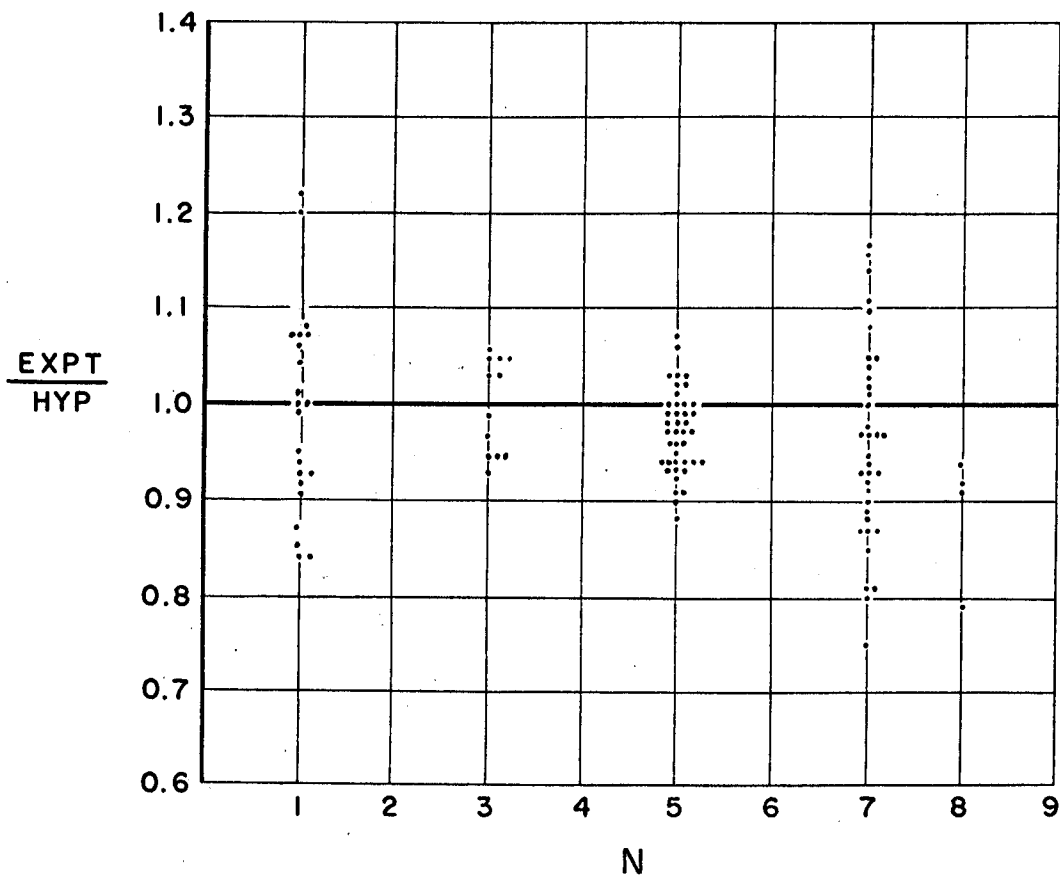
Figure 23. Scatter diagram of variation of pillar loading with N.

## Analysis of Data for f(h)

Pillar loading, according to the hypothesis, although not according to the tributary area theory, is a function of the height of the pillar, H, or the normalized parameter $h = H/L$. To examine the appropriateness of the functional relation between pillar loadings and h, a scatter diagram is plotted of the ratio of experimental to calculated values against h. The results of the series of models A, B, E, F, T, V and S as expressed in Tables 11 to 15 have been used.

By examining the scatter diagram of Figure 24, it seems that the dispersion of values cannot be attributed to the functional relations between loading and h having some strong relationship different from that included in the hypothesis. There is no conspicuous trend away from the x-axis as h increases.

## Analysis of Data for f(k)

The hypothesis shows that the pillar loadings should vary with the magnitude of the field stress acting parallel to the span of the mining zone, $S_t$. This component of the field stress has been included in the parameter $k = S_t/S_o$. Figure 25 was plotted to determine if the hypothesis predicts the proper dependence between pillar loading and k. Model series C and D have not been included in this scatter diagram because they have pillars of unequal breadths, and the pillar loading, as seen above, is so strongly dependent on the parameter b that it is judged preferable to exclude this variation when examining the dependence of pillar loading on other parameters.

Figure 25 shows the ratio of experimental to calculated values normalized to $k = 0$ (i.e., expressed as a ratio of the value at $k = 0$) versus k. For this figure, model series E, F, U and S have been used with the results shown in Tables 17 and 18. Model series U has been included in this diagram as, in spite of the inadequate edge distance, it is probable that the relative values are a reasonable representation of the variation of loading with k.

The scatter diagram shows a rather large dispersion. Within the dispersion it seems that a rising trend with k may be occurring in the ratio EXPT/HYP. It is possible that with a slot, as opposed to a circular or elliptical hole, the deflection due to $S_t$ does not vary with x. Model series S indicated that this would be a reasonable deduction.

Based on this concept and on the empirical data the hypothesis can be modified by separating the elements of δ, whose origin can be seen in the original derivation (1), and by deriving the equations again to make the deflection due to $S_t$ independent of x. Equations 4 and 6 are changed to:

## TABLE 17

### Analysis of Data from Araldite Models for f(k)

$$N = 1, \ x = 0, \ \mu = 0.435, \ n = 1$$

| No. | R | h | b | k | $\sigma_p{}'$ EXPT | $\sigma_p{}'$ TA | $\dfrac{\sigma_p(k)}{\sigma_p(0)}$ EXPT | $\dfrac{\sigma_p(k)}{\sigma_p(0)}$ HYP$^x$ |
|-----|------|------|------|-----|------|------|------|------|
| E-1 | 0.667 | 0.333 | 0.333 | 0 | 1.9 | 1.50 | 1 | 1 |
|     |       |       |       | 1/3 | 1.9 | 1.50 | 1 | 0.95 |
|     |       |       |       | 1 | 1.8 | 1.50 | 0.95 | 0.86 |
| E-2 | 0.800 | 0.400 | 0.200 | 0 | 2.6 | 2.50 | 1 | 1 |
|     |       |       |       | 1/3 | 2.5 | 2.50 | 0.96 | 0.97 |
|     |       |       |       | 1 | 2.3 | 2.50 | 0.88 | 0.84 |
| E-3 | 0.889 | 0.444 | 0.111 | 0 | 3.7 | 4.52 | 1 | 1 |
|     |       |       |       | 1/3 | 3.4 | 4.52 | 0.92 | 0.94 |
|     |       |       |       | 1 | 3.1 | 4.52 | 0.84 | 0.82 |
| F-1 | 0.574 | 0.344 | 0.427 | 0 | 1.8 | 1.67 | 1 | 1 |
|     |       |       |       | 1/3 | 1.7 | 1.67 | 0.94 | 0.96 |
|     |       |       |       | 1 | 1.6 | 1.67 | 0.89 | 0.86 |
| F-2 | 0.762 | 0.457 | 0.238 | 0 | 2.55 | 2.60 | 1 | 1 |
|     |       |       |       | 1/3 | 2.45 | 2.60 | 0.96 | 0.94 |
|     |       |       |       | 1 | 2.25 | 2.60 | 0.88 | 0.82 |
| F-3 | 0.904 | 0.543 | 0.096 | 0 | 3.85 | 5.71 | 1 | 1 |
|     |       |       |       | 1/3 | 3.7 | 5.71 | 0.96 | 0.93 |
|     |       |       |       | 1 | 3.4 | 5.71 | 0.88 | 0.79 |
| U-1 | 0.867 | 0.157 | 0.133 | 0 | 4.3 | 4.26 | 1 | 1 |
|     |       |       |       | 1/3 | 4.6 | 4.26 | 1.08 | 0.98 |
|     |       |       |       | 1 | 4.0 | 4.26 | 0.92 | 0.93 |
|     |       |       |       | 3 | 2.8 | 4.26 | 0.65 | 0.78 |

HYP$^x$ = modified hypothesis as included in Equation 6.

Figure 25.  Scatter diagram of variation of pillar loading with k.

## TABLE 17

### Analysis of Data from Araldite Models for f(k)

$$N = 1, \ x = 0, \ \mu = 0.435, \ n = 1$$

| No. | R | h | b | k | $\sigma_p'$ EXPT | $\sigma_p'$ TA | $\dfrac{\sigma_p(k)}{\sigma_p(0)}$ EXPT | $\dfrac{\sigma_p(k)}{\sigma_p(0)}$ HYP$^x$ |
|---|---|---|---|---|---|---|---|---|
| E-1 | 0.667 | 0.333 | 0.333 | 0 | 1.9 | 1.50 | 1 | 1 |
| | | | | 1/3 | 1.9 | 1.50 | 1 | 0.95 |
| | | | | 1 | 1.8 | 1.50 | 0.95 | 0.86 |
| E-2 | 0.800 | 0.400 | 0.200 | 0 | 2.6 | 2.50 | 1 | 1 |
| | | | | 1/3 | 2.5 | 2.50 | 0.96 | 0.97 |
| | | | | 1 | 2.3 | 2.50 | 0.88 | 0.84 |
| E-3 | 0.889 | 0.444 | 0.111 | 0 | 3.7 | 4.52 | 1 | 1 |
| | | | | 1/3 | 3.4 | 4.52 | 0.92 | 0.94 |
| | | | | 1 | 3.1 | 4.52 | 0.84 | 0.82 |
| F-1 | 0.574 | 0.344 | 0.427 | 0 | 1.8 | 1.67 | 1 | 1 |
| | | | | 1/3 | 1.7 | 1.67 | 0.94 | 0.96 |
| | | | | 1 | 1.6 | 1.67 | 0.89 | 0.86 |
| F-2 | 0.762 | 0.457 | 0.238 | 0 | 2.55 | 2.60 | 1 | 1 |
| | | | | 1/3 | 2.45 | 2.60 | 0.96 | 0.94 |
| | | | | 1 | 2.25 | 2.60 | 0.88 | 0.82 |
| F-3 | 0.904 | 0.543 | 0.096 | 0 | 3.85 | 5.71 | 1 | 1 |
| | | | | 1/3 | 3.7 | 5.71 | 0.96 | 0.93 |
| | | | | 1 | 3.4 | 5.71 | 0.88 | 0.79 |
| U-1 | 0.867 | 0.157 | 0.133 | 0 | 4.3 | 4.26 | 1 | 1 |
| | | | | 1/3 | 4.6 | 4.26 | 1.08 | 0.98 |
| | | | | 1 | 4.0 | 4.26 | 0.92 | 0.93 |
| | | | | 3 | 2.8 | 4.26 | 0.65 | 0.78 |

HYP$^x$ = modified hypothesis as included in Equation 6.

## TABLE 18

### Analysis of Data from Steel Models for f(k)

$$\mu = 0.290$$

| No. | N | R | h | b | x | k | n | $\sigma_p'$ EXPT | $\sigma_p'$ TA | $\dfrac{\sigma_p(k)}{\sigma_p(0)}$ EXPT | $\dfrac{\sigma_p(k)}{\sigma_p(0)}$ HYPx |
|---|---|---|---|---|---|---|---|---|---|---|---|
| S-4 | 1 | 0.800 | 0.201 | 0.200 | 0 | 0 | 1.732 | 2.17 | 3.0 | 1 | 1 |
| S-5 | 1 | 0.800 | 0.201 | 0.200 | 0 | 1/3 | 1.732 | 2.14 | 3.0 | 0.99 | 0.97 |
| | | | | | | 1 | | 2.09 | 3.0 | 0.96 | 0.91 |
| | | | | | | 3 | | 1.93 | 3.0 | 0.89 | 0.72 |
| S-6 | 1 | 0.800 | 0.401 | 0.200 | 0 | 0 | 1 | 2.15 | 3.0 | 1 | 1 |
| | | | | | 0 | 1/3 | 1 | 2.09 | 3.0 | 0.97 | 0.95 |
| | | | | | | 1 | | 1.98 | 3.0 | 0.92 | 0.83 |
| | | | | | | 3 | | 1.65 | 3.0 | 0.77 | 0.50 |
| S-8 | 1 | 0.800 | 0.401 | 0.200 | 0 | 0 | 1.416 | 1.92 | 3.0 | 1 | 1 |
| S-9 | 1 | 0.800 | 0.401 | 0.200 | 0 | 1/3 | 1.416 | 1.87 | 3.0 | 0.97 | 0.94 |
| | | | | | | 1 | | 1.78 | 3.0 | 0.93 | 0.83 |
| | | | | | | 3 | | 1.51 | 3.0 | 0.79 | 0.50 |
| S-12 | 3 | 0.644 | 0.162 | 0.119 | 0 | 0 | 1.250 | 2.12 | 2.36 | 1 | 1 |
| | | | | 0.118 | 0.560 | | | 2.05 | 2.36 | 1 | 1 |
| | | | | 0.115 | 0.560 | | | 2.06 | 2.36 | 1 | 1 |
| S-14 | 3 | 0.644 | 0.162 | 0.119 | 0 | 1/3 | 1.250 | 2.05 | 2.36 | 0.97 | 0.96 |
| | | | | 0.118 | 0.560 | | | 1.99 | 2.36 | 0.97 | 0.97 |
| | | | | 0.115 | 0.560 | | | 1.96 | 2.36 | 0.95 | 0.97 |
| | | | | 0.119 | 0 | 1 | 1.250 | 1.92 | 2.36 | 0.91 | 0.92 |
| | | | | 0.118 | 0.560 | | | 1.86 | 2.36 | 0.91 | 0.92 |
| | | | | 0.115 | 0.560 | | | 1.81 | 2.36 | 0.88 | 0.92 |
| | | | | 0.119 | 0 | 3 | 1.250 | 1.52 | 2.36 | 0.72 | 0.78 |
| | | | | 0.118 | 0.560 | | | 1.48 | 2.36 | 0.72 | 0.77 |
| | | | | 0.115 | 0.560 | | | 1.21 | 2.36 | 0.59 | 0.77 |
| S-13 | 3 | 0.644 | 0.162 | 0.119 | 0 | 0 | 1.695 | 1.94 | 2.36 | 1 | 1 |
| | | | | 0.118 | 0.560 | | | 1.82 | 2.36 | 1 | 1 |
| | | | | 0.115 | 0.560 | | | 1.85 | 2.36 | 1 | 1 |
| S-15 | 3 | 0.644 | 0.162 | 0.119 | 0 | 1/3 | 1.695 | 1.90 | 2.36 | 0.97 | 0.98 |
| | | | | 0.118 | 0.560 | | | 1.76 | 2.36 | 0.97 | 0.97 |
| | | | | 0.115 | 0.560 | | | 1.79 | 2.36 | 0.97 | 0.97 |
| | | | | 0.119 | 0 | 1 | 1.695 | 1.80 | 2.36 | 0.93 | 0.92 |
| | | | | 0.118 | 0.560 | | | 1.63 | 2.36 | 0.90 | 0.92 |
| | | | | 0.115 | 0.560 | | | 1.68 | 2.36 | 0.91 | 0.92 |
| | | | | 0.119 | 0 | 3 | 1.695 | 1.51 | 2.36 | 0.78 | 0.78 |
| | | | | 0.118 | 0.560 | | | 1.24 | 2.36 | 0.68 | 0.77 |
| | | | | 0.115 | 0.560 | | | 1.33 | 2.36 | 0.72 | 0.77 |
| S-18 | 5 | 0.630 | 0.151 | 0.074 | 0 | 0 | 1.262 | 2.08 | 3.33 | 1 | 1 |
| | | | | | 0.357 | | | 2.01 | 3.33 | 1 | 1 |
| | | | | | 0.357 | | | 1.98 | 3.33 | 1 | 1 |
| | | | | | 0.715 | | | 1.87 | 3.33 | 1 | 1 |
| | | | | | 0.715 | | | 1.87 | 3.33 | 1 | 1 |

(Continued)

TABLE 18 (Concluded)

| No. | N | R | h | b | x | k | n | $\sigma_p'$ EXPT | $\sigma_p'$ TA | $\dfrac{\sigma_p(k)}{\sigma_p(0)}$ EXPT | $\dfrac{\sigma_p(k)}{\sigma_p(0)}$ HYP[x] |
|---|---|---|---|---|---|---|---|---|---|---|---|
| S-21 | 5 | 0.630 | 0.151 | 0.074 | 0 | 1/3 | 1.262 | 2.07 | 3.33 | 1 | 0.98 |
| | | | | | 0.357 | | | 2.01 | 3.33 | 1 | 0.98 |
| | | | | | 0.357 | | | 1.98 | 3.33 | 1 | 0.98 |
| | | | | | 0.715 | | | 1.87 | 3.33 | 1 | 0.97 |
| | | | | | 0.715 | | | 1.85 | 3.33 | 0.99 | 0.97 |
| | | | | | 0 | 1 | 1.262 | 2.06 | 3.33 | 0.99 | 0.93 |
| | | | | | 0.357 | | | 2.01 | 3.33 | 1 | 0.93 |
| | | | | | 0.357 | | | 1.98 | 3.33 | 1 | 0.93 |
| | | | | | 0.715 | | | 1.86 | 3.33 | 1 | 0.93 |
| | | | | | 0.715 | | | 1.82 | 3.33 | 0.97 | 0.93 |
| | | | | | 0 | 3 | 1.262 | 2.02 | 3.33 | 0.97 | 0.79 |
| | | | | | 0.357 | | | 2.01 | 3.33 | 1 | 0.79 |
| | | | | | 0.357 | | | 1.98 | 3.33 | 1 | 0.79 |
| | | | | | 0.715 | | | 1.84 | 3.33 | 0.98 | 0.79 |
| | | | | | 0.715 | | | 1.72 | 3.33 | 0.92 | 0.79 |
| S-19 | 5 | 0.630 | 0.151 | 0.074 | 0 | 0 | 1.665 | 2.06 | 3.33 | 1 | 1 |
| | | | | | 0.357 | | | 2.03 | 3.33 | 1 | 1 |
| | | | | | 0.357 | | | 2.01 | 3.33 | 1 | 1 |
| | | | | | 0.715 | | | 1.86 | 3.33 | 1 | 1 |
| | | | | | 0.715 | | | 1.88 | 3.33 | 1 | 1 |
| S-22 | 5 | 0.630 | 0.151 | 0.074 | 0 | 1/3 | 1.665 | 2.05 | 3.33 | 1 | 0.98 |
| | | | | | 0.357 | | | 2.02 | 3.33 | 0.99 | 0.98 |
| | | | | | 0.357 | | | 2.00 | 3.33 | 0.99 | 0.98 |
| | | | | | 0.715 | | | 1.84 | 3.33 | 0.99 | 0.98 |
| | | | | | 0.715 | | | 1.85 | 3.33 | 0.98 | 0.98 |
| | | | | | 0 | 1 | | 2.04 | 3.33 | 0.99 | 0.94 |
| | | | | | 0.357 | | | 2.00 | 3.33 | 0.98 | 0.93 |
| | | | | | 0.357 | | | 1.97 | 3.33 | 0.98 | 0.93 |
| | | | | | 0.715 | | | 1.80 | 3.33 | 0.97 | 0.93 |
| | | | | | 0.715 | | | 1.80 | 3.33 | 0.96 | 0.93 |
| | | | | | 0 | 3 | | 1.99 | 3.33 | 0.97 | 0.79 |
| | | | | | 0.357 | | | 1.93 | 3.33 | 0.95 | 0.79 |
| | | | | | 0.357 | | | 1.88 | 3.33 | 0.94 | 0.79 |
| | | | | | 0.715 | | | 1.67 | 3.33 | 0.90 | 0.79 |
| | | | | | 0.715 | | | 1.66 | 3.33 | 0.88 | 0.79 |
| S-23 | 5 | 0.630 | 0.151 | 0.074 | 0 | 1/3 | 1.665 | 2.03 | 3.33 | 0.99 | 0.98 |
| | | | | | 0.357 | | | 2.01 | 3.33 | 0.99 | 0.98 |
| | | | | | 0.357 | | | 2.00 | 3.33 | 0.99 | 0.98 |
| | | | | | 0.715 | | | 1.83 | 3.33 | 0.98 | 0.98 |
| | | | | | 0.715 | | | 1.83 | 3.33 | 0.97 | 0.98 |
| | | | | | 0 | 1 | | 1.98 | 3.33 | 0.96 | 0.94 |
| | | | | | 0.357 | | | 1.96 | 3.33 | 0.97 | 0.93 |
| | | | | | 0.357 | | | 1.95 | 3.33 | 0.97 | 0.93 |
| | | | | | 0.715 | | | 1.77 | 3.33 | 0.95 | 0.93 |
| | | | | | 0.715 | | | 1.75 | 3.33 | 0.93 | 0.93 |
| | | | | | 0 | 3 | | 1.82 | 3.33 | 0.88 | 0.79 |
| | | | | | 0.357 | | | 1.81 | 3.33 | 0.89 | 0.79 |
| | | | | | 0.357 | | | 1.80 | 3.33 | 0.89 | 0.79 |
| | | | | | 0.715 | | | 1.58 | 3.33 | 0.85 | 0.79 |
| | | | | | 0.715 | | | 1.52 | 3.33 | 0.81 | 0.79 |

HYP[x] = modified hypothesis as included in Equation 6.

$$\frac{\Delta \sigma_p}{S_o} = \frac{2R(1 - x/5 + h) - kh(1 - w + w_p n)}{hn + 1.8(1 - R)(1 + 1/N)(1 + h/(1 - x/5)) + 2Rb(1 - w)/\pi} \qquad \text{Eq. 9}$$

and

$$\frac{\sigma_p}{S_o} = \frac{(2 + h)(1 - x/5 + h) - kh}{hn + 1.8(1 - R)(1 + R/(1 + N - R))(1 + h/(1 - x/5)) + 2Rb(1 - \mu)/\pi} \qquad \text{Eq. 10}$$

The corresponding changes in Equations 7 and 8 lead to:

$$\frac{\Delta \sigma_p}{S_o} = \frac{2R(1 - x/5 + h) - kh(1 - w + w_p n)}{hn + 1.8(1 - r)(1 + h/(1 - x/5)) + 2Rb(1 - w)/\pi} \qquad \text{Eq. 11}$$

$$\frac{\sigma_p}{S_o} = \frac{(2 + h)(1 - x/5 + h) - kh}{hn + 1.8(1 - r)(1 + h/(1 - x/5)) + 2Rb(1 - \mu)/\pi} \qquad \text{Eq. 12}$$

The calculated values using Equation 10 are shown in Tables 19 and 20. The scatter diagram for the alternate function is shown in Figure 26. A reduction in the range of dispersion can be seen and the coefficient of variation (standard deviation over mean) is reduced by the alternate function from 10.9 per cent to 8.1 per cent. It is therefore judged that the alternate form of the equations is preferable.

The corresponding equation for shallow mining zones is changed from Equation 5 to:

$$\frac{\Delta \sigma_p}{S_o} = \frac{2R(1 - x/5 + 2h) + R K_b' - kh(1 - w + 2 w_p n)}{2hn + (1.8(1 + h/(1 - x/5)) + (2K_b'/3)(1 + h/(1 - x^2)))(1 - r) + 4Rb(1 - w)/\pi}$$

$$\text{Eq. 13}$$

With this change in f(k) it was considered necessary to re-examine f(x). However, the only data that included k greater than zero were model series T and V. Owing to the small values of k and h in these experiments, it was found that the differences in calculated pillar loadings using Equation 12 instead of Equation 1 were small enough not to be noticeable on the scatter diagram. Hence, it would not influence the derived f(x).

## TABLE 19

Analysis of Data from Araldite Models for Alternate f(k)

$N = 1$, $x = 0$, $\mu = 0.435$, $n = 1$

| No. | R | h | b | k | $\sigma_p{}'$ EXPT | $\sigma_p{}'$ TA | $\dfrac{\sigma_p(k)}{\sigma_p(0)}$ EXPT | $\dfrac{\sigma_p(k)}{\sigma_p(0)}$ HYP$^{xk}$ |
|-----|-----|-----|-----|-----|-----|-----|-----|-----|
| E-1 | 0.667 | 0.333 | 0.333 | 0 | 1.9 | 1.50 | 1 | 1 |
|     |       |       |       | 1/3 | 1.9 | 1.50 | 1 | 0.97 |
|     |       |       |       | 1 | 1.8 | 1.50 | 0.95 | 0.90 |
| E-2 | 0.800 | 0.400 | 0.200 | 0 | 2.6 | 2.50 | 1 | 1 |
|     |       |       |       | 1/3 | 2.5 | 2.50 | 0.96 | 0.96 |
|     |       |       |       | 1 | 2.3 | 2.50 | 0.88 | 0.88 |
| E-3 | 0.889 | 0.444 | 0.111 | 0 | 3.7 | 4.52 | 1 | 1 |
|     |       |       |       | 1/3 | 3.4 | 4.52 | 0.92 | 0.95 |
|     |       |       |       | 1 | 3.1 | 4.52 | 0.84 | 0.87 |
| F-1 | 0.574 | 0.344 | 0.427 | 0 | 1.8 | 1.67 | 1 | 1 |
|     |       |       |       | 1/3 | 1.7 | 1.67 | 0.94 | 0.96 |
|     |       |       |       | 1 | 1.6 | 1.67 | 0.89 | 0.89 |
| F-2 | 0.762 | 0.457 | 0.238 | 0 | 2.55 | 2.60 | 1 | 1 |
|     |       |       |       | 1/3 | 2.45 | 2.60 | 0.96 | 0.96 |
|     |       |       |       | 1 | 2.25 | 2.60 | 0.88 | 0.87 |
| F-3 | 0.904 | 0.543 | 0.096 | 0 | 3.85 | 5.71 | 1 | 1 |
|     |       |       |       | 1/3 | 3.7 | 5.71 | 0.96 | 0.97 |
|     |       |       |       | 1 | 3.4 | 5.71 | 0.88 | 0.88 |
| U-1 | 0.867 | 0.157 | 0.133 | 0 | 4.3 | 4.26 | 1 | 1 |
|     |       |       |       | 1/3 | 4.6 | 4.26 | 1.08 | 0.98 |
|     |       |       |       | 1 | 4.0 | 4.26 | 0.92 | 0.94 |
|     |       |       |       | 3 | 2.8 | 4.26 | 0.65 | 0.81 |

HYP$^{xk}$ = modified hypothesis as included in Equation 10.

## TABLE 20

### Analysis of Data from Steel Models for Alternate $f(k)$

$$\mu = 0.290$$

| No. | N | R | h | b | x | k | n | $\sigma_p'$ EXPT | $\sigma_p'$ TA | $\dfrac{\sigma_p(k)}{\sigma_p(0)}$ EXPT | $\dfrac{\sigma_p(k)}{\sigma_p(0)}$ HYP$^{\times k}$ |
|---|---|---|---|---|---|---|---|---|---|---|---|
| S-4 | 1 | 0.800 | 0.201 | 0.200 | 0 | 0 | 1.732 | 2.17 | 3.0 | 1 | 1 |
| S-5 | 1 | 0.800 | 0.201 | 0.200 | 0 | 1/3 | 1.732 | 2.14 | 3.0 | 0.99 | 0.97 |
|  |  |  |  |  |  | 1 |  | 2.09 | 3.0 | 0.96 | 0.92 |
|  |  |  |  |  |  | 3 |  | 1.93 | 3.0 | 0.89 | 0.77 |
| S-6 | 1 | 0.800 | 0.401 | 0.200 | 0 | 0 | 1 | 2.15 | 3.0 | 1 | 1 |
| S-7 | 1 | 0.800 | 0.401 | 0.200 | 0 | 1/3 | 1 | 2.09 | 3.0 | 0.97 | 0.96 |
|  |  |  |  |  |  | 1 |  | 1.98 | 3.0 | 0.92 | 0.88 |
|  |  |  |  |  |  | 3 |  | 1.65 | 3.0 | 0.77 | 0.64 |
| S-8 | 1 | 0.800 | 0.401 | 0.200 | 0 | 0 | 1.416 | 1.92 | 3.0 | 1 | 1 |
| S-9 | 1 | 0.800 | 0.401 | 0.200 | 0 | 1/3 | 1.416 | 1.87 | 3.0 | 0.97 | 0.96 |
|  |  |  |  |  |  | 1 |  | 1.78 | 3.0 | 0.93 | 0.88 |
|  |  |  |  |  |  | 3 |  | 1.51 | 3.0 | 0.79 | 0.64 |
| S-12 | 3 | 0.644 | 0.162 | 0.119 | 0 | 0 | 1.250 | 2.12 | 2.36 | 1 | 1 |
|  |  |  |  | 0.118 | 0.560 |  |  | 2.05 | 2.36 | 1 | 1 |
|  |  |  |  | 0.115 | 0.560 |  |  | 2.06 | 2.36 | 1 | 1 |
| S-14 | 3 | 0.644 | 0.162 | 0.119 | 0 | 1/3 | 1.250 | 2.05 | 2.36 | 0.97 | 0.98 |
|  |  |  |  | 0.118 | 0.560 |  |  | 1.99 | 2.36 | 0.97 | 0.97 |
|  |  |  |  | 0.115 | 0.560 |  |  | 1.96 | 2.36 | 0.95 | 0.97 |
|  |  |  |  | 0.119 | 0 | 1 | 1.250 | 1.92 | 2.36 | 0.91 | 0.93 |
|  |  |  |  | 0.118 | 0.560 |  |  | 1.86 | 2.36 | 0.91 | 0.92 |
|  |  |  |  | 0.115 | 0.560 |  |  | 1.81 | 2.36 | 1.88 | 0.92 |
|  |  |  |  | 0.119 | 0 | 3 | 1.250 | 1.52 | 2.36 | 0.72 | 0.80 |
|  |  |  |  | 0.118 | 0.560 |  |  | 1.48 | 2.36 | 0.72 | 0.78 |
|  |  |  |  | 0.115 | 0.560 |  |  | 1.21 | 2.36 | 0.59 | 0.78 |
| S-13 | 3 | 0.644 | 0.162 | 0.119 | 0 | 0 | 1.695 | 1.94 | 2.36 | 1 | 1 |
|  |  |  |  | 0.118 | 0.560 |  |  | 1.82 | 2.36 | 1 | 1 |
|  |  |  |  | 0.115 | 0.560 |  |  | 1.85 | 2.36 | 1 | 1 |
| S-15 | 3 | 0.644 | 0.162 | 0.119 | 0 | 1/3 | 1.695 | 1.90 | 2.36 | 0.97 | 0.98 |
|  |  |  |  | 0.118 | 0.560 |  |  | 1.76 | 2.36 | 0.97 | 0.97 |
|  |  |  |  | 0.115 | 0.560 |  |  | 1.79 | 2.36 | 0.97 | 0.97 |
|  |  |  |  | 0.119 | 0 | 1 | 1.695 | 1.80 | 2.36 | 0.93 | 0.93 |
|  |  |  |  | 0.118 | 0.560 |  |  | 1.63 | 2.36 | 0.90 | 0.92 |
|  |  |  |  | 0.115 | 0.560 |  |  | 1.68 | 2.36 | 0.91 | 0.92 |
|  |  |  |  | 0.119 | 0 | 3 | 1.695 | 1.51 | 2.36 | 0.78 | 0.80 |
|  |  |  |  | 0.118 | 0.560 |  |  | 1.24 | 2.36 | 0.68 | 0.78 |
|  |  |  |  | 0.115 | 0.560 |  |  | 1.33 | 2.36 | 0.72 | 0.78 |
| S-18 | 5 | 0.630 | 0.151 | 0.074 | 0 | 0 | 1.262 | 2.08 | 3.33 | 1 | 1 |
|  |  |  |  |  | 0.357 |  |  | 2.01 | 3.33 | 1 | 1 |
|  |  |  |  |  | 0.357 |  |  | 1.98 | 3.33 | 1 | 1 |
|  |  |  |  |  | 0.715 |  |  | 1.87 | 3.33 | 1 | 1 |
|  |  |  |  |  | 0.715 |  |  | 1.87 | 3.33 | 1 | 1 |

(Continued)

TABLE 20 (Concluded)

| No. | N | R | h | b | x | k | n | $\sigma_p'$ EXPT | $\sigma_p'$ TA | $\dfrac{\sigma_p(k)}{\sigma_p(0)}$ EXPT | $\dfrac{\sigma_p(k)}{\sigma_p(0)}$ HYP$^{xk}$ |
|---|---|---|---|---|---|---|---|---|---|---|---|
| S-21 | 5 | 0.630 | 0.151 | 0.074 | 0 | 1/3 | 1.262 | 2.07 | 3.33 | 1 | 0.98 |
| | | | | | 0.357 | | | 2.01 | 3.33 | 1 | 0.98 |
| | | | | | 0.357 | | | 1.98 | 3.33 | 1 | 0.98 |
| | | | | | 0.715 | | | 1.87 | 3.33 | 1 | 0.97 |
| | | | | | 0.715 | | | 1.85 | 3.33 | 0.99 | 0.97 |
| | | | | | 0 | 1 | 1.262 | 2.06 | 3.33 | 0.99 | 0.94 |
| | | | | | 0.357 | | | 2.01 | 3.33 | 1 | 0.94 |
| | | | | | 0.357 | | | 1.98 | 3.33 | 1 | 0.94 |
| | | | | | 0.715 | | | 1.86 | 3.33 | 1 | 0.93 |
| | | | | | 0.715 | | | 1.82 | 3.33 | 0.97 | 0.93 |
| | | | | | 0 | 3 | 1.262 | 2.02 | 3.33 | 0.97 | 0.82 |
| | | | | | 0.357 | | | 2.01 | 3.33 | 1 | 0.81 |
| | | | | | 0.357 | | | 1.98 | 3.33 | 1 | 0.81 |
| | | | | | 0.715 | | | 1.84 | 3.33 | 0.98 | 0.79 |
| | | | | | 0.715 | | | 1.72 | 3.33 | 0.92 | 0.79 |
| S-19 | 5 | 0.630 | 0.151 | 0.074 | 0 | 0 | 1.665 | 2.06 | 3.33 | 1 | 1 |
| | | | | | 0.357 | | | 2.03 | 3.33 | 1 | 1 |
| | | | | | 0.357 | | | 2.01 | 3.33 | 1 | 1 |
| | | | | | 0.715 | | | 1.86 | 3.33 | 1 | 1 |
| | | | | | 0.715 | | | 1.88 | 3.33 | 1 | 1 |
| S-22 | 5 | 0.630 | 0.151 | 0.074 | 0 | 1/3 | 1.665 | 2.05 | 3.33 | 1 | 0.98 |
| | | | | | 0.357 | | | 2.02 | 3.33 | 0.99 | 0.98 |
| | | | | | 0.357 | | | 2.00 | 3.33 | 0.99 | 0.98 |
| | | | | | 0.715 | | | 1.84 | 3.33 | 0.99 | 0.97 |
| | | | | | 0.715 | | | 1.85 | 3.33 | 0.98 | 0.97 |
| | | | | | 0 | 1 | | 2.04 | 3.33 | 0.99 | 0.94 |
| | | | | | 0.357 | | | 2.00 | 3.33 | 0.98 | 0.93 |
| | | | | | 0.357 | | | 1.97 | 3.33 | 0.98 | 0.93 |
| | | | | | 0.715 | | | 1.80 | 3.33 | 0.97 | 0.93 |
| | | | | | 0.715 | | | 1.80 | 3.33 | 0.96 | 0.93 |
| | | | | | 0 | 3 | | 1.99 | 3.33 | 0.97 | 0.81 |
| | | | | | 0.357 | | | 1.93 | 3.33 | 0.95 | 0.80 |
| | | | | | 0.357 | | | 1.88 | 3.33 | 0.94 | 0.80 |
| | | | | | 0.715 | | | 1.67 | 3.33 | 0.90 | 0.79 |
| | | | | | 0.715 | | | 1.66 | 3.33 | 0.88 | 0.79 |
| S-23 | 5 | 0.630 | 0.151 | 0.074 | 0 | 1/3 | 1.665 | 2.03 | 3.33 | 0.99 | 0.98 |
| | | | | | 0.357 | | | 2.01 | 3.33 | 0.99 | 0.98 |
| | | | | | 0.357 | | | 2.00 | 3.33 | 0.99 | 0.98 |
| | | | | | 0.715 | | | 1.83 | 3.33 | 0.98 | 0.97 |
| | | | | | 0.715 | | | 1.83 | 3.33 | 0.97 | 0.97 |
| | | | | | 0 | 1 | | 1.98 | 3.33 | 0.96 | 0.94 |
| | | | | | 0.357 | | | 1.96 | 3.33 | 0.97 | 0.93 |
| | | | | | 0.357 | | | 1.95 | 3.33 | 0.97 | 0.93 |
| | | | | | 0.715 | | | 1.77 | 3.33 | 0.95 | 0.93 |
| | | | | | 0.715 | | | 1.75 | 3.33 | 0.93 | 0.93 |
| | | | | | 0 | 3 | | 1.82 | 3.33 | 0.88 | 0.81 |
| | | | | | 0.357 | | | 1.81 | 3.33 | 0.89 | 0.80 |
| | | | | | 0.357 | | | 1.80 | 3.33 | 0.89 | 0.80 |
| | | | | | 0.715 | | | 1.58 | 3.33 | 0.85 | 0.79 |
| | | | | | 0.715 | | | 1.52 | 3.33 | 0.81 | 0.79 |

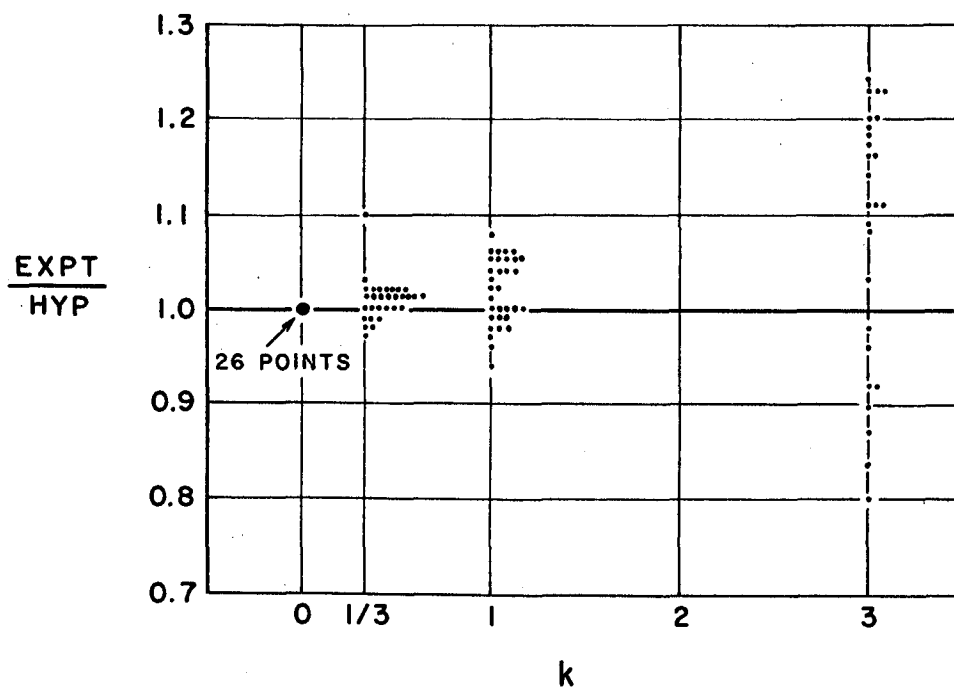HYP$^{xk}$ = modified hypothesis for $f(x)$ and $f(k)$ as included in Equation 10.

Figure 26. Scatter diagram of variation of pillar loading with k with the hypothesis modified.

Analysis of Data for f(n)

        The hypothesis indicates that pillar loading should vary with the relative deformability of the pillar rock. This relative deformability is represented by the parameter $n = E/E_p$. To examine the validity of the function contained in the hypothesis, a scatter diagram was plotted of the ratio of experimental to calculated values normalized to n = 1 (i.e., expressed as a ratio of the value at n = 1) against n. In this case, only the results of model series S are used, as shown in Table 21 using Equation 10; the deformability of the pillars was constant in all other series.

        Figure 27 shows this scatter diagram. This figure suggests that the functional relation as contained in the hypothesis is a good representation of the variation of pillar loadings with n. The mean of these ratios is 0.98 and the coefficient of variation 3.2 per cent.

Analysis of Data for f(R) or f(r)

        The most significant parameter governing pillar loadings is, of course, the extraction ratio, R, or, as shown above, the local extraction ratio, r. A scatter diagram is plotted of the ratio of experimental to calculated values (using Equations 11, 12, and 13) against the local extraction ratio, r. Model series A, B, C, D, E, F, T, V, and S have been used for this scatter diagram. Model series U has been excluded for the reason mentioned previously. Where necessary owing to new empirical functions, the hypothesis values have been recalculated and are included in Tables 22 to 25.

        Figure 28 shows the scatter diagram and indicates that the average of all the experimental data is close to the calculated values. The dispersion of values is greater than is desirable; however, when the sources of errors in the various experimental techniques are considered, the amount of dispersion becomes more acceptable. Indeed, because results for the various series have been independently determined it is considered that the correspondence with the hypothesis is very good. The actual mean value of EXPT/HYP is 0.99 and the coefficient of variation is 8.7 per cent.

### TABLE 21

Analysis of Data from Steel Models for $f(n)$

$k = 0, \mu = 0.290$

| No. | N | R | h | b | x | n | $\dfrac{\sigma_p(n > 1)}{\sigma_p(n = 1)}$ EXPT | $\dfrac{\sigma_p(n > 1)}{\sigma_p(n = 1)}$ HYP$^{xk}$ |
|-----|---|---|---|---|---|---|------|------|
| S-3 | 1 | 0.800 | 0.201 | 0.200 | 0 | 1.300 | 0.930 | 0.943 |
| S-4 | 1 | 0.800 | 0.201 | 0.200 | 0 | 1.732 | 0.885 | 0.875 |
| S-8 | 1 | 0.800 | 0.401 | 0.200 | 0 | 1.416 | 0.894 | 0.887 |
| S-12 | 3 | 0.644 | 0.162 | 0.119 | 0 | 1.250 | 0.960 | 0.965 |
|  |  |  |  | 0.118 | 0.560 |  | 0.950 | 0.966 |
|  |  |  |  | 0.115 | 0.560 |  | 0.950 | 0.966 |
| S-13 | 3 | 0.644 | 0.162 | 0.119 | 0 | 1.695 | 0.878 | 0.901 |
|  |  |  |  | 0.118 | 0.560 |  | 0.843 | 0.903 |
|  |  |  |  | 0.115 | 0.560 |  | 0.854 | 0.903 |
| S-18 | 5 | 0.630 | 0.151 | 0.074 | 0 | 1.262 | 0.950 | 0.962 |
|  |  |  |  |  | 0.357 |  | 0.922 | 0.964 |
|  |  |  |  |  | 0.357 |  | 0.912 | 0.964 |
|  |  |  |  |  | 0.715 |  | 0.886 | 0.961 |
|  |  |  |  |  | 0.715 |  | 0.886 | 0.961 |
| S-19 | 5 | 0.630 | 0.151 | 0.074 | 0 | 1.665 | 0.940 | 0.912 |
|  |  |  |  |  | 0.357 |  | 0.931 | 0.915 |
|  |  |  |  |  | 0.357 |  | 0.926 | 0.915 |
|  |  |  |  |  | 0.715 |  | 0.882 | 0.908 |
|  |  |  |  |  | 0.715 |  | 0.890 | 0.908 |

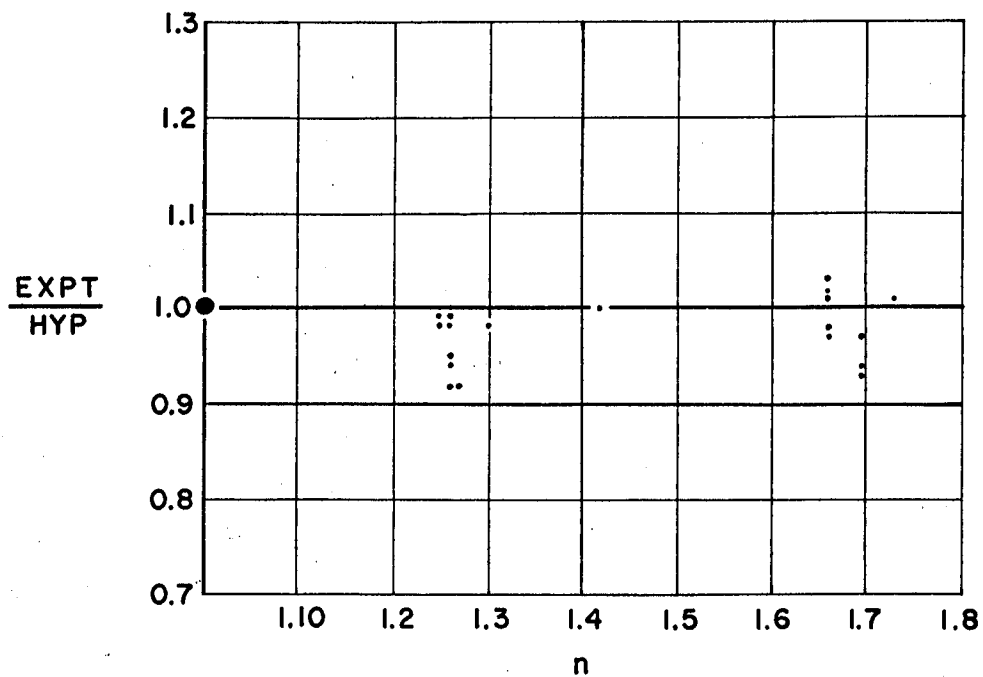HYP$^{xk}$ = modified hypothesis as included in Equation 10.

Figure 27. Scatter diagram of variation of pillar loading with n.

## TABLE 22

Analysis of Data from Gelatin Models for $f(R)$ with Alternate $f(k)$

$k = 0.5, \ \mu = 0.5, \ n = 1$

| No. | N | R | h | b | x | $\Delta\sigma_p'$ EXPT | $\Delta\sigma_p'$ TA | $\Delta\sigma_p'$ HYP$^{xk}$ |
|-----|---|---|---|---|---|------|----|--------|
| T-1 | 7 | 0.604 | 0.226 | 0.057 | 0 | 1.12 | 1.33 | 1.10 |
|  |  |  |  |  | 0.264 | 1.03 | 1.33 | 1.05 |
|  |  |  |  |  | 0.528 | 1.00 | 1.33 | 1.00 |
|  |  |  |  |  | 0.792 | 0.75 | 1.33 | 0.95 |
| T-2 | 7 | 0.656 | 0.197 | 0.049 | 0 | 1.35 | 1.67 | 1.39 |
|  |  |  |  |  | 0.262 | 1.22 | 1.67 | 1.36 |
|  |  |  |  |  | 0.525 | 1.22 | 1.67 | 1.26 |
|  |  |  |  |  | 0.787 | 1.11 | 1.67 | 1.17 |
| T-3 | 7 | 0.696 | 0.174 | 0.043 | 0 | 1.77 | 2.00 | 1.70 |
|  |  |  |  |  | 0.261 | 1.56 | 2.00 | 1.60 |
|  |  |  |  |  | 0.522 | 1.51 | 2.00 | 1.49 |
|  |  |  |  |  | 0.783 | 1.35 | 2.00 | 1.41 |
| T-4 | 7 | 0.728 | 0.156 | 0.039 | 0 | 2.06 | 2.34 | 2.00 |
|  |  |  |  |  | 0.260 | 2.06 | 2.34 | 1.89 |
|  |  |  |  |  | 0.520 | 1.56 | 2.34 | 1.77 |
|  |  |  |  |  | 0.780 | 1.36 | 2.34 | 1.66 |
| T-5 | 7 | 0.753 | 0.141 | 0.035 | 0 | 2.17 | 2.87 | 2.25 |
|  |  |  |  |  | 0.259 | 2.00 | 2.87 | 2.12 |
|  |  |  |  |  | 0.518 | 1.84 | 2.87 | 1.99 |
|  |  |  |  |  | 0.777 | 1.55 | 2.87 | 1.85 |
| T-6 | 7 | 0.696 | 0.087 | 0.043 | 0 | 1.61 | 2.00 | 1.89 |
|  |  |  |  |  | 0.261 | 1.55 | 2.00 | 1.79 |
|  |  |  |  |  | 0.522 | 1.46 | 2.00 | 1.68 |
|  |  |  |  |  | 0.783 | 1.38 | 2.00 | 1.59 |
| T-7 | 7 | 0.696 | 0.130 | 0.043 | 0 | 1.56 | 2.00 | 1.78 |
|  |  |  |  |  | 0.261 | 1.56 | 2.00 | 1.69 |
|  |  |  |  |  | 0.522 | 1.51 | 2.00 | 1.59 |
|  |  |  |  |  | 0.783 | 1.38 | 2.00 | 1.49 |
| T-9 | 7 | 0.696 | 0.232 | 0.043 | 0 | 1.78 | 2.00 | 1.58 |
|  |  |  |  |  | 0.261 | 1.56 | 2.00 | 1.50 |
|  |  |  |  |  | 0.522 | 1.51 | 2.00 | 1.41 |
|  |  |  |  |  | 0.783 | 1.38 | 2.00 | 1.33 |
| T-10 | 7 | 0.696 | 0.290 | 0.043 | 0 | 1.72 | 2.00 | 1.49 |
|  |  |  |  |  | 0.261 | 1.55 | 2.00 | 1.41 |
|  |  |  |  |  | 0.522 | 1.43 | 2.00 | 1.34 |
|  |  |  |  |  | 0.783 | 0.94 | 2.00 | 1.24 |
| T-11 | 1 | 0.727 | 1.090 | 0.273 | 0 | 0.83 | 1.33 | 0.78 |
| T-12 | 1 | 0.800 | 0.800 | 0.200 | 0 | 1.16 | 2.00 | 1.20 |
| T-13 | 1 | 0.833 | 0.632 | 0.158 | 0 | 1.50 | 2.50 | 1.45 |
| T-14 | 1 | 0.800 | 0.400 | 0.200 | 0 | 1.30 | 2.00 | 1.40 |
| T-15 | 1 | 0.800 | 1.333 | 0.200 | 0 | 1.05 | 2.00 | 1.00 |
| V-1 | 8 | 0.600 | 0.200 | 0.050 | 0.117 | 1.03 | 1.33 | 1.11 |
|  |  |  |  |  | 0.350 | 0.97 | 1.33 | 1.05 |
|  |  |  |  |  | 0.584 | 0.91 | 1.33 | 0.99 |
|  |  |  |  |  | 0.817 | 0.74 | 1.33 | 0.92 |

HYP$^{xk}$ = hypothesis modified as included in Equation 11.

TABLE 23

Analysis of Data from Araldite Models for f(R) with Alternate f(k)

$k = 0$, $\mu = 0.435$, $n = 1$

| No. | N | R | h | b | k | $\sigma_p'$ EXPT | $\sigma_p'$ TA | $\sigma_p'$ HYP$^{xk}$ |
|-----|---|------|------|------|------|------|------|------|
| E-1 | 1 | 0.667 | 0.333 | 0.333 | 0 | 1.9 | 1.5 | 1.92 |
|     |   |       |       |       | 0.333 | 1.9 | 1.5 | 1.86 |
|     |   |       |       |       | 1 | 1.8 | 1.5 | 1.73 |
| E-2 | 1 | 0.800 | 0.400 | 0.200 | 0 | 2.6 | 2.5 | 2.58 |
|     |   |       |       |       | 0.333 | 2.5 | 2.5 | 2.48 |
|     |   |       |       |       | 1 | 2.3 | 2.5 | 2.28 |
| E-3 | 1 | 0.889 | 0.444 | 0.111 | 0 | 3.7 | 4.52 | 3.54 |
|     |   |       |       |       | 0.333 | 3.4 | 4.52 | 3.32 |
|     |   |       |       |       | 1 | 3.1 | 4.52 | 2.91 |
| F-1 | 1 | 0.572 | 0.345 | 0.429 | 0 | 1.8 | 1.67 | 1.67 |
|     |   |       |       |       | 0.333 | 1.7 | 1.67 | 1.61 |
|     |   |       |       |       | 1 | 1.6 | 1.67 | 1.49 |
| F-2 | 1 | 0.762 | 0.457 | 0.238 | 0 | 2.55 | 2.60 | 2.35 |
|     |   |       |       |       | 0.333 | 2.45 | 2.60 | 2.26 |
|     |   |       |       |       | 1 | 2.25 | 2.60 | 2.05 |
| F-3 | 1 | 0.904 | 0.543 | 0.096 | 0 | 3.85 | 5.71 | 3.61 |
|     |   |       |       |       | 0.333 | 3.7 | 5.71 | 3.52 |
|     |   |       |       |       | 1 | 3.4 | 5.71 | 3.19 |

HYP$^{xk}$ = modified hypothesis as included in Equation 12.

TABLE 24

Analysis of Data from Mortar Models for f(R) with Alternate f(k)

$x = 0$, $k = 0.1$, $\mu = 0.1$, $n = 1$

| No. | N | R | h | b | z/ℓ | $\sigma_p'$ EXPT | $\sigma_p'$ TA | $\sigma_p'$ HYP$^{xk}$ |
|-----|---|-------|-------|-------|------|------|------|------|
| T-16 | 1 | 0.727 | 1.09 | 0.273 | 5.45 | 1.90 | 2.33 | 2.25 |
| T-17 | 1 | 0.800 | 0.800 | 0.200 | 4.00 | 2.36 | 3.00 | 2.51 |
| T-18 | 1 | 0.833 | 0.632 | 0.158 | 3.16 | 2.74 | 3.50 | 2.73 |
| T-19 | 1 | 0.800 | 0.400 | 0.200 | 4.00 | 2.51 | 3.00 | 2.49 |
| T-20 | 1 | 0.800 | 1.333 | 0.200 | 4.00 | 2.34 | 3.00 | 2.70 |

HYP$^{xk}$ = hypothesis modified as included in Equation 12.

## TABLE 25

Analysis of Data from Steel Models for f(R) with Alternate f(b,k)

$$\mu = 0.290$$

| No. | N | R | h | b | x | k | n | $\sigma'_p$ EXPT | $\sigma'_p$ TA | $\sigma'_p$ HYP×bk |
|-----|---|---|---|---|---|---|---|------|----|--------|
| S-5 | 1 | 0.800 | 0.201 | 0.200 | 0 | 1/3 | 1.732 | 2.14 | 3.0 | 2.26 |
|     |   |       |       |       |   | 1   |       | 2.09 | 3.0 | 2.14 |
|     |   |       |       |       |   | 3   |       | 1.93 | 3.0 | 1.78 |
| S-7 | 1 | 0.800 | 0.401 | 0.200 | 0 | 1/3 | 1 | 2.09 | 3.0 | 2.46 |
|     |   |       |       |       |   | 1   | 1 | 1.98 | 3.0 | 2.25 |
|     |   |       |       |       |   | 3   | 1 | 1.65 | 3.0 | 1.63 |
| S-9 | 1 | 0.800 | 0.401 | 0.200 | 0 | 1/3 | 1.416 | 1.87 | 3.0 | 2.18 |
|     |   |       |       |       |   | 1   | 1.416 | 1.78 | 3.0 | 2.00 |
|     |   |       |       |       |   | 3   | 1.416 | 1.51 | 3.0 | 1.46 |
| S-14 | 3 | 0.644 | 0.162 | 0.119 | 0 | 1/3 | 1.250 | 2.05 | 2.36 | 2.19 |
|      |   |       |       |       |   | 1   |       | 1.88 | 2.36 | 2.09 |
|      |   |       |       |       |   | 3   |       | 1.42 | 2.36 | 1.80 |
|      |   |       |       | 0.118 | 0.560 | 1/3 |    | 1.97 | 2.36 | 1.94 |
|      |   |       |       |       |   | 1   |       | 1.81 | 2.36 | 1.84 |
|      |   |       |       |       |   | 3   |       | 1.35 | 2.36 | 1.55 |
|      |   |       |       | 0.115 | 0.560 | 1/3 |    | 1.96 | 2.36 | 1.94 |
|      |   |       |       |       |   | 1   |       | 1.80 | 2.36 | 1.84 |
|      |   |       |       |       |   | 3   |       | 1.28 | 2.36 | 1.55 |
| S-15 | 3 | 0.644 | 0.162 | 0.119 | 0 | 1/3 | 1.695 | 1.92 | 2.36 | 2.04 |
|      |   |       |       |       |   | 1   |       | 1.83 | 2.36 | 1.95 |
|      |   |       |       |       |   | 3   |       | 1.54 | 2.36 | 1.68 |
|      |   |       |       | 0.118 | 0.560 | 1/3 |    | 1.82 | 2.36 | 1.81 |
|      |   |       |       |       |   | 1   |       | 1.69 | 2.36 | 1.72 |
|      |   |       |       |       |   | 3   |       | 1.29 | 2.36 | 1.45 |
|      |   |       |       | 0.115 | 0.560 | 1/3 |    | 1.79 | 2.36 | 1.81 |
|      |   |       |       |       |   | 1   |       | 1.68 | 2.36 | 1.72 |
|      |   |       |       |       |   | 3   |       | 1.33 | 2.36 | 1.45 |
| S-21 | 5 | 0.630 | 0.151 | 0.074 | 0 | 1/3 | 1.262 | 2.07 | 3.33 | 2.26 |
|      |   |       |       |       |   | 1   |       | 2.06 | 3.33 | 2.17 |
|      |   |       |       |       |   | 3   |       | 2.02 | 3.33 | 1.89 |
|      |   |       |       |       | 0.357 | 1/3 |  | 2.01 | 3.33 | 2.11 |
|      |   |       |       |       |   | 1   |       | 2.01 | 3.33 | 2.02 |
|      |   |       |       |       |   | 3   |       | 2.01 | 3.33 | 1.74 |
|      |   |       |       |       | 0.357 | 1/3 |  | 1.98 | 3.33 | 2.11 |
|      |   |       |       |       |   | 1   |       | 1.98 | 3.33 | 2.02 |
|      |   |       |       |       |   | 3   |       | 1.98 | 3.33 | 1.74 |
|      |   |       |       |       | 0.715 | 1/3 | 1.262 | 1.87 | 3.33 | 1.94 |
|      |   |       |       |       |   | 1   |       | 1.86 | 3.33 | 1.85 |
|      |   |       |       |       |   | 3   |       | 1.84 | 3.33 | 1.57 |
|      |   |       |       |       | 0.715 | 1/3 |  | 1.85 | 3.33 | 1.94 |
|      |   |       |       |       |   | 1   |       | 1.82 | 3.33 | 1.85 |
|      |   |       |       |       |   | 3   |       | 1.72 | 3.33 | 1.57 |

(Continued)

TABLE 25 (Concluded)

| No. | N | R | h | b | x | k | n | $\sigma_p'$ EXPT | $\sigma_p'$ TA | $\sigma_p'$ HYP$^{xbk}$ |
|---|---|---|---|---|---|---|---|---|---|---|
| S-22 | 5 | 0.630 | 0.151 | 0.074 | 0 | 1/3 | 1.665 | 2.05 | 3.33 | 2.14 |
| | | | | | | 1 | | 2.04 | 3.33 | 2.05 |
| | | | | | | 3 | | 1.99 | 3.33 | 1.78 |
| | | | | | 0.357 | 1/3 | | 2.02 | 3.33 | 2.00 |
| | | | | | | 1 | | 2.00 | 3.33 | 1.91 |
| | | | | | | 3 | | 1.93 | 3.33 | 1.64 |
| | | | | | 0.357 | 1/3 | | 2.00 | 3.33 | 2.00 |
| | | | | | | 1 | | 1.97 | 3.33 | 1.91 |
| | | | | | | 3 | | 1.88 | 3.33 | 1.04 |
| | | | | | 0.715 | 1/3 | | 1.84 | 3.33 | 1.83 |
| | | | | | | 1 | | 1.80 | 3.33 | 1.74 |
| | | | | | | 3 | | 1.67 | 3.33 | 1.49 |
| | | | | | 0.715 | 1/3 | | 1.85 | 3.33 | 1.83 |
| | | | | | | 1 | | 1.80 | 3.33 | 1.74 |
| | | | | | | 3 | | 1.66 | 3.33 | 1.49 |
| S-23 | 5 | 0.630 | 0.151 | 0.074 | 0 | 1/3 | 1.665 | 2.03 | 3.33 | 2.14 |
| | | | | | | 1 | | 1.98 | 3.33 | 2.05 |
| | | | | | | 3 | | 1.82 | 3.33 | 1.78 |
| | | | | | 0.357 | 1/3 | | 2.01 | 3.33 | 2.00 |
| | | | | | | 1 | | 1.96 | 3.33 | 1.91 |
| | | | | | | 3 | | 1.81 | 3.33 | 1.04 |
| | | | | | 0.357 | 1/3 | | 2.00 | 3.33 | 2.00 |
| | | | | | | 1 | | 1.95 | 3.33 | 1.91 |
| | | | | | | 3 | | 1.80 | 3.33 | 1.64 |
| | | | | | 0.715 | 1/3 | | 1.83 | 3.33 | 1.83 |
| | | | | | | 1 | | 1.77 | 3.33 | 1.74 |
| | | | | | | 3 | | 1.58 | 3.33 | 1.49 |
| | | | | | 0.715 | 1/3 | | 1.83 | 3.33 | 1.83 |
| | | | | | | 1 | | 1.75 | 3.33 | 1.74 |
| | | | | | | 3 | | 1.52 | 3.33 | 1.49 |
| S-30 | 5 | 0.621 | 0.148 | 0.0708 | 0 | 1/3 | 1 | 2.30 | -- | 2.40 |
| | | | | | | 1 | | 2.27 | -- | 2.31 |
| | | | | | | 3 | | 2.17 | -- | 2.02 |
| | | | | 0.0651 | 0.342 | 1/3 | | 2.31 | -- | 2.32 |
| | | | | | | 1 | | 2.28 | -- | 2.25 |
| | | | | | | 3 | | 2.18 | -- | 1.96 |
| | | | | 0.0887 | 0.367 | 1/3 | | 2.11 | -- | 1.99 |
| | | | | | | 1 | | 2.05 | -- | 1.90 |
| | | | | | | 3 | | 1.86 | -- | 1.61 |
| | | | | 0.0893 | 0.705 | 1/3 | | 2.01 | -- | 1.83 |
| | | | | | | 1 | | 1.95 | -- | 1.74 |
| | | | | | | 3 | | 1.78 | -- | 1.45 |
| | | | | 0.0651 | 0.729 | 1/3 | | 2.18 | -- | 2.17 |
| | | | | | | 1 | | 2.10 | -- | 2.08 |
| | | | | | | 3 | | 1.87 | -- | 1.79 |

HYP$^{xbk}$ = hypothesis modified as included in Equation 12.

Figure 28. Scatter diagram of variation of pillar loading with r.

TABLE 25 (Concluded)

| No. | N | R | h | b | x | k | n | $\sigma_p'$ EXPT | $\sigma_p'$ TA | $\sigma_p'$ HYP$^{xbk}$ |
|---|---|---|---|---|---|---|---|---|---|---|
| S-22 | 5 | 0.630 | 0.151 | 0.074 | 0 | 1/3 | 1.665 | 2.05 | 3.33 | 2.14 |
| | | | | | | 1 | | 2.04 | 3.33 | 2.05 |
| | | | | | | 3 | | 1.99 | 3.33 | 1.78 |
| | | | | | 0.357 | 1/3 | | 2.02 | 3.33 | 2.00 |
| | | | | | | 1 | | 2.00 | 3.33 | 1.91 |
| | | | | | | 3 | | 1.93 | 3.33 | 1.64 |
| | | | | | 0.357 | 1/3 | | 2.00 | 3.33 | 2.00 |
| | | | | | | 1 | | 1.97 | 3.33 | 1.91 |
| | | | | | | 3 | | 1.88 | 3.33 | 1.04 |
| | | | | | 0.715 | 1/3 | | 1.84 | 3.33 | 1.83 |
| | | | | | | 1 | | 1.80 | 3.33 | 1.74 |
| | | | | | | 3 | | 1.67 | 3.33 | 1.49 |
| | | | | | 0.715 | 1/3 | | 1.85 | 3.33 | 1.83 |
| | | | | | | 1 | | 1.80 | 3.33 | 1.74 |
| | | | | | | 3 | | 1.66 | 3.33 | 1.49 |
| S-23 | 5 | 0.630 | 0.151 | 0.074 | 0 | 1/3 | 1.665 | 2.03 | 3.33 | 2.14 |
| | | | | | | 1 | | 1.98 | 3.33 | 2.05 |
| | | | | | | 3 | | 1.82 | 3.33 | 1.78 |
| | | | | | 0.357 | 1/3 | | 2.01 | 3.33 | 2.00 |
| | | | | | | 1 | | 1.96 | 3.33 | 1.91 |
| | | | | | | 3 | | 1.81 | 3.33 | 1.04 |
| | | | | | 0.357 | 1/3 | | 2.00 | 3.33 | 2.00 |
| | | | | | | 1 | | 1.95 | 3.33 | 1.91 |
| | | | | | | 3 | | 1.80 | 3.33 | 1.64 |
| | | | | | 0.715 | 1/3 | | 1.83 | 3.33 | 1.83 |
| | | | | | | 1 | | 1.77 | 3.33 | 1.74 |
| | | | | | | 3 | | 1.58 | 3.33 | 1.49 |
| | | | | | 0.715 | 1/3 | | 1.83 | 3.33 | 1.83 |
| | | | | | | 1 | | 1.75 | 3.33 | 1.74 |
| | | | | | | 3 | | 1.52 | 3.33 | 1.49 |
| S-30 | 5 | 0.621 | 0.148 | 0.0708 | 0 | 1/3 | 1 | 2.30 | -- | 2.40 |
| | | | | | | 1 | | 2.27 | -- | 2.31 |
| | | | | | | 3 | | 2.17 | -- | 2.02 |
| | | | | 0.0651 | 0.342 | 1/3 | | 2.31 | -- | 2.32 |
| | | | | | | 1 | | 2.28 | -- | 2.25 |
| | | | | | | 3 | | 2.18 | -- | 1.96 |
| | | | | 0.0887 | 0.367 | 1/3 | | 2.11 | -- | 1.99 |
| | | | | | | 1 | | 2.05 | -- | 1.90 |
| | | | | | | 3 | | 1.86 | -- | 1.61 |
| | | | | 0.0893 | 0.705 | 1/3 | | 2.01 | -- | 1.83 |
| | | | | | | 1 | | 1.95 | -- | 1.74 |
| | | | | | | 3 | | 1.78 | -- | 1.45 |
| | | | | 0.0651 | 0.729 | 1/3 | | 2.18 | -- | 2.17 |
| | | | | | | 1 | | 2.10 | -- | 2.08 |
| | | | | | | 3 | | 1.87 | -- | 1.79 |

HYP$^{xbk}$ = hypothesis modified as included in Equation 12.

Figure 28. Scatter diagram of variation of pillar loading with r.

# CONCLUSIONS

1. The empirically modified hypothesis for the loading of pillars in long, deep mining zones provides good agreement with measured values and is represented by

$$\frac{\Delta \sigma_p}{S_o} = \frac{2R(1 - x/5 + h) - kh(1 - w + w_p n)}{hn + 1.8(1 - R)(1 + 1/N)(1 + h/(1 - x/5)) + 2Rb(1 - w)/\pi} \qquad \text{Eq. 9}$$

$$\frac{\Delta \sigma_p}{S_o} = \frac{2R(1 - x/5 + h) - kh(1 - w + w_p n)}{hn + 1.8(1 - r)(1 + h/(1 - x/5)) + 2Rb(1 - w)/\pi} \qquad \text{Eq. 10}$$

Equation 9 can be used when the general extraction ratio, R, is known and the local extraction ratio, r, is difficult to determine (e.g., when the breadths of the pillars and openings are irregular). Equation 10 can be used when the local extraction ratios, r, are easily determined.

The hypothesis should be applicable for the ranges in the various parameters covered by the empirical data. Presumably, some extrapolation would be valid, but there is the danger that inaccuracies in the functional relations would become more significant for distinctly different ranges of some of the parameters.

2. The location of the pillar within the mining zone, the parameter x, has been shown by the model studies to be less important than the unmodified hypothesis indicated. The decrease in pillar stress from the centre of the mining zone to the abutments, other things being equal, should only be of the order of 20 per cent.

For this parameter the range in values covered by the empirical data, from zero to 0.8, is substantially the full range that occurs in practice.

3. The laboratory work has substantiated the effect of pillar height as represented by the dimensionless parameter h. The hypothesis indicates that for two mining geometries that are similar, except that in one case a very narrow vein is being mined whereas in the second case a very wide vein is being mined, the pillar loading in the first case could be as much as three times greater than in the second case (see Figure 29). The implications with respect to rockbursts are that a narrow vein would tend to produce pillars having higher stored strain energy densities.

The range in values of the parameter h in the experimental data was from 0.08 to 1.3. There is little likelihood that this range would be exceeded on the high side; however, actual mine geometries could include pillar heights as small as 0.01 of the semi-span of the mining zone. Considering how h affects the mechanics of the problem, it is improbable that the range not covered by the experimental data, i.e., 0.01 to 0.08, would not be predicted by the hypothesis.

4. The breadth of pillar, as contained in the parameter b, for mining geometries with equal widths of stopes and equal breadths of pillars has been shown by this work to be relatively insignificant. However, the laboratory experiments have shown that where the breadths of pillars vary, the pillar loadings could vary greatly, so that the narrower pillars could have average stresses, or energy densities, many times those of the wide pillars.

The range in the parameter b in the experimental work extended from 0.01 to 0.43, which probably covers more than the common range of pillar breadths. Also, the relative difference in breadths of adjacent pillars in the empirical data has been between 1 and 5, which again should cover the majority of actual mine geometries.

5. It was originally thought, as a result of the analyses preceding the formulation of the hypothesis, that the transverse field stress, $S_t$, or the parameter k, would be very important. The modified hypothesis, based on the laboratory experimental data, now indicates that this parameter is relatively insignificant. It would seem that a difference in pillar loading of a maximum of possibly 30 per cent could occur as a result of variation over the probable range of values of k (see Figure 30).

The range in values included in the experimental data for the parameter k was from 0 to 3. Because the actual range in k that can occur in the earth's crust is not known, it must be assumed that the experimental range can be exceeded. Consequently, the hypothesis would have to be used with caution when values of k make it necessary to extrapolate beyond the experimental data.

6. The number of pillars, N, has been shown to be very important in the use of the general extraction ratio to predict pillar loadings.

For the parameter N the range included in the experimental data was from 1 to 8, beyond which N tends to become insignificant.
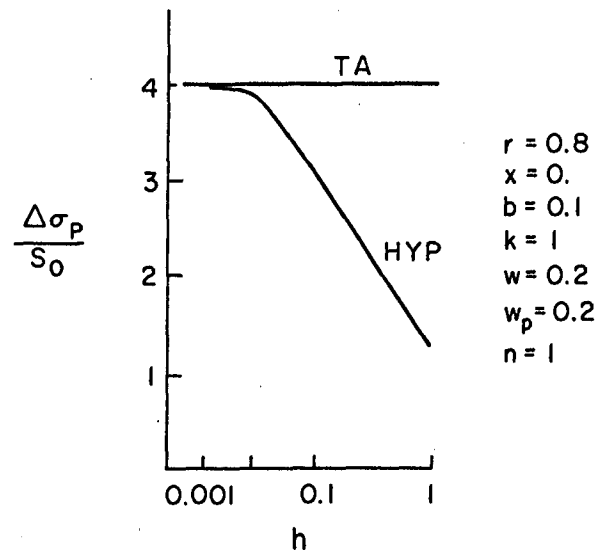
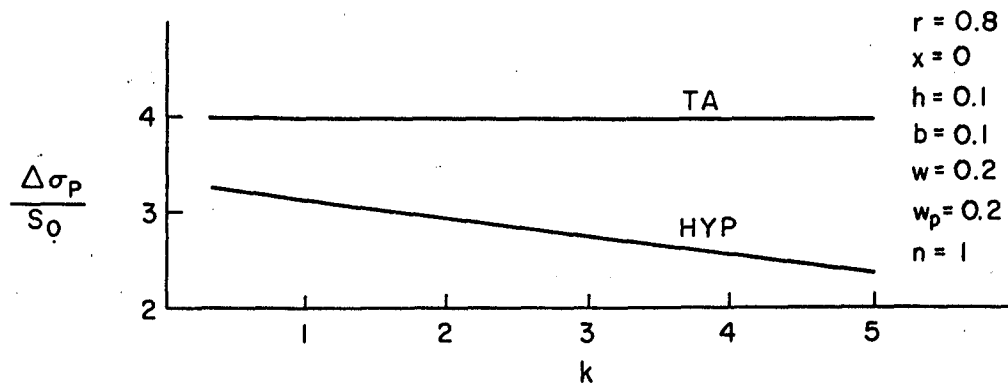Figure 29. Effect of h on pillar loading.



Figure 30. Effect of k on pillar loading.

7.  The hypothesis indicates, and the laboratory work confirms, that the compressibility of the pillar, as represented by the parameter n, is a very important factor in determining pillar stresses. As is indicated by Figure 31, it seems quite possible for pillar loadings to differ considerably with differences in their compressibility. Again, the implications with respect to the stored strain energy and rockbursts are obvious: relatively incompressible pillars could contain stored strain energy of an order of magnitude higher than could pillars with moderate compressibility.

The range in the parameter n covered by the experimental data is from 1 to 1.7. For values of n outside this range, the hypothesis would have to be used with caution.

8.  The extraction ratio R is, of course, the most important parameter governing pillar loading. The range in values covered by the experimental data was from 0.5 to 0.9 for the general extraction ratio, R, and from 0.1 to 0.9 for the local extraction ratio, r, substantially covering the full range required for these parameters.

9.  From observations made during the laboratory work, it seems that the basic mechanisms included in the hypothesis are the effective aspects of the ground reaction resulting from the mining out of openings and the creation of pillars. For example, aside from the numerical corroboration, the shape of the inward deflection curve of the wall rocks was illustrated by the photoelastic experiments which showed a higher concentration of corner stresses on the sides of the pillars towards the centreline of the mining zone.
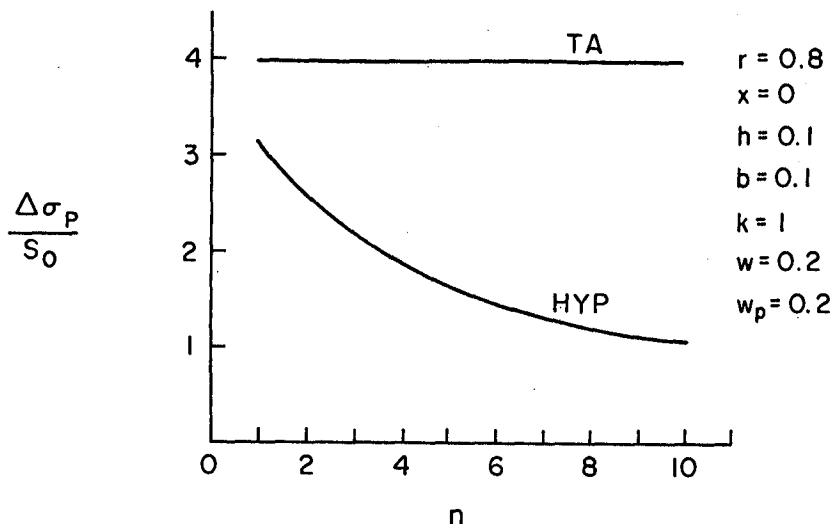
Figure 31. Effect of n on pillar loading.

Also, in experiments with the mortar models, removal of a thin slice of a pillar, which effectively increased the deflection, clearly showed a reduction in the loading resulting from the increased deflection of the walls.

The magnitudes of the stresses between the pillars and the walls associated with the local penetration postulated by the hypothesis were clearly illustrated by all of the photoelastic experiments, and the depth into the walls of these stress concentrations could be seen to be proportional to the breadth of the pillar, supporting the hypothesis which stated that the local penetration was also proportional to the breadth.

Another significant finding in the laboratory work is that joints in rock are unlikely to affect pillar loadings. This was established by placing joints in some of the models in the only area where tensile stresses could occur. Since the remaining zones would not contain tensile stresses, the compressive stresses would be transmitted across the joints in the same way as they would without joints. This, of course, does not include the cases where joints, brecciated or gouge zones, or zones of incompetent secondary mineralization, could provide planes of weak shear resistance.

This additional information is useful because it provides some basis for judging whether the equations of the hypothesis can be used for cases containing parameters outside the ranges that have been empirically substantiated.

10. The equations resulting from the hypothesis for long, shallow mining zones, which have received substantiation from the empirical data applicable to this case, are as follows:

$$\frac{\Delta \sigma_p}{S_o} = \frac{2R(1-x/5+2h)+RK_b'-kh(1-w+2w_p n)}{2hn+(1.8(1+h/(1-x/5))+(2K_b'/3)(1+h/(1-x^2)))(1-R)(1+1/N)+4Rb(1-w)/\pi}$$

Eq. 14

$$\frac{\Delta \sigma_p}{S_o} = \frac{2R(1-x/5+2h)+RK_b'-kh(1-w+2w_p n)}{2hn+(1.8(1+h/(1-x/5))+(2K_b'/3)(1+h/(1-x^2)))(1-r)+4Rb(1-w)/\pi}$$

Eq. 13

One implication of the differentiation between deep and shallow mining zones is that the depth ratio for horizontal workings, $z/L$, is important. Where $z/L$ is small the pillar stress ratio, $\Delta \sigma_p/S_o$, becomes greater than for similar pillars in a deep mining zone.

Another implication of the shallow case is that where z/L is very small the pillar loads can be as much as 50 per cent greater than those produced by the tributary area theory.

The laboratory work indicated that the range of applicability of the equations for shallow mining zones is smaller than the theoretical analysis originally suggested. It seems now that the equation for deep mining zones can be used for values of z/L greater than about 0.4.

## ACKNOWLEDGEMENTS

- - - -

DFC:DV

# BIBLIOGRAPHY

1. Coates, D.F., "Pillar Loading: I. Literature Survey and New Hypothesis", Mines Branch Research Report R 168, Canada Department of Mines and Technical Surveys, Ottawa (1965).

2. Buckingham, E., "On Physically Similar Systems: Illustrations of the Use of Dimensional Equations", Phys. Rev., Vol. 4, p. 345 (1914).

3. Coker, E. and Filon, L., "A Treatise on Photoelasticity", Cambridge University Press, London, p. 473 (1957).

4. Peterson, R., "Stress Concentration Design Factors ", John Wiley and Sons, New York (1953).

5. Bruggeman, J. et al., "Stresses and Pore Pressures Around Circular Openings Near a Boundary", USBR Tech. Memo 597, Denver (1940).

6. Trumbachev, V. and Molodtsova, L., "The Application of the Optical Method for Investigation of Stress Conditions of Rocks Around Mine Workings", Academy of Sciences, Moscow (1963).

7. Trumbachev, V. and Melnikov, E., "Distribution of Stress in Inter-room Pillars and the Immediate Roof", Gosgortekhizdat, Moscow (1961).

8. Crisp, J.D.C., "The Use of Gelatin Models in Structural Analysis", Inst. Mech. Eng. Proc., Vol. 1B, No. 1-12 (1952-1953).

9. Ellis, J.S. and Gent, K.W., "The Use of Gelatin Model in the Photo-elastic Analysis of a Gravity Dam", Eng. J., No. 11 (1953).

10. Murray, N.W., "Discussion on Paper by J.D.C. Crisp", Inst. Mech. Eng. Proc., Vol. 1B, No. 1-12 (1952-1953).

11. Gyenge, M. and Coates, D.F., "Stress Distribution in Slopes Using Photoelasticity - I", unpublished report (1964).

12. Frocht, M.M., "Photoelasticity", John Wiley and Sons, London, Vol. 1 (1941).

13. Avershin, S., "Experiences in Rock Pressure Research", Internat. Strata Control Congress, Leipzig (1958).

14. Hiramatsu, Y. and Oka, Y., "Photoelastic Investigations into the Earth Pressure Acting on Pillars", J. MM Japan, Vol. 79, No. 905 (1963).

15. Nair, O. and Udd, J., "Stresses Around Openings in a Plate Due to Biaxial Loads Through a Superpositioning Technique", Proc. Rock Mech. Symp., Univ. of Toronto; Mines Branch (1965).

16. Ilstein, A., "The Problem of Applying Room System of Mining With Periodical Succession in the Distribution of Barrier and Inter-chamber Pillars", Symp. Methods for the Determination of Dimensions of Support Pillars and Arch Pillars, Academy, of Sciences, Moscow (1962).

17. Hiramatsu, Y., letter (1964).

18. Filon, L., "On the Elastic Equilibrium of Circular Cylinders under Certain Practical Systems of Load", Phil. Trans., Series A, Vol. 198, p. 147 (1902).

19. Pickett, G., "Application of the Fourier Method to the Solution of Certain Boundary Problems in the Theory of Elasticity", J. App. Mech., A 176 (Sept. 1944).

20. Habib, M., "Determination of the Moduli of Elasticity of Rocks In Situ", Inst. Tech. Bat. Trav. Pub. Ann., No. 145, p. 27 (1950).

21. Low, I., "Model Stress Analysis Using the Moire Method", Proc. Rock Mech. Symp., Univ. of Toronto; Mines Branch (1965).

22. Howland, R., "On the Stresses in the Neighbourhood of a Circular Hole in a Strip under Tension", Phil. Trans. Roy. Soc. A., Vol. 229, p. 49 (1929).

23. Reed, J., "Case History in Pillar Recovery", Min. Eng., Vol. 2, p. 701 (July 1959).

APPENDIX

GLOSSARY OF ABBREVIATIONS

(Note:  After many of the terms, letters in brackets
indicate the fundamental dimensions of the physical
quantity; e.g., L stands for length, M for mass,
F for force, T for time, and D signifies that the
quantity is dimensionless.)

| | |
|---|---|
| $a(L)$ | - radius of a circle or major semi-axis of an ellipse |
| $A_o(L^2)$ | - total area of walls adjacent to the mined out rooms or stopes of the entire mining zone |
| $A_p(L^2)$ | - area of a pillar parallel to the walls |
| $A_t(L^2)$ | - area of walls tributary to a pillar |
| $A_T(L^2)$ | - area of walls adjacent to the entire mining zone |
| $b(D)$ | - width of pillar $(B/L)$ |
| $b(L)$ | - minor semi-axis of an ellipse |
| $b_o(D)$ | - width of opening $(B_o/L)$ |
| $B(L)$ | - width of pillar |
| $B_o(L)$ | - width of opening (stope or room) |
| $c\,c(L)$ | - centre to centre |
| $cc(L^3)$ | - cubic centimetre |
| $cf(L^3)$ | - cubic foot |
| $c(FL^{-2})$ | - cohesion |
| $ci(L^3)$ | - cubic inch |
| $cm(L)$ | - centimetre |
| $cpn$ | - compression |
| $C_b(D)$ | - coefficient of $\dfrac{WL^3}{EI}$ for calculating the deflection of a beam due to bending moment |
| $C_s(D)$ | - coefficient of $\dfrac{WL^3}{EI}$ for calculating the deflection of a beam due to shear force |
| $d(D)$ | - parameter of an ellipse $(3-4\mu)$ in plane strain and $(3-\mu)/(1+\mu)$ in plane stress |
| $dia(L)$ | - diameter |
| Eq. | - equation |
| $E(FL^{-2})$ | - modulus of linear deformation (Young's modulus) |

$E_p (FL^{-2})$ — modulus of deformation of pillar rock

ft(L) — feet

$F_s (D)$ — factor of safety

$G (FL^{-2})$ — modulus of shear deformation

h' (L) — semi-height of a pillar

h (D) — dimensionless height of a pillar (H /L)

H (L) — height of pillar

i (D) — angle of dip to horizontal

in. (L) — inch

$I (L^4 \text{ or } ML^2)$ — moment of inertia

k (D) — $S_t/S_o$ or $\sigma_h/\sigma_v$

$k_s (L^3 F^{-1})$ — coefficient of subgrade reaction, $\delta/q$

ksc — kilograms per square centimetre

l — semi-span of a mining zone (L/2)

ln a — natural logarithm of a

log a — logarithm of a to base 10

LF — linear foot

L (L) — breadth of mining zone

max — maximum

m (D) — Poisson's number

m (D) — parameter of an ellipse (a-b)/(a+b)

min — minimum

$M (FL^{-2})$ — $E/(1-\mu^2)$

M (FL)      - moment

n (D)      - ratio of moduli of deformation (M/Mp or E/Ep)

N (D)      - number of pillars

p $(FL^{-2})$      - contact pressure

pcf $(FL^{-3})$      - pounds per cubic foot

psf $(FL^{-2})$      - pounds per square foot

psi $(FL^{-2})$      - pounds per square inch

P (F)      - a pillar load

q $(FL^{-2})$      - bearing pressure

$Q_B$ $(FL^{-2})$      - uniaxial compressive strength of a sample of width B

$Q_o$ $(FL^{-2})$      - uniaxial compressive strength for a sample of unit width

$Q_u$ $(FL^{-2})$      - uniaxial compressive strength

r (D)      - local extraction ratio, i.e. based on tributary area to single pillar

r (L)      - radius or radial distance

R (D)      - extraction ratio (wall area excavated/total wall area); parameter of an ellipse (a+b)/2

R (L)      - radius or radial distance

sf $(L^2)$      - square foot

si $(L^2)$      - square inch

S $(L^{-3})$      - section modulus

$S_h$ $(FL^{-2})$      - field stress in the horizontal direction

$S_t$ $(FL^{-2})$      - field stress parallel to the seam or vein and normal to strike

$S_v$ $(FL^{-2})$      - field stress in the vertical direction

| | |
|---|---|
| $S_o$ $(FL^{-2})$ | - field stress normal to seam or vein |
| $S_p$ $(FL^{-2})$ | - average pillar pressure on walls $\Sigma P / \Sigma A_t$ |
| $S_x$ $(FL^{-2})$ | - field stress in the x-direction |
| $S_y$ $(FL^{-2})$ | - field stress in the y-direction |
| $S_z$ $(FL^{-2})$ | - field stress in the z-direction |
| tsn | - tension |
| TA | - tributary area |
| $v_r$ (L) | - radial displacement |
| $v_\theta$ (L) | - tangential displacement |
| V (F) | - shear force |
| w (D) | - $\mu / (1 - \mu)$ |
| wrt | - with respect to |
| W (F or $MLT^{-2}$) | - load or weight |
| x (L or D) | - linear displacement or co-ordinate or dimensionless distance (x'/L) in direction of x-axis |
| x' (L) | - linear displacement or co-ordinate in direction of x-axis |
| y (L) | - linear displacement or co-ordinate in direction of y-axis |
| z' (L) | - dimensionless co-ordinate (z/L) in direction of z-axis |
| z (L or D) | - linear displacement or co-ordinate in direction of z-axis |
| $\delta$ (L) | - inward displacement of wall normal to vein or seam; or just displacement |
| $\delta'$ (L) | - reverse displacement of wall due to average pillar pressure |
| $\delta A$ (L) | - abutment compression or deformation |

| | |
|---|---|
| $\delta_c(L)$ | - displacement of wall normal to vein or seam at centreline |
| $\delta_e(L)$ | - inward displacement of wall normal to vein (or seam), resulting from excavation of stopes or rooms |
| $\delta'_p(L)$ | - local penetration of a pillar into the wall |
| $\delta_x(L)$ | - displacement of wall normal to vein or seam at x from centreline |
| $\gamma(d)$ | - shear strain |
| $\gamma(FL^{-3})$ | - unit weight (bulk density) |
| $\epsilon(D)$ | - linear strain |
| $\epsilon_r(D)$ | - linear strain in the radial direction |
| $\epsilon_t(D)$ | - linear strain in the tangential direction |
| $\epsilon_\theta(D)$ | - linear strain in the tangential direction |
| $\mu(D)$ | - Poisson's ratio |
| $\rho(L)$ | - radius of curvature |
| $\sigma(FL^{-2})$ | - normal stress |
| $\sigma_p(FL^{-2})$ | - pillar stress $P/A_p$ |
| $\bar{\sigma}_p'(D)$ | - $\sigma_p/S_o$ |
| $\sigma_p(FL^{-2})$ | - average pillar stress $\Sigma P/\Sigma A_p$ |
| $\Delta\sigma_p(FL^{-2})$ | - increase in pillar stress due to mining |
| $\Delta\sigma_p'(D)$ | - $\Delta\sigma_p/S_o$ |
| $\sigma_r(FL^{-2})$ | - radial stress |
| $\sigma_\theta(FL^{-2})$ | - tangential stress |
| $\sigma_t(FL^{-2})$ | - tangential stress |

$\sigma_1 \, (FL^{-2})$        - major principal stress

$\sigma_2 \, (FL^{-2})$        - intermediate principal stress

$\sigma_3 \, (FL^{-2})$        - minor principal stress

$\tau \, (FL^{-2})$        - shear stress